UNIVERSITY OF NAPLES FEDERICO II

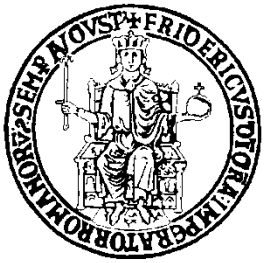

DEPARTMENT OF CHEMICAL, MATERIALS AND PRODUCTION ENGINEERING (DICMAPI)

PHD PROGRAM IN INDUSTRIAL PRODUCT AND PROCESS ENGINEERING

- XXXII Cycle -

"New method of production of orthopedic back brace for the treatment of scoliosis through Additive Manufacturing techniques: an application case"

Academic Tutor:
Prof. Giuseppe Mensitieri

PhD student:
Valentina Abbate

External Tutors:
Eng. Mario Montanino
Dr. Alfredo Ronca

TABLE OF CONTENT

Abstract

Chapter 1: The role of 3D printing in Industry 4.0

1. INTRODUCTION 5
2. INDUSTRY 4.0 7
3. 3D PRINTING IN INDUSTRY 4.0 11
   - 3.1 Classification of AM techniques 15
     - 3.1.1 Liquid polymer 16
       - 3.1.1.1 Stereolithography 17
       - 3.1.1.2 Two photon stereolithography 18
     - 3.1.2 Process involving discrete particles 19
       - 3.1.2.1 Selective laser sintering (SLS) 19
       - 3.1.2.2 Three dimensional printing (3DP) 20
     - 3.1.3 Solidification of molten material 22
       - 3.1.3.1 Fused Deposition Modelling 22
4. APPLICATION FIELDS OF 3DP 24
   - 4.1 Medical application of AM 26
     - 4.1.1 Custom made orthosis and prosthesis using AM 27

   References 30

Chapter 2: Back brace for scoliosis

1. INTRODUCTION 37
2. SCOLIOSIS 38
   - 2.1 Idiopathic scoliosis 40
   - 2.2 Osteogenesis Imperfecta 44
   - 2.3 Treatments for scoliosis 45
3. BACK BRACE FOR SCOLIOSIS 48
   - 3.1 Types of Scoliosis Braces 48
     - 3.1.1 Boston Brace 49
     - 3.1.2 Wilmington Brace 49
     - 3.1.3 Milwaukee Brace 50
     - 3.1.4 Providence and Charleston Brace 51
   - 3.2 Back brace manufacturing techniques traditional vs proposed approach 51
     - 3.2.1 Traditional approach 52
     - 3.2.2 Modern approach 53
     - 3.2.3 Proposed approach 54
4. ENVIRONMENTAL IMPACT OF 3D PRINTING 57

References 60
Chapter 3: An innovative process to produce back brace scoliosis by 3D printing
1. INTRODUCTION 65
2. MATERIALS AND METHODS 67
2.1 Preliminary material screening 67
2.2 Polylactic acid (PLA) 71
2.3 Polyethylene terephthalate glycol (PETG) 72
2.4 Characterization of 3D printed samples 73
2.4.1 Tensile test 73
2.4.2 Charpy impact test 74
2.4.3 Differential scanning calorimetry 75
2.4.4 Surface morphological analysis 75
2.5 Brace manufacturing by FDM 75
2.5.1 Virtual design of the back brac 75
2.5.2 Back brace manufacturing process 77
3. RESULTS AND DISCUSSIONS 78
3.1 Preliminary materials screening 78
3.2 Mechanical morphological and thermal characterization of selected polymers 79
3.3 3D printing of the back brace 84
3.4 Cost model for the realization of the back brace by FDM technique 85
4. CONCLUSIONS 90
References 91
Chapter 4: Clinical Trials
1. INTRODUCTION 94
2. INCLUSION AND EXCLUSION CRITERIA 94
3. PLANNED ACTIVITIES 95
3.1 Recruiting 95
3.2 First visit 96
3.3 Realization of the back brace 97
3.4 Second visit 99
3.5 Third visit 100
3.6 Data analysis and tolerability evaluation criteria 100
4. LIMITATIONS 103
5. CONCLUSIONS 103
References 104

Abstract

The latest industrial revolution, Industry 4.0, is encouraging the integration of intelligent production systems and advanced information technologies. Additive manufacturing (AM) is considered to be an essential ingredient in this new movement. In the medical sector use of scanning technologies combined with computer aided design (CAD) and AM are gaining attention in the fabrication of customized medical devices, implants and products. Particularly, in orthopedic the patient-specific analysis is essential to obtain an accurate medical imaging data of the individual patient. Building end-use functional parts, like back brace for scoliosis, with additive manufacturing (AM) technologies is a challenging task and it will be described in the present work.

This aim of the present thesis is the design and fabrication of a customized orthopedic back brace by Additive Manufacturing technique.

Chapter 1 provides an analysis of Industry 4.0 and how it is changing the industrial scenario in Europe. AM is considered to be an essential ingredient in this new movement and the author provides a comprehensive review on AM technologies together with its contributions to Industry 4.0 and potential uses. In particular, the authors focus its attention on the possible application of AM in the medical field.

Chapter 2 gives an overview on idiopathic scoliosis with a focus on the commercial back braces present on the market. Moreover, the authors proposed a comparison between three different manufacturing processes for back brace: the old, the present and the proposed approach. In particular, the proposed approach is based on the combination of 3D medical imaging and AM technologies to realize customized back braces for scoliosis.

Chapter 3 describes in details the methods to design and manufacture an orthopedic back brace from the material testing to the final back brace design and manufacturing. Mechanical, thermal and morphological properties of two commercial polymers (PLA and PETG) have been investigated to determine the best 3D printer material for developing the back brace. Starting from the patient imaging an orthopedic back brace have been designed by dedicated software (Rodin4D). Fused deposition modeling (FDM) have been selected for the realization of the back brace due to its ease of use and the possibility to have a wide range of processable materials.

Finally, **Chapter 4** reports the pre-clinical trial of the realized back braces on ten patients in collaboration with the orthopedic clinic “La Nostra Famiglia -

Eugenio Medea" of Bosisio Parini (Lecco). The pre-clinical investigation is a pilot study that will involve pediatric patients suffering from rachis alterations (idiopathic scoliosis and osteogenesis imperfecta) whose main objective will be the evaluation of the acceptance, safety and satisfaction of patients in the use of 3D printed back braces respect to the traditional ones with consolidated clinical effectiveness.

Chapter 1
The role of 3D Printing in Industry 4.0

1. INTRODUCTION

According to statistics of the American economist W. Rostow, beginning of the 20th century marked the domination of industrial production: while in 1870 its share constituted 19.5%, in 1900 it was 58.7% (1913—100%). Due to growth of production and development of transport, turnover of the global trade increased by three times. In order to explain the causal factors that constitute the essence of genesis of global revolutionary transitions, it is necessary to determine the role of these revolutions in the historical context [1]. In literature, it was common to distinguish the following industrial revolutions: steam engine and railroad transport (late 18th century); electrification, division of labour, and mass production (late 19th century); electronics, IT industry, and automatized production (late 20th century) and Cyber physical system (21th century) as depicted in *Figure 1* [1-3]. The fourth industrial revolution, namely Industry 4.0, is the recent movement on intelligent automation technology. A continuous concern for manufacture Industry 4.0 dictates the end of traditional centralized applications for production control and it assumes preparation of a computerized, intelligent manufacturing environment, guaranteeing flexibility and high efficiency of production, integration of different activities and effective communication between a client and a producer, as well as between the producer and suppliers [4, 5]. One of the most radical changes is the shift from computers to smart devices utilizing the infrastructure services based on cloud computing [1, 6]. This new beginning of the Internet era, marked by an integrated computer-based automation and ubiquitous computing systems, is moreover being connected to the wireless network by the Internet [7, 8] firms is the mismatch between supply and demand within value chains [2, 3, 9, 10].

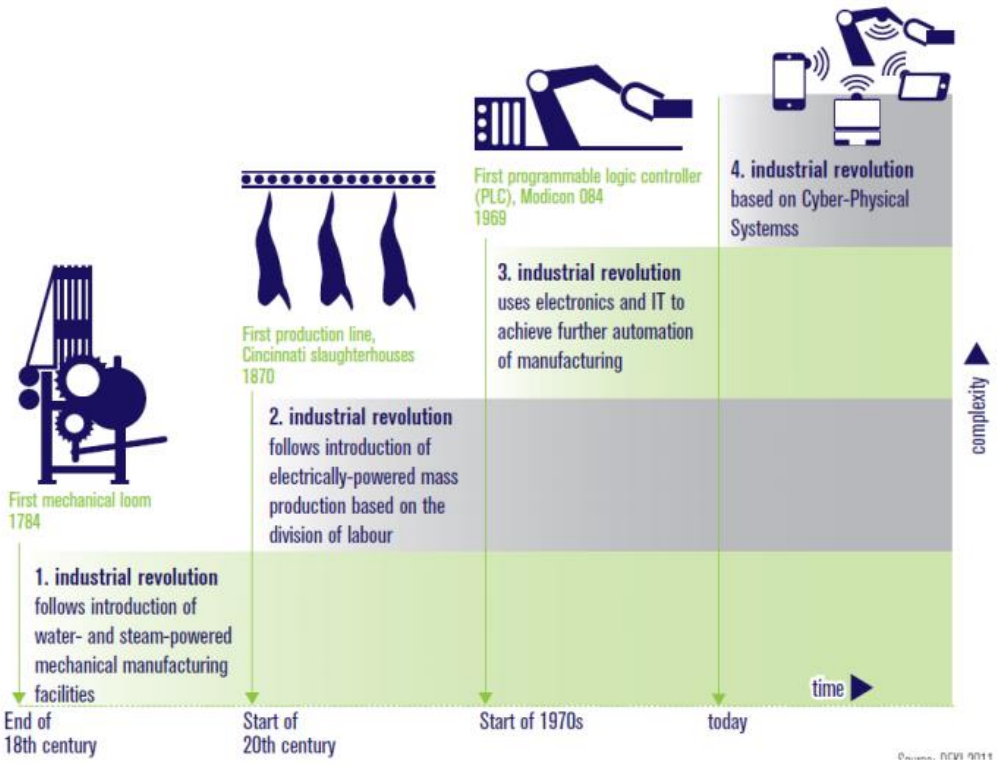

Figure 1The four industrial revolutions

Industry 4.0 responds to customer demands for tailored products by technology enablers such as 3D printing, Internet of Things (IoT), Cloud computing, Mobile Devices and Big Data, creating a totally new environment by redefining the role of humans (*Figure 2*) [3]. With respect to the cyber-physical systems, IoT is described as the concept of gathering information from physical objects using computer networks or accelerated wireless connections [11, 12]. As a whole, this large quantity of data is defined as Big Data, which is another major notion in Industry 4.0 [13, 14]. Moreover, cloud computing, which is related to the processing of all the available information, can also be considered as one of the most significant terms in virtual industrial world [15]. All of these cyber technologies help to ensure the effective utilization of existing information for smart manufacturing of future [4, 16]. In this scenario, additive manufacturing (AM) is considered to be an essential ingredient of this revolution. Due to the necessity for mass customization in Industry 4.0, AM may become a key technology for fabricating customized products due to its ability to create sophisticated objects with advanced attributes (new materials, shapes)[17, 18].

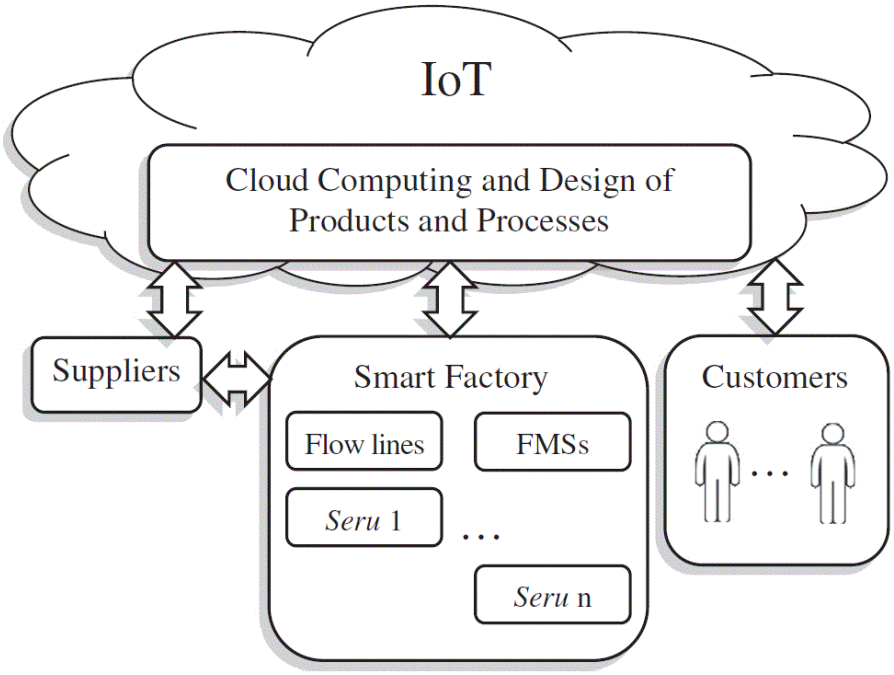

Figure 2 An example of a smart manufacturing system for Industry 4.0 as reported by Yong et al. [2].

Thanks to increased product quality, AM is currently being used in various industries such as aerospace, biomedical and manufacturing mass customization in Industry 4.0 [19].

This chapter give an overview about the correlation between Industry 4.0 and AM technologies. Due to its significant role in Industry 4.0, AM is the main scope of this paper and so after a first introduction to industry 4.0 all the AM technologies will be explained with a deepening of their application in the biomedical field.

2. INDUSTRY 4.0

The concept of Industry 4.0 was born in Germany in 2011 under the term of "Smart Factory" and later defined 4.0 to emphasize the principle that sees the beginning of the fourth industrial revolution [2, 20]. Similar promotions are advocated in other industrial countries. For example, the United States proposed a smart manufacturing plan and suggested connecting everything using IoT [7, 21-23]. The Japanese Government published "Society 5.0" – a smart system that covers smart community, smart infrastructure, smart factory and others. China created a plan of

“Chinese Manufacturing 2025” to foster Chinese manufacturing shifting to high value-added and becoming a global leader. Industry 4.0 specifically involves a radical shift in how production shop floors currently operate. Defined by many as a global transformation of the manufacturing industry by the introduction of digitalization and the Internet, these transformations consider revolutionary improvements in the design and manufacturing processes, operations and services of manufacturing products and systems [5]. All the industrial revolutions listed are linked to inventions based on scientific discoveries: steam engines, electricity, PCs and telecommunications [24].

The first industrial revolution is generally considered the steam machine that made the steam power exploitable opening the industry age. The second industrial revolution is generally seen as the discovery, or better the application, of electricity and how to use it, namely allowing automotive mass production. The third industrial revolution is generally linked to the computer and the possibility of data processing for computer integrated manufacturing (CIM), leading to the present era of information technology *Figure 1* [2, 25]. Within the context of Industry 4.0, the factory of the future will enable the connection between machines and human-beings in Cyber-Physical-Systems (CPSs). These new systems focus their resources on the introduction of intelligent products and industrial processes that will allow the industry to face rapid changes in shopping patterns [26, 27].

The concept of Industry 4.0, on the other hand, is a technological revolution not closely linked to a scientific discovery but is depicted as a connection of components that generate a further connected system [28]. The implementation of innovative technologies enables companies to reduce costs, increase flexibility and customize the product. Industry 4.0 involves automated systems including Artificial Intelligence (AI), robots, drones, nanotechnologies and a variety of inputs that enable customization, flexibility and rapid manufacturing (*Figure 3*) [20].

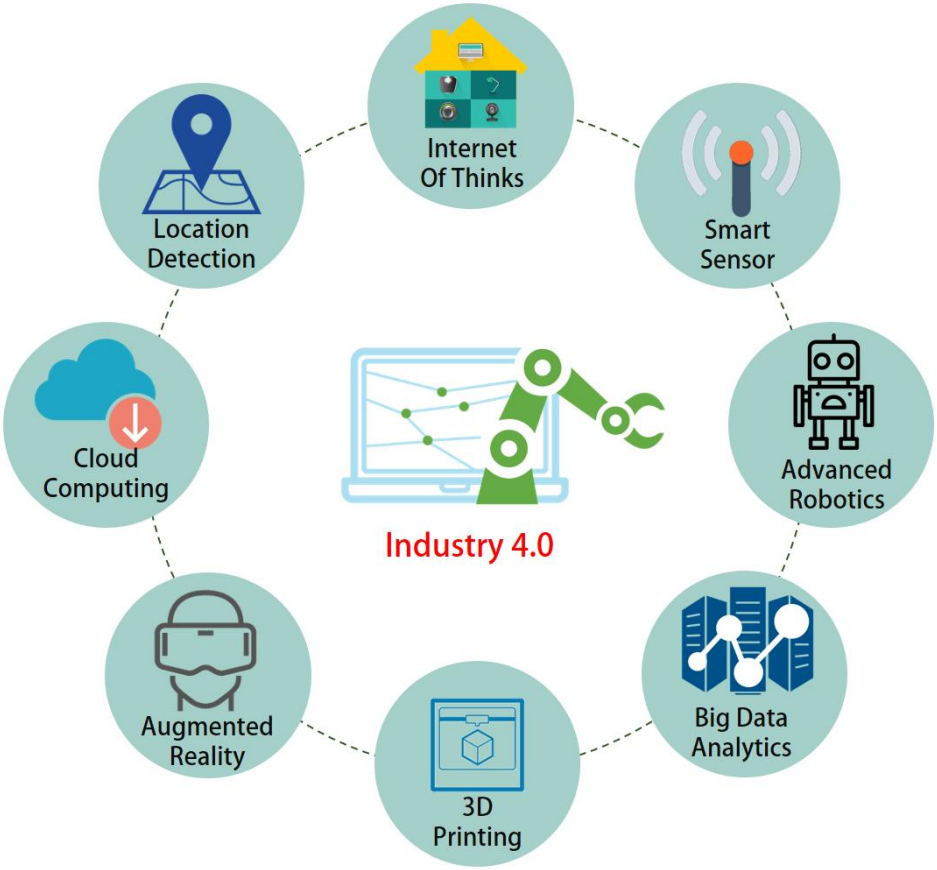

Figure 3 Industry 4.0 Framework

From a production point of view, Industry 4.0, represents the ability to improve a product through the study and implementation of algorithms that analyze a huge amount of data about that product and how it should be made [8]. Practically all production is based on the concept that collecting as much data as possible on the product (BIG DATA), transmitting and analyzing them, are much more economical and performing processes for the production of the product itself [24]. Thanks to the connectivity it is now possible to manage a large amount of data, the Big Data precisely, the innovation is therefore all in the daily use of connectivity and then in the continuous transmission of this data. The production will therefore be the final part of a mechanism that starts from the collection of Big Data, which are then "translated" by algorithms (Analysis phase) that optimize the production process that will then take place in close collaboration between man and machines [29]. This creates an integrated, innovative, smart and fast production system that promotes the integration between big data, IoT and Artificial Intelligence (AI). In this way it will possible to envisages an environment whereby smart machines can

communicate with one another, not only to enable the automation of production lines but also to analyse and understand a certain level of production issues and to solve them [10, 14].

An important competitive advantage for a company is its capability to realise individual requirements of diverse customers. The paradigm of mass customization emerged in the late 1980's as demand for product variety increased [30-32]. The number of varieties offered by consumer product manufacturers has increased significantly since then. An example used in is the number of distinct automobile vehicle models in the U.S. which increased from 44 in 1969 to 165 in 2006 [33, 34]. To implement MC manufacturers should apply appropriate management and control principles to organise manufacturing systems to realise individual customer requirements. Traditional manufacturing systems may find it difficult to achieve these requirements because its responsiveness is slow [3, 35].

Additive manufacturing (AM), also called 3D printing (3DP), is one of the vital components of Industry 4.0 and it may become a key technology for fabricating customized products [36-38]. The core principle of this method is that materials are added in a layer by layer fashion rather than subtracted as happens in conventional [39].

Figure 4 CAD image of a teacup with further images showing the effects of building using different layer thicknesses [40]

AM technologies is a relatively recent technology that provides the production of an object through the progressive addition of material in a layer-by-layer fashion,

with the realization of the piece that proceeds section by section based on a three-dimensional CAD model (*Figure 4*) [41-43]. Garrett et al suggests that the impact of 3D printing may be disruptive and revolutionary, and that the impact could last for several decades in the areas of manufacturing, value chains, environments, global economies and geopolitics [37]. AM is already a proven "general purpose" technology that is being used for an enormous range of applications such as fabricating spare and new parts for planes, trains and automobiles and thousands of items in between [44-46]. Initially limited to one realization of models and prototypes, the additive technology has started to move towards the production of semi-finished components suitable for long-term use [40, 41, 43]. The advantages that can derive from this innovation do not place any limit on the geometric complexity of the obtainable piece and are present in a wide range of types of materials ranging from polymers, on which the first additive techniques initially concentrated, to metals and also, used, to composite materials [47, 48]. Moreover, 3DP has greater resource efficiency compared to most conventional, subtractive production methods [39]. This has led some authors to propose that the rapid success of 3DP will initiate a change of view on natural resources with respect to material savings during production, smart redesign of components, and the ability to utilize recycled materials for the printing process [49]. It is of paramount importance that in the next chapter we analyze the different 3D printing technologies and their potential impact in different market.

3. 3D PRINTING IN INDUSTRY 4.0

The ASTM F42 Technical Committee defines AM as the "*process of joining materials to make objects from three-dimensional (3D) model data, usually layer upon layer, as opposed to subtractive manufacturing methodologies*" [50]. AM was officially born in 1982, when Mr. Chuck Hull invented stereolithography (SLA) and founding the 3D Systems. He created the first commercial example of rapid prototyping, and of the STL format (*Figure 5*) [4, 37, 40, 41, 43]. He laid the groundwork and paved the way for all those who followed him, while remaining himself and his company at step with innovations; his patented concept of physical objects created as a sequence of 2D layers overlapping is, in fact, still valid today.

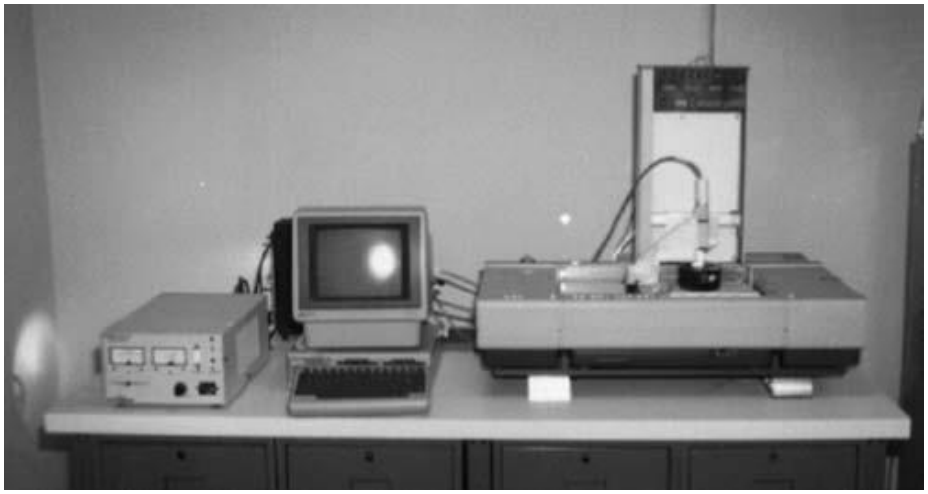

Figure 5 The first AM technology from Hull, who founded 3D systems [51]

In 1986 Carl Deckard, Joe Beaman and Paul Forderhase studied the ideas of Chuck Hull and developed Selective Laser Sintering (SLS), sintering, a process completely similar to the one previously discovered, but which brings an important modification: the liquid was replaced with powder [52]. One of the most advantages was that the powder being a solid does not require specific supports as in the previous technology. In 1988 Mr. Crump patented Fused Deposition Modeling, that is, printing with molten material. Both the laser and the dust were set aside and he began to use molten plastic that it was "spread" layer by layer according to the object [43]. Later he founded Stratasys, a company also a leader in the sector. In 1995 the Germans of the Fraunhofer Institute developed the method of the Selective Laser Melting (SLM) [53]. For the first time, the world of 3D printers experienced the possibility of produce truly solid objects, with a density that had little to envy to traditional industry. The adjective "Additive" indicates that the object is formed by the progressive addition of material, rather than the removal of excess material from a block. *Figure 6* shows the different approach in the realization of the same component of the additive methods with respect to conventional subtractive ones.

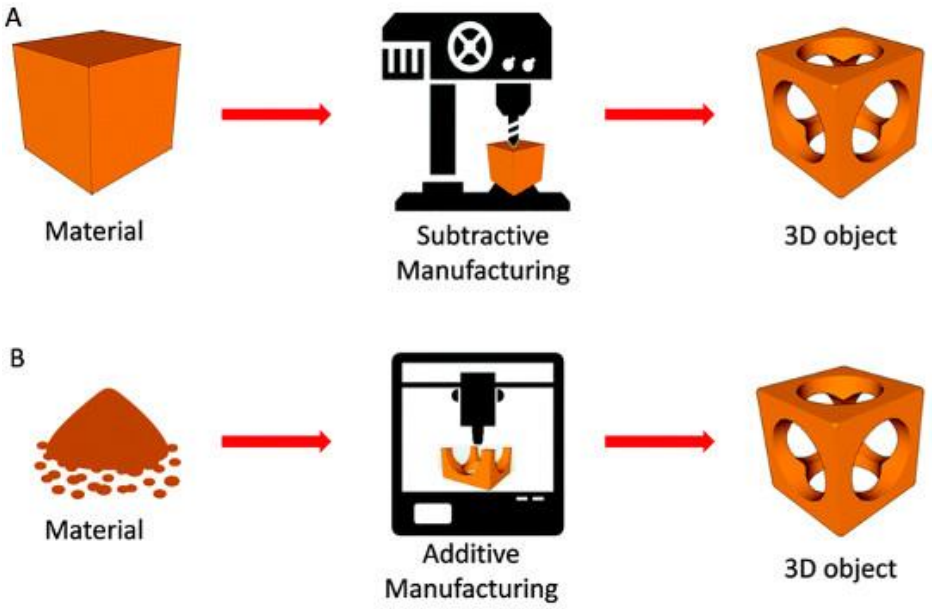

Figure 6 Manufacturing process of a metal component using additive (A) or subtractive technologies (B).

What drives research in the direction of using AM techniques to fabricate long-term and fully functional components is the possibility of drastically reduce the "time-to-market" of the product. The AM in fact allows both to set a cycle production composed of a single step, and to eliminate, in many cases, all types of processing to the tool making. Today, thanks to the progress made it is possible to produce in little time realistic objects that do not require additional finishes. Furthermore, additive production absorbs less subtractive production energy, a key point for producers. On the other hand, additive technologies manufacturing can be very advantageous for the freedom they grant in the component design. In fact, these techniques offer a unique possibility to produce light components, functional gradients of composition, complex geometries and dimensions micrometer.
Generally AM involves a number of steps that move from the virtual CAD description to the physical model part as depicted in *Figure 7* [40]. At later stages of the process, parts may require cleaning and post-processing (including sanding, surface preparation and painting) before they are used, with AM being useful here because of the complexity of form that can be created without having to consider tooling [40].

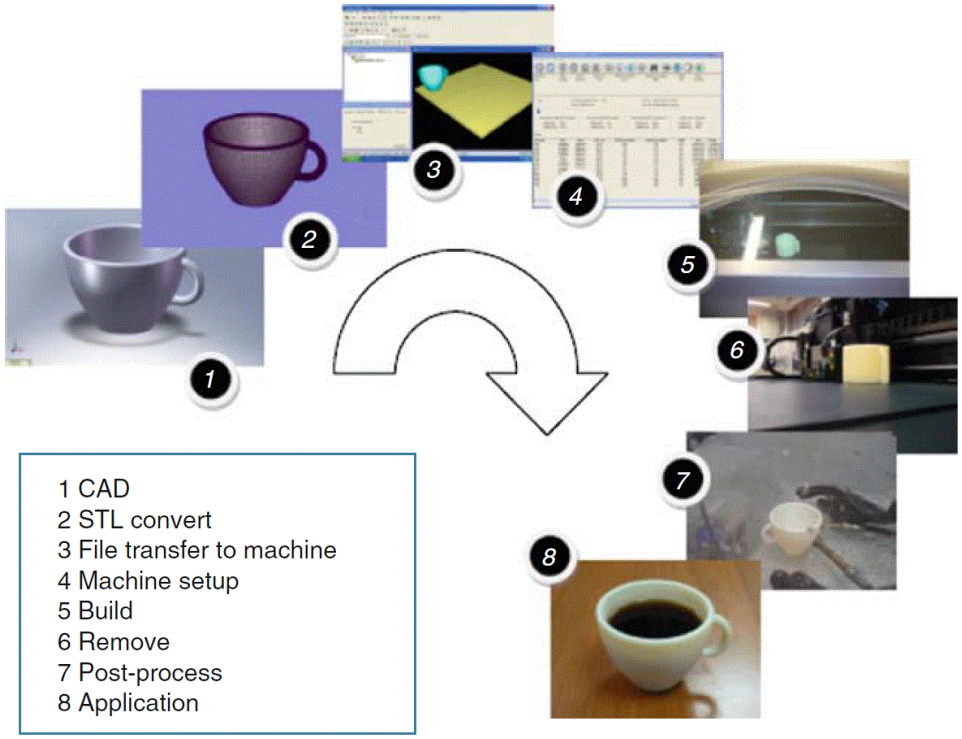

Figure 7 Generic process of CAD to part, showing all 8 stages

In 2005, thanks to the principle of the Self Replicating Rapid Prototyper, there was the real one breakthrough in the world of 3D printers. A 3D printer was created that could reproduce itself. He was born consequently the RepRap project, still active today, completely open source, is free e downloadable for anyone wishing to try their hand at rebuilding their 3D printer. According to the 2014 Wohlers Report, consumers of 3D printers are classified as those that cost less than $ 5000 [54]. The Cornell University and the University of Bath have designed the first open-source 3D printers which are widely recognised in the area: Fab@home and RepRap [55, 56]. However, at present time, it is not yet adopted in the manufacturing sector, but scientists, medical doctors, students and professors, market researchers, and artists use it [57-59]. Areas of interest which have used AM to create objects include aeronautics, architecture, automotive industries, art, dentistry, fashion, food, jewellery, medicine, pharmaceuticals, robotics and toys [60]. Medical industries are particularly interested in AM technology because of the ease in which 3D medical imaging data can be converted into solid objects. In this way, devices can be customised to suit the needs of an individual patient [61]. Thus, each AM technology have advantages and disadvantages for own applications and we

propose to have an overview of the main 3D printing techniques in the next paragraph [41].

3.1 Classification of AM techniques

There are numerous ways to classify AM technologies. A popular approach is to classify them according to baseline technology, like whether the process uses lasers, printer technology, extrusion technology, etc. [62, 63]. Another approach is to collect processes together according to the type of raw material input [64]. These vary according to the materials used (liquids, solids and powders) and to the way in which the various layers are deposited one above the other as showed in *Figure 8*. The processes that use liquid material are divided into those that use photopolymers (which cross-link due to ultraviolet radiation) and those based on melting, depositing and resolidification (thermoplastic materials).

Other processes, on the other hand, consolidate granules of powder by melting along the contact area of the particles or by adding a suitable adhesive. Finally, other methods start from solid material reduced to thin sheets glued one on top of the other and shaped in an appropriate manner.

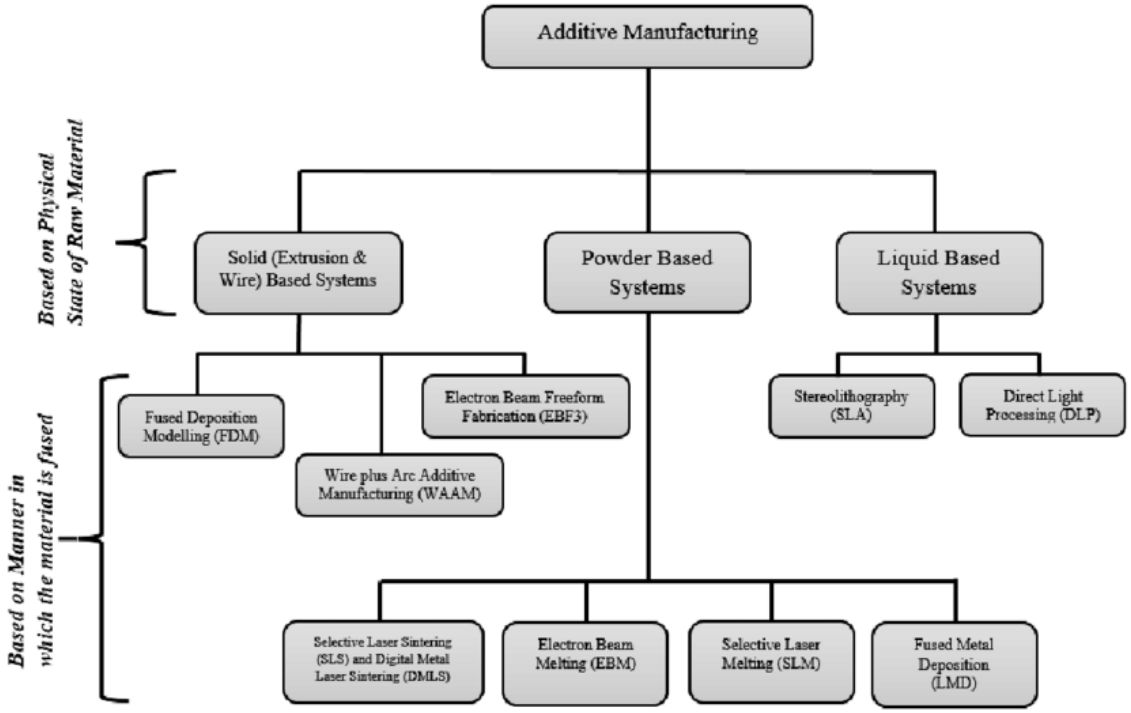

Figure 8 Classification of different AM processes

An excellent and comprehensive classification method is described by Pham et al [65], which uses a two-dimensional classification method as shown in *Figure 9*. The first dimension relates to the method by which the layers are constructed. Earlier technologies used a single point source to draw across the surface of the base material. The first dimension relates to the method by which the layers are constructed.

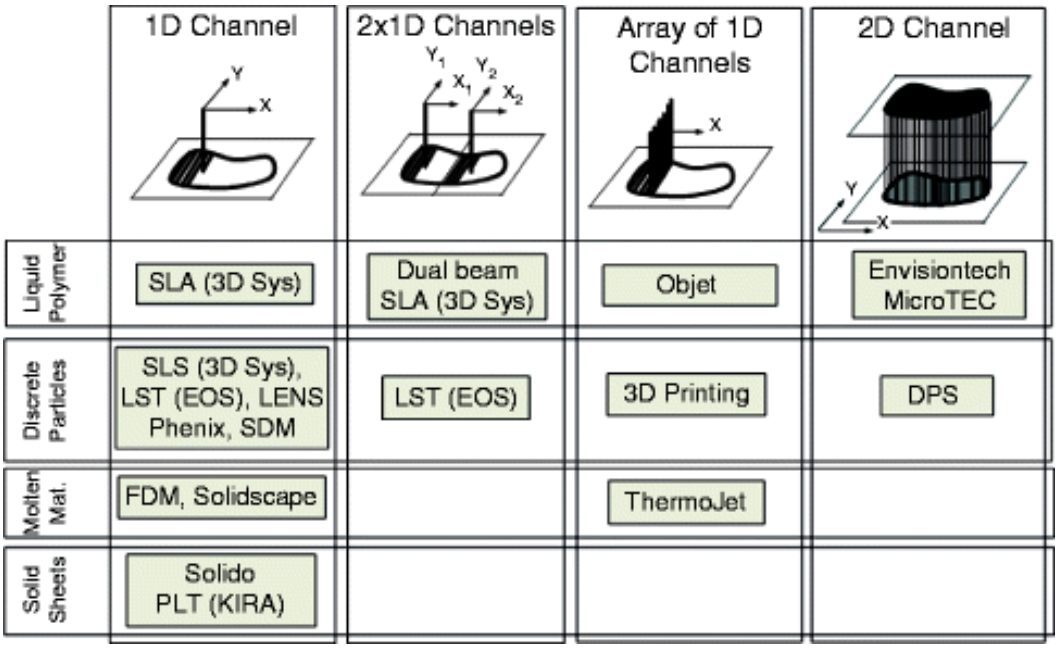

Figure 9 Layered Manufacturing (LM) processes as classified by Pham et al. (note that this diagram has been amended to include some recent AM technologies) [65]

Earlier technologies used a single point source to draw across the surface of the base material. Later systems increased the number of sources to increase the throughput, which was made possible with the use of droplet deposition technology, for example, which can be constructed into a one dimensional array of deposition heads. Pham uses four separate material classifications; liquid polymer, discrete particles, molten material, and laminated sheets. Furthermore, there may come systems in the future that use 3D holography to project and fabricate complete objects in a single pass.

3.1.1 Liquid polymer

Liquid polymers system appears to be one of the most popular between the AM technologies. The first commercial system was the 3D Systems Stereolithography process based on liquid photopolymers. A large portion of systems in use today are,

in fact, not just liquid polymer systems but more specifically liquid photopolymer systems [40].

3.1.1.1 Stereolithography

Stereolithography is an additive fabrication process using a liquid UV-curable photopolymer and a UV laser to build structures a layer at a time. Stereolithographic processes produce 3D solid objects in a multi-layer procedure through the selective photo-initiated cure reaction of a polymer [66, 67]. These processes usually employ two distinct methods of irradiation. The first method is the mask-based method in which an image is transferred to a liquid polymer by irradiating through a patterned mask. The irradiated part of the liquid polymer is then solidified. These systems generally require the generation of many masks with precise mask alignments. In the second method, a direct writing process using a focused UV beam produces polymer structures.

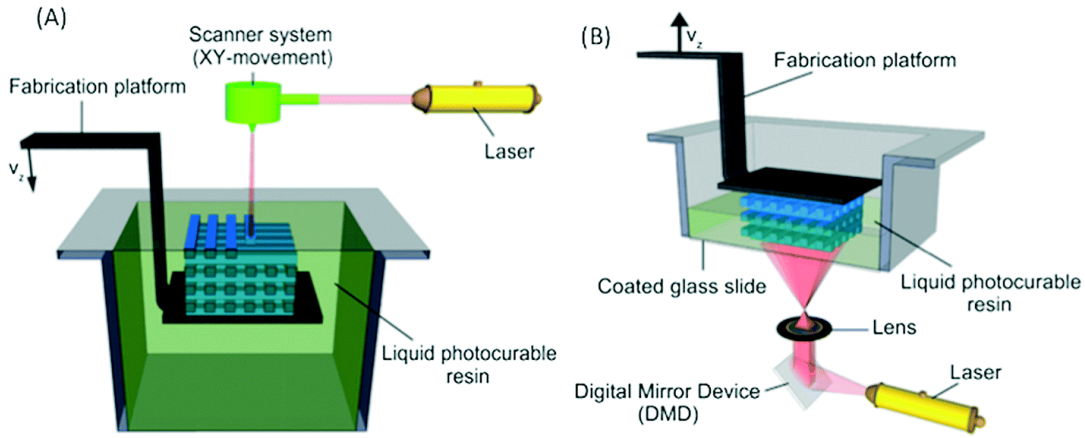

Figure 10 Conventional Stereolithography system as reported by waheed et al.[68]

Generally, SL is considered to provide the greatest accuracy and best surface finish of any RP technology [69-71]. The model material is robust, slightly brittle, and relatively light, although it is hydroscopic and may physically warp over time (a few months) if exposed to high humidity. Although fine structures can be produced by the laser SL technique, the process is usually slow because of the nature of point-by-point laser scanning [72]. One solution for this problem is the use of a Liquid Crystal Display (LCD) or a digital processing projection system as a flexible mask. Microstereolithography (μ-SL) is a relatively recent development, similar to conventional stereolithography [73]. There are three methods of μ-SL and they have differences in the solidification processes. The first is free-surface method where an UV curable resin is exposed to UV laser beam above the free-

surface of the resin and the resin at the surface is solidified [74]. The second is fixed-surface method. In this method, UV curable resin is exposed to UV beam toward flatly transparent window that is immersed in the resin and the resin at the surface formed by this window is solidified [75]. This method has a higher resolution than free-surface method. However, the yield of this method is low because adhesion between the resin and the window causes destruction of a solidified structure. The third is inside-solidification method [76]. Unlike the two methods described above, in this method resin is solidified at not the surface, but a point inside the UV curable resin.

3.1.1.2 Two photon stereolithography

Even if micro-stereolithography (μ-SLA) remains one of the most powerful and versatile of all SFF techniques there are limitations to μ-SL in terms of the spatial resolution of fabricated structures [77]. The minimum thickness of layers is inevitably affected by the viscosity and surface tension of the resin and so it is very difficult to use μ-SL to fabricate ultraprecise microstructures that have a nano-detail or submicrometer scale. In this context, two-photon stereolithography (TPS), established by Kawata and his group, appears of high interest since it offers intrinsically sub-100 nm resolution [78]. Normally in conventional SLA techniques polymerization is induced by absorption of a single photon, TPS, instead, is based on two photon non-linear absorption (TPA) process [78]. In this system, they used a high-power Ti:Sapphire femtosecond-laser, with wavelength 790 nm and during the process the photoinitiator requires two photons to strike and to form a free radical that can initiate polymerization. Taking advantage of these effects, photopolymerization is confined at the focal point of the laser irradiation, in a 3D volume, typically of less than 1 μm^3 [79]. A schematic of a typical research setup for this process is shown in *Figure 11*. Therefore, the main advantage of TPS, compared to single photon absorption, is that excitation is localized within the focal volume of a laser beam. Consequently, it gives access to 3D microfabrication since the polymerization threshold is not reached out of the focal volume [80]. Moreover, another advantage is that parts can be built inside the resin vat, not just at the vat surface, which eliminates the need for recoating with a great improves in speed production.

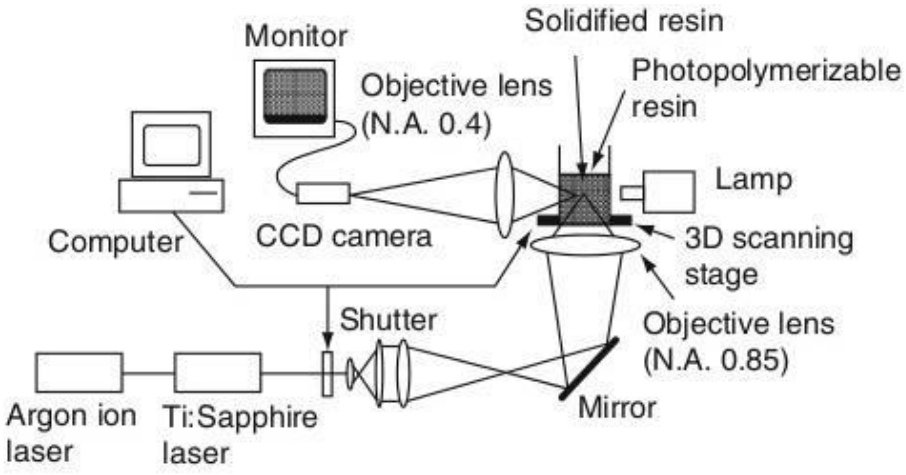

Figure 11 Schematic of typical two-photon equipment by Gibson et al [80]

Nano-sized structures formed by this technique have many other promising applications especially in the field of photonic crystals, micromechanical parts, rapid prototyping of micro/nanofluidics, small-scale production of micro-optics components and 3D frameworks for cell biology. Despite the possibilities to fabricate 3D objects with sub-100 nm features in a single step, TPS appears as an extremely slow technique for mass production in industry due to the point by point writing process. However, these drawbacks appear to be a fantastic and appealing field of research for the next decades since it is expected that the TPS will take a position as a powerful process for the fabrication of 3D nano/microdevices applicable to diverse research fields.

3.1.2 Process involving discrete particles

These processes build the part by joining powder grains together using either a laser or a separate binding material.

3.1.2.1 Selective laser sintering (SLS)

SLS uses a fine powder of material which is heated with CO_2 laser of power in the range of 25-50W such that the surface tension of the grain are overcome and they fuse together [52]. Before the powder is sintered, the entire bed is heated to just below the melting point of the material in order to minimize thermal distortion and facilitate fusion to the previous layer [81].

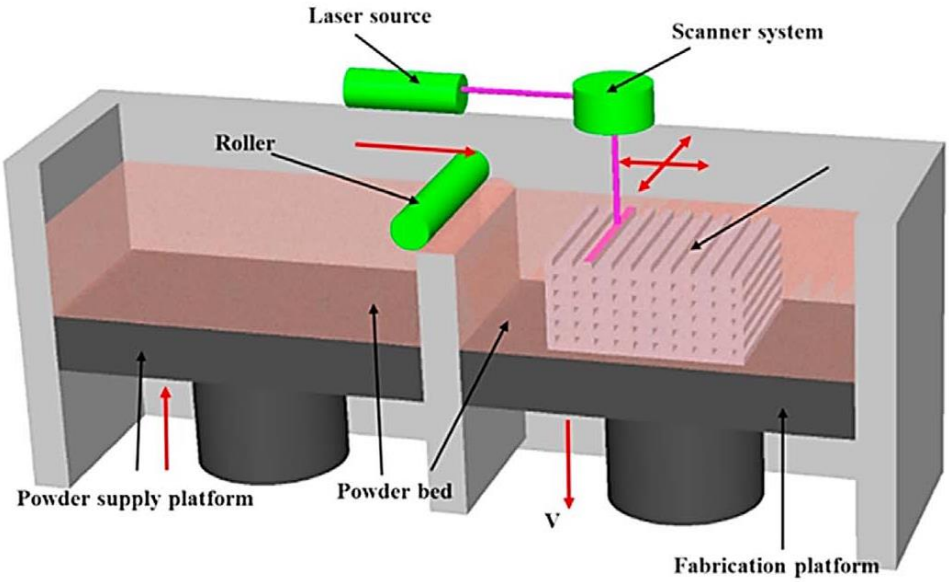

Figure 12 Schematic view of the selective laser sintering techniques.

Each layer is drawn in the powder bed using the laser to sinter the material. Then the bed is lowered and a powder-feed chamber raised. A new layer of powder is deposited and spread by a counter rotating roller [82]. The sintered material forms the desired structure while the undesired powder remains in place to support the structure and may be cleaned away and recycled once the process is completed as depicted in *Figure 12*. There is a large range of materials available for this process, basically any material which can be pulverised may be employed. At present, nylon, thermoplastic Polyurethane (TPU), Polylactic acid (PLA), Polycarbonate, composites and metals are commonly used in SLS, and it is claimed that these materials have engineering grade properties [83]. They are cheaper than the resins used for SL, are non-toxic and safe and may be sintered with relatively low-powered lasers. However, parts need a long cooling cycle on the machine before they can be removed.

3.1.2.2 Three dimensional printing (3DP)

The binder jetting process is another AM technique that employs inkjet head (IJH) technology for processing materials. In this system, the head prints a liquid binder onto thin layers of powders based on object profiles that have been generated by software [52].

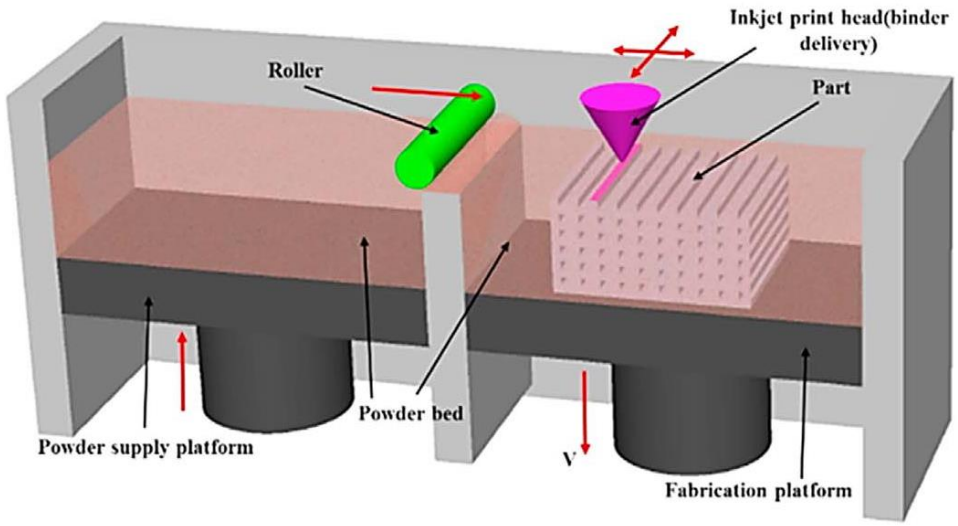

Figure 13 Schematic layout of the inkjet printing process.

In general, a wide range of powders including ceramics and polymers can be processed by inkjet 3DP; however, binder selection is a key factor in successful part fabrication [84]. The materials used as a binder must have suitable properties to prevent spreading from nozzles. To be compatible with the type of printing head, the viscosity and surface tension of the binder must be 5–20 Pa.s and 35–40 mJ N^{-1} respectively. Three different types of binders are commonly used in the inkjet 3DP method: i) water-based binders such as certain commercial ones, ii) phosphoric acid–based and citric acid–based binders, and iii) polymer solution binders such as PVA and poly(D,L-lactic acid) (PDLLA)[52, 83, 84]. For powder materials, a broad range of polymers, ceramics, and composites can be applied in this technique. The resolution is dependent on the size of the binder droplets and the powder grains, the placement accuracy of the nozzle and the way that the binder diffuses through the powder due to capillary action. Parts made using this process do not require supports to brace overhanging features. They do however need to include a hole so that excess powder can be removed [20]. Disadvantages of this technology are that the final parts may be fragile and porous, and it can be hard to remove the excess powder from any cavities. A further drawback is that the layers are raster-scanned by the printhead that leads to a stair-stepping effect in the X–Y plane as well as in the build direction. Another drawback is that the recycled powders require sieving to ensure that no globules are present that would interfere

with the smooth application of the next powder layer. The system also requires an inert nitrogen atmosphere in which to sinter the materials.

3.1.3 Solidification of molten material

3.1.3.1 Fused Deposition Modelling

The FDM process was developed in the 1980s and was commercialized by Stratasys Inc., USA, in the early 1990s [85]. The FDM machine consists of a movable head which deposits a thread of molten material onto a substrate. The build material is heated above its melting point so that it rapidly solidifies after extrusion and cold welds to the previous layers (*Figure 14*). At the completion of the layer deposition, the sample stage is lowered and a new layer is deposited. In this fashion, the technique fabricates a 3D structure [86, 87]. Factors to be taken into consideration are the necessity for a steady nozzle speed and material extrusion rate, the addition of a support structure for overhanging parts, and the speed of the head which affects the overall layer thickness [88]. A benefit of this method is the absence of organic solvents in the fabrication process. The computer-aided process is controlled by the use of CAD data in the design of the part.

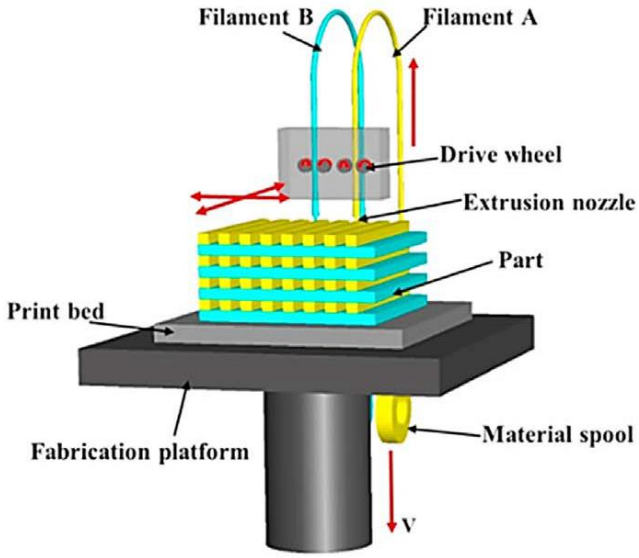

Figure 14 Schematic description of fused deposition modelling

FDM is being widely used in AM technology recently in producing various products across various manufacturing sectors because of its reliability, cost-effectiveness in producing 3D objects with good resolution, dimensional stability [89], wide material customization, simple fabrication process and its ability to

fabricate complicated geometrical parts safely in a favorable environment [90]. FDM is the most commonly used in producing conceptual models, prototypes and engineering components.

The characteristics of the final product such as strength, surface finish and porosity are extremely dependent on the process parameters of the FDM process. Currently, polymers are treated as most suitable for the FDM process due to their melting temperature which are in the range of commercially available machine and they also provide sufficient strength to the final parts that can be utilized for wide-ranging applications [91].

Thermoplastic polymers are mostly used in FDM, and ABS and PLA are the most popular. Some frequently used polymer materials in the FDM process include polyethylene terephthalate glycole (PETG) polyamide or nylon (PA), polycarbonate (PC), polyethylene (PE) and polypropylene (PP). Some research is also done using a combination of the polymer materials such as ABS and PC, PLA and PC, PE and PP. Recently polymers are used as base matrix materials, and metals mostly in powder form are used as reinforcement which results in a material having particular properties from both materials [92]. Properties such as adhesiveness, flexibility, conductivity, process ability, toughness and strength depend on the composition of the matrix and reinforcement materials. Bio-composites have brought significant advancements in the field of bio-medical and modern health-care sector and helped in the development of artificial human organs and tissue engineering [93]. They are based on ceramics such as TiO_2, ZrO_2, Al_2O_3 used as reinforcement materials with polymer matrices such as polyamide (PA), polypropylene (PP) and PLA. Bio-composites/materials, made of those substances are highly compatible with the simulated body fluid that resembles close to that of human blood plasma.

Most of the research on the FDM materials has been concentrated on the suitability of the material, optimizing the process parameters, rheological and mechanical properties, finding applicability in new areas such as tissue engineering and dimensional accuracy [94, 95]. Development of new material for FDM is done along with optimization of the process parameters that is a critical criterion for achieving quality parts with enriched material, mechanical and thermal properties. Currently, there are different types of FDM machines available in the market with specifications regarding the flow ability of the material to be used for best results [96]. There is also a need to work on the FDM machine such as improving the range of melting temperature in order to include high melting point materials. Moreover, due to the increasing environmental consciousness in the world, there is

a need to do extensive research on natural fiber-reinforced composites as they have a huge potential in replacing glass-filled reinforced composites that are not environmental friendly. Recently, most of the manufacturing industries are focusing on developing infrastructure for executing research on FDM technology as it possess huge potential for changing the manufacturing scenario by generating huge profits without compromising on product quality. These future works will help in improving the FDM process further and making it an ideal AM process for various manufacturing applications including bio-medical with high part quality, dimensional accuracy and other desired properties.

4. APPLICATION FIELDS OF 3DP

The development of innovative, advanced AM techniques has progressed greatly in recent years, yielding broader and broader industry applications *Figure 15*.

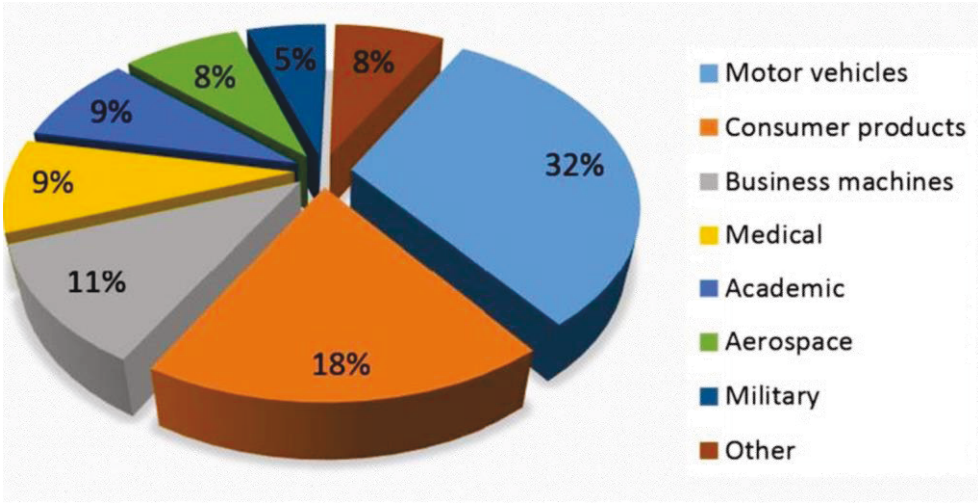

Figure 15 Main application field of 3DP

Customized functional products are currently becoming the trend in 3D printing as predicted by Wohlers Associates, who envisioned that about 50% of 3D printing will revolve around the manufacturing of commercial products in 2020 [97, 98]. The growing consensus of adapting the 3D manufacturing system over traditional techniques is attributed to several advantages including fabrication of complex geometry with high precision, maximum material savings, flexibility in design, and personal customization. AM is capable of fabricating objects with any degree of customization (*Figure 16*). This includes products that can be custom-fit to an existing person or object, products that can be personalized based on individual or

group preferences, and mass-customized products that can be produced with infinite variations.

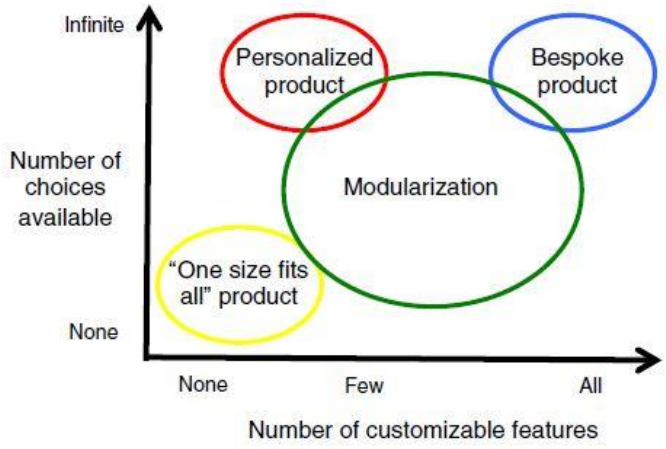

Figure 16 Types of customization available in AM process [99]

However, the precision of the printed parts is dependent on the accuracy of the employed method and the scale of printing. For instance, micro-scale 3D printing poses challenges with the resolution, surface finish and layer bonding, which sometimes require post-processing techniques. However, the inferior mechanical properties and anisotropic behavior of 3D printed parts still limit the potential of large-scale printing. Moreover, the limited materials available for 3D printing pose challenges in utilizing this technology in various industries. Hence, there is a need for developing suitable materials that can be used for 3D printing. Further developments are also needed to enhance the mechanical properties of 3D printed parts [97]. The advantages of 3DP technology will continue to emerge through continuing research efforts, which must be undertaken to understand and eliminate constraints that inhibit the use of this technology.

A distinguished advantage of 3D printing is mass customization i.e., production of a series of personalized goods such that each product can be different while maintaining a low price due to mass production. 3D printing is devoid of the added cost due to mold making and tooling for a customized product. Therefore, mass production of a number of identical parts can be as cost-effective as the same number of different personalized goods. The change between different designs is straightforward with negligible added cost and no need for special preparation. Compared with subtractive manufacturing, AM is particularly suitable for producing low volumes of products, especially for parts with complex geometries.

AM processes also offer great potential for customization, such as fabricating personalized implants for hip and knee replacements [50]. AM gives a flexible solution in orthopaedics area, where customised implants can be formed as per the required shape and size and can help substitution with customised products. A 3D model created by this technology gain an accurate perception of patient's anatomy which is used to perform mock surgeries and is helpful for highly complex surgical pathologies [100]. AM provides a perfect fit implant for the specific patient by unlimited geometric freedom and this is why can help to solve present-day challenges in the biomedical field as reported in the next paragraphs.

4.1 Medical application of AM

As reported by Wohler's The biomedical market represents 11% of the total AM market share today and is going to be one of the drivers for AM evolution and growth [98]. AM is able to 3D print small quantities of customized products with relatively low costs. This is specifically useful in the medical field, where high complexity, customization and patient specific necessities are typically required. Moreover, small production quantities are another of the main requirement of the biomedical market. For example in surgical applications, this technology is used to create a model which gives a better understanding of complex pathology and anatomy of the patient easily produces specific custom implants and patient-specific instruments which help surgeon during the surgery of the patient [101, 102]. In the orthopedic field the patient-specific analysis is essential to obtain an accurate medical imaging data of the individual patient. Magnetic resonance imaging (MRI), modern multi-row detector Computer Tomography (MDCT), Computer tomography (CT) scan, X-rays and 3D scanners provide an accurate, fast, high-resolution data and easily prepare a 3D view of patient's anatomy. AM convert the digital medical image into a 3D physical model. This conversion takes place in three steps as depicted in *Figure 17*.

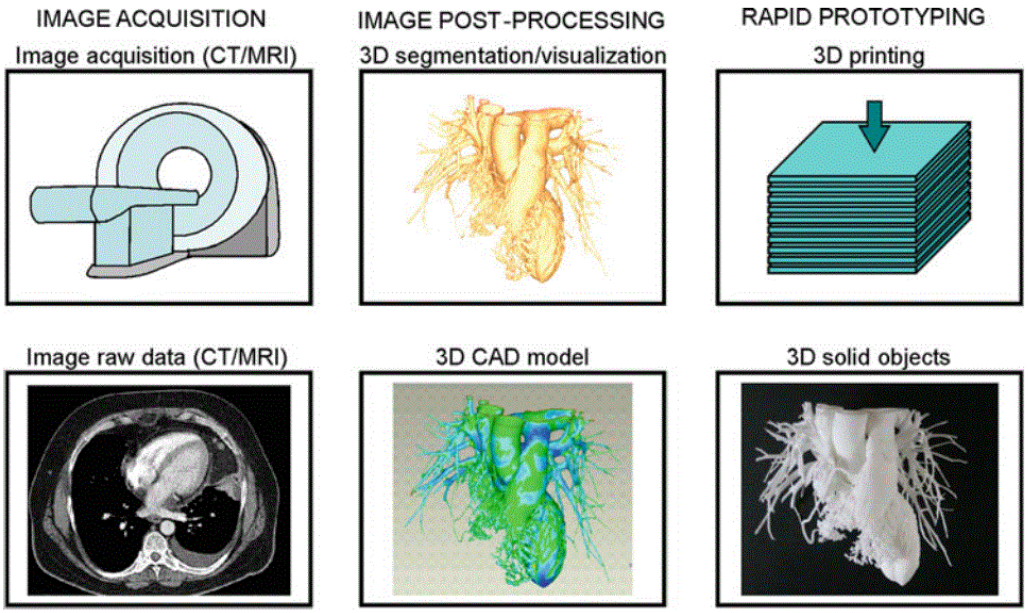

Figure 17 Overview of established step to convert medical imaging in 3D printed object

In the last decades, rapid prototyping has been used in a variety of medical applications including bioprinting of tissue, surgical planning and custom-made orthosis.

4.1.1 Custom made orthosis and prosthesis using AM

Orthoses and prostheses (O&P) are assistive devices that help people with disabilities. Orthoses, colloquially known as braces, support and modify the structural and functional characteristics of human neuromuscular and musculoskeletal systems. O&P can be either custom fabricated or prefabricated [103]. Prefabricated O&P are less expensive and are readily available as off-the shelf products.

Figure 18 Manufacturing processes for foot orthosis: (a) conventional and (b) AM[103].

However, custom O&P have better fit to the patient's body and perform better than the prefabricated O&P. Traditionally, custom O&P are manufactured using a labor intensive plaster molding technique as it will be discussed in the following chapter. In this scenario, the potential for AM has been demonstrated for rapid and cost-

effective fabrication and transformative service of the custom O&P. The traditional plaster molding technique to fabricate a custom orthosis is shown in *Figure 18a* and require several step from the measurement of the body segment to the creation of the positive model till the final shaping of the orthosis. The duration for traditional manufacturing of an orthosis usually takes about one week. In a central fabrication setting with technicians working three shifts, the manufacturing time of an orthosis can be shortened to one day. For AM of orthosis, as shown in *Figure 18b*, Step 1 is the 3D scanning of the body segment of the patient. In Step 2, the scan data is processed using a CAD software to obtain a suitable file for 3D printing machine. In Step 4, the path and support structure for AM of orthosis are designed. Finally, the orthosis is fabricated and ready for use.

Even if a number of research studies have been conducted for the application of AM in the design and fabrication of O&P, Several barriers need to be overcome in order to enable the adoption of AM in the orthotics and prosthetics industry. These barriers include: the lack of clinical and design interface for an AM system, uneconomic throughput and material cost, and limited material strength [104-107]

References

[1] U.A. Pozdnyakova, V.V. Golikov, I.A. Peters, I.A. Morozova, Genesis of the revolutionary transition to industry 4.0 in the 21st century and overview of previous industrial revolutions, Industry 4.0: Industrial Revolution of the 21st Century, Springer2019, pp. 11-19.
[2] Y. Yin, K.E. Stecke, D. Li, The evolution of production systems from Industry 2.0 through Industry 4.0, International Journal of Production Research 56(1-2) (2018) 848-861.
[3] P. Zawadzki, K. Żywicki, Smart product design and production control for effective mass customization in the Industry 4.0 concept, Management and Production Engineering Review 7(3) (2016) 105-112.
[4] U.M. Dilberoglu, B. Gharehpapagh, U. Yaman, M. Dolen, The role of additive manufacturing in the era of industry 4.0, Procedia Manufacturing 11 (2017) 545-554.
[5] B. Tjahjono, C. Esplugues, E. Ares, G. Pelaez, What does industry 4.0 mean to supply chain?, Procedia Manufacturing 13 (2017) 1175-1182.
[6] Y.A. Sukhodolov, The notion, essence, and peculiarities of industry 4.0 as a sphere of industry, Industry 4.0: Industrial Revolution of the 21st Century, Springer2019, pp. 3-10.
[7] H. Kagermann, W. Wahlster, J. Helbig, Securing the future of German manufacturing industry, Recommendations for implementing the strategic initiative INDUSTRIE 4(199) (2013) 14.
[8] L. Thames, D. Schaefer, Software-defined cloud manufacturing for industry 4.0, Procedia cirp 52 (2016) 12-17.
[9] D. Ivanov, A. Dolgui, B. Sokolov, F. Werner, M. Ivanova, A dynamic model and an algorithm for short-term supply chain scheduling in the smart factory industry 4.0, International Journal of Production Research 54(2) (2016) 386-402.
[10] J. Lee, B. Bagheri, H.-A. Kao, A cyber-physical systems architecture for industry 4.0-based manufacturing systems, Manufacturing letters 3 (2015) 18-23.
[11] M. Wollschlaeger, T. Sauter, J. Jasperneite, The future of industrial communication: Automation networks in the era of the internet of things and industry 4.0, IEEE industrial electronics magazine 11(1) (2017) 17-27.
[12] A. Gilchrist, Industry 4.0: the industrial internet of things, Apress2016.
[13] J. Lee, H.-A. Kao, S. Yang, Service innovation and smart analytics for industry 4.0 and big data environment, Procedia Cirp 16 (2014) 3-8.
[14] S. Wang, J. Wan, D. Zhang, D. Li, C. Zhang, Towards smart factory for industry 4.0: a self-organized multi-agent system with big data based feedback and coordination, Computer Networks 101 (2016) 158-168.
[15] F. Shrouf, J. Ordieres, G. Miragliotta, Smart factories in Industry 4.0: A review of the concept and of energy management approached in production based on the Internet of Things paradigm, 2014 IEEE international conference on industrial engineering and engineering management, IEEE, 2014, pp. 697-701.
[16] L. Wang, G. Wang, Big data in cyber-physical systems, digital manufacturing and industry 4.0, International Journal of Engineering and Manufacturing (IJEM) 6(4) (2016) 1-8.

[17] M.K. Thompson, G. Moroni, T. Vaneker, G. Fadel, R.I. Campbell, I. Gibson, A. Bernard, J. Schulz, P. Graf, B. Ahuja, Design for Additive Manufacturing: Trends, opportunities, considerations, and constraints, CIRP annals 65(2) (2016) 737-760.
[18] S. Singh, S. Ramakrishna, R. Singh, Material issues in additive manufacturing: A review, Journal of Manufacturing Processes 25 (2017) 185-200.
[19] D. Herzog, V. Seyda, E. Wycisk, C. Emmelmann, Additive manufacturing of metals, Acta Materialia 117 (2016) 371-392.
[20] A.T.C.C. Finance, Industry 4.0 Challenges and solutions for the digital transformation and use of exponential technologies, Finance, Audit Tax Consulting Corporate: Zurich, Swiss (2015).
[21] S.M.L. Coalition, Implementing 21st century smart manufacturing, Workshop summary report, 2011.
[22] M.E. Porter, J.E. Heppelmann, How smart, connected products are transforming competition, Harvard business review 92(11) (2014) 64-88.
[23] M.E. Porter, J.E. Heppelmann, How smart, connected products are transforming companies, Harvard business review 93(10) (2015) 96-114.
[24] F. Almada-Lobo, The Industry 4.0 revolution and the future of Manufacturing Execution Systems (MES), Journal of innovation management 3(4) (2015) 16-21.
[25] B.G. Rüttimann, M.T. Stöckli, Lean and industry 4.0—Twins, partners, or contenders? A due clarification regarding the supposed clash of two production systems, Journal of Service Science and Management 9(6) (2016) 485-500.
[26] R. Geissbauer, J. Vedsø, S. Schrauf, A Strategist's Guide to Industry 4.0: Global businesses are about to integrate their operations into a seamless digital whole, and thereby change the world, Strategy and Business (2016).
[27] M. Brettel, N. Friederichsen, M. Keller, M. Rosenberg, How virtualization, decentralization and network building change the manufacturing landscape: An Industry 4.0 Perspective, International journal of mechanical, industrial science and engineering 8(1) (2014) 37-44.
[28] L.D. Xu, E.L. Xu, L. Li, Industry 4.0: state of the art and future trends, International Journal of Production Research 56(8) (2018) 2941-2962.
[29] R. Strange, A. Zucchella, Industry 4.0, global value chains and international business, Multinational Business Review 25(3) (2017) 174-184.
[30] G. Da Silveira, D. Borenstein, F.S. Fogliatto, Mass customization: Literature review and research directions, International journal of production economics 72(1) (2001) 1-13.
[31] F.S. Fogliatto, G.J. Da Silveira, D. Borenstein, The mass customization decade: An updated review of the literature, International Journal of production economics 138(1) (2012) 14-25.
[32] B.J. Pine, J. Pine, B.J.I. Pine, Mass customization: the new frontier in business competition, Harvard business press1993.
[33] S.J. Hu, J. Ko, L. Weyand, H.A. ElMaraghy, T.K. Lien, Y. Koren, H. Bley, G. Chryssolouris, N. Nasr, M. Shpitalni, Assembly system design and operations for product variety, CIRP annals 60(2) (2011) 715-733.
[34] A. Wards, Wards Automotive Yearbook, Wards Communications, Inc., Detroit, MI, 1970.

[35] W. Hopp, J., Spearman, ML: Factory Physics, Mcgraw-Hill Publ. Comp, 2001.
[36] N. Koleva, Industry 4.0's opportunities and challenges for production engineering and managemnet, Innovations 6(1) (2018) 17-18.
[37] B. Garrett, 3D printing: new economic paradigms and strategic shifts, Global Policy 5(1) (2014) 70-75.
[38] Y. Long, J. Pan, Q. Zhang, Y. Hao, 3D printing technology and its impact on Chinese manufacturing, International Journal of Production Research 55(5) (2017) 1488-1497.
[39] T. Campbell, C. Williams, O. Ivanova, B. Garrett, Could 3D printing change the world, Technologies, Potential, and Implications of Additive Manufacturing, Atlantic Council, Washington, DC 3 (2011).
[40] I. Gibson, D.W. Rosen, B. Stucker, Additive manufacturing technologies, Springer2014.
[41] J. Gardan, Additive manufacturing technologies: state of the art and trends, International Journal of Production Research 54(10) (2016) 3118-3132.
[42] M. Baumers, P. Dickens, C. Tuck, R. Hague, The cost of additive manufacturing: machine productivity, economies of scale and technology-push, Technological forecasting and social change 102 (2016) 193-201.
[43] K.V. Wong, A. Hernandez, A review of additive manufacturing, ISRN Mechanical Engineering 2012 (2012).
[44] S. Mohr, O. Khan, 3D printing and its disruptive impacts on supply chains of the future, Technology Innovation Management Review 5(11) (2015) 20.
[45] K. Pierrakakis, C.D. Gkritzali, M. Kandias, D. Gritzalis, 3D printing: a paradigm shift in political economy, Proc. of the 65th International Studies Association's Annual Convention, Citeseer, 2015.
[46] X. Yao, Y. Lin, Emerging manufacturing paradigm shifts for the incoming industrial revolution, The International Journal of Advanced Manufacturing Technology 85(5-8) (2016) 1665-1676.
[47] D. Bak, Rapid prototyping or rapid production? 3D printing processes move industry towards the latter, Assembly Automation 23(4) (2003) 340-345.
[48] C. McAlister, J. Wood, The potential of 3D printing to reduce the environmental impacts of production, Proceeding of the ECEEE (2014) 213-221.
[49] P. Reeves, Additive Manufacturing–A supply chain wide response to economic uncertainty and environmental sustainability, Econolyst Limited, The Silversmiths, Crown Yard, Wirksworth, Derbyshire, DE4 4ET, UK (2009).
[50] N. Guo, M.C. Leu, Additive manufacturing: technology, applications and research needs, Frontiers of Mechanical Engineering 8(3) (2013) 215-243.
[51] I. Gibson, D. Rosen, B. Stucker, Development of additive manufacturing technology, Additive manufacturing technologies, Springer2015, pp. 19-42.
[52] S.F.S. Shirazi, S. Gharehkhani, M. Mehrali, H. Yarmand, H.S.C. Metselaar, N.A. Kadri, N.A.A. Osman, A review on powder-based additive manufacturing for tissue engineering: selective laser sintering and inkjet 3D printing, Science and technology of advanced materials 16(3) (2015) 033502.

[53] C.Y. Yap, C.K. Chua, Z.L. Dong, Z.H. Liu, D.Q. Zhang, L.E. Loh, S.L. Sing, Review of selective laser melting: Materials and applications, Applied physics reviews 2(4) (2015) 041101.
[54] T. Wohlers, T. Caffrey, Wohlers Report 2014 Annual Worldwide Progress Report. Wohlers Associates, Inc. Fort Collins, CO (2014).
[55] E. Sells, S. Bailard, Z. Smith, A. Bowyer, V. Olliver, RepRap: the replicating rapid prototyper: maximizing customizability by breeding the means of production, Handbook of Research in Mass Customization and Personalization: (In 2 Volumes), World Scientific2010, pp. 568-580.
[56] E. Malone, H. Lipson, Fab@ Home: the personal desktop fabricator kit, Rapid Prototyping Journal 13(4) (2007) 245-255.
[57] R. Noorani, Rapid prototyping: principles and applications, (2006).
[58] J. Flowers, M. Moniz, Rapid prototyping in technology education: rapid prototyping, while costly, can afford students a unique opportunity to bring their ideas to reality, The Technology Teacher 62(3) (2002) 7-12.
[59] C.K. Chua, S.M. Chou, S.C. Lin, K.H. Eu, K.F. Lew, Rapid prototyping assisted surgery planning, The International Journal of Advanced Manufacturing Technology 14(9) (1998) 624-630.
[60] D.L. Bourell, D.W. Rosen, M.C. Leu, The roadmap for additive manufacturing and its impact, 3D Printing and Additive Manufacturing 1(1) (2014) 6-9.
[61] I. Campbell, D. Bourell, I. Gibson, Additive manufacturing: rapid prototyping comes of age, Rapid prototyping journal 18(4) (2012) 255-258.
[62] J.-P. Kruth, M.-C. Leu, T. Nakagawa, Progress in additive manufacturing and rapid prototyping, Cirp Annals 47(2) (1998) 525-540.
[63] M. Burns, Automated fabrication: improving productivity in manufacturing, (1993).
[64] C.K. Chua, K.F. Leong, C.S. Lim, Liquid-based rapid prototyping systems, Rapid Prototyping: Principles & Applications in Manufacturing, Wiley, New York, NY (1998).
[65] D.T. Pham, R.S. Gault, A comparison of rapid prototyping technologies, International Journal of machine tools and manufacture 38(10-11) (1998) 1257-1287.
[66] P. Bartolo, G. Mitchell, Stereo-thermal-lithography: a new principle for rapid prototyping, Rapid Prototyping Journal (2003).
[67] P.F. Jacobs, Fundamentals of stereolithography, 1992 International Solid Freeform Fabrication Symposium, 1992.
[68] S. Waheed, J.M. Cabot, N.P. Macdonald, T. Lewis, R.M. Guijt, B. Paull, M.C. Breadmore, 3D printed microfluidic devices: enablers and barriers, Lab on a Chip 16(11) (2016) 1993-2013.
[69] A. Ronca, L. Ambrosio, D.W. Grijpma, Design of porous three-dimensional PDLLA/nano-hap composite scaffolds using stereolithography, Journal of applied biomaterials & functional materials 10(3) (2012) 249-258.
[70] A. Ronca, L. Ambrosio, D.W. Grijpma, Preparation of designed poly (D, L-lactide)/nanosized hydroxyapatite composite structures by stereolithography, Acta biomaterialia 9(4) (2013) 5989-5996.
[71] F.P. Melchels, J. Feijen, D.W. Grijpma, A review on stereolithography and its applications in biomedical engineering, Biomaterials 31(24) (2010) 6121-6130.

[72] R.F. Pereira, P.J. Bártolo, Photocrosslinkable materials for the fabrication of tissue-engineered constructs by stereolithography, Tissue engineering, Springer2014, pp. 149-178.
[73] Y. Lu, G. Mapili, G. Suhali, S. Chen, K. Roy, A digital micro-mirror device-based system for the microfabrication of complex, spatially patterned tissue engineering scaffolds, Journal of Biomedical Materials Research Part A: An Official Journal of The Society for Biomaterials, The Japanese Society for Biomaterials, and The Australian Society for Biomaterials and the Korean Society for Biomaterials 77(2) (2006) 396-405.
[74] K. Ikuta, S. Maruo, T. Fujisawa, A. Yamada, Micro concentrator with opto-sense micro reactor for biochemical IC chip family. 3D composite structure and experimental verification, Technical Digest. IEEE International MEMS 99 Conference. Twelfth IEEE International Conference on Micro Electro Mechanical Systems (Cat. No. 99CH36291), IEEE, 1999, pp. 376-381.
[75] K. Kobayashi, K. Ikuta, Development of free-surface microstereolithography with ultra-high resolution to fabricate hybrid 3-D microdevices, IEEE International Symposium on Micro-NanoMechatronics and Human Science, 2005, IEEE, 2005, pp. 273-278.
[76] S. Maruo, K. Ikuta, Submicron stereolithography for the production of freely movable mechanisms by using single-photon polymerization, Sensors and Actuators A: Physical 100(1) (2002) 70-76.
[77] A. Bertsch, S. Jiguet, P. Bernhard, P. Renaud, Microstereolithography: a review, MRS Online Proceedings Library Archive 758 (2002).
[78] S. Maruo, O. Nakamura, S. Kawata, Three-dimensional microfabrication with two-photon-absorbed photopolymerization, Optics letters 22(2) (1997) 132-134.
[79] L.P.C. Gomez, A. Spangenberg, X.A. Ton, Y. Fuchs, F. Bokeloh, J.P. Malval, B. Tse Sum Bui, D. Thuau, C. Ayela, K. Haupt, Rapid Prototyping of Chemical Microsensors Based on Molecularly Imprinted Polymers Synthesized by Two-Photon Stereolithography, Advanced Materials 28(28) (2016) 5931-5937.
[80] B. Mueller, Additive manufacturing technologies–Rapid prototyping to direct digital manufacturing, Assembly Automation 32(2) (2012).
[81] H. Lee, C.H.J. Lim, M.J. Low, N. Tham, V.M. Murukeshan, Y.-J. Kim, Lasers in additive manufacturing: A review, International Journal of Precision Engineering and Manufacturing-Green Technology 4(3) (2017) 307-322.
[82] J.-P. Kruth, X. Wang, T. Laoui, L. Froyen, Lasers and materials in selective laser sintering, Assembly Automation (2003).
[83] K. Zeng, D. Pal, B. Stucker, A review of thermal analysis methods in laser sintering and selective laser melting, Proceedings of Solid Freeform Fabrication Symposium Austin, TX, 2012, pp. 796-814.
[84] C. Kullmann, N.C. Schirmer, M.-T. Lee, S.H. Ko, N. Hotz, C.P. Grigoropoulos, D. Poulikakos, 3D micro-structures by piezoelectric inkjet printing of gold nanofluids, Journal of Micromechanics and Microengineering 22(5) (2012) 055022.
[85] T. Wohlers, T. Gornet, History of additive manufacturing, Wohlers report 24(2014) (2014) 118.
[86] S. Au, P.K. Wright, Comparative study of rapid prototyping technology, ASME DES ENG DIV PUBL DE, ASME, NEW YORK, NY,(USA), 1993 66 (1993) 73-82.

[87] S. Upcraft, R. Fletcher, The rapid prototyping technologies, Assembly Automation 23(4) (2003) 318-330.
[88] R. Singh, Process capability analysis of fused deposition modelling for plastic components, Rapid Prototyping Journal 20(1) (2014) 69-76.
[89] W. Harun, S. Sharif, M. Idris, K. Kadirgama, Characteristic studies of collapsibility of ABS patterns produced from FDM for investment casting, Materials Research Innovations 13(3) (2009) 340-343.
[90] S. Masood, W. Song, Development of new metal/polymer materials for rapid tooling using fused deposition modelling, Materials & design 25(7) (2004) 587-594.
[91] A. Salem Bala, S. bin Wahab, Elements and materials improve the FDM products: A review, Advanced Engineering Forum, Trans Tech Publ, 2016, pp. 33-51.
[92] Y. Iwai, T. Honda, T. Miyajima, Y. Iwasaki, M. Surappa, J. Xu, Dry sliding wear behavior of Al2O3 fiber reinforced aluminum composites, Composites science and technology 60(9) (2000) 1781-1789.
[93] M. Ahlhelm, P. Günther, U. Scheithauer, E. Schwarzer, A. Günther, T. Slawik, T. Moritz, A. Michaelis, Innovative and novel manufacturing methods of ceramics and metal-ceramic composites for biomedical applications, Journal of the European Ceramic Society 36(12) (2016) 2883-2888.
[94] F.P. Melchels, M.A. Domingos, T.J. Klein, J. Malda, P.J. Bartolo, D.W. Hutmacher, Additive manufacturing of tissues and organs, Progress in Polymer Science 37(8) (2012) 1079-1104.
[95] H. Chim, D. Hutmacher, A. Chou, A. Oliveira, R. Reis, T.C. Lim, J.-T. Schantz, A comparative analysis of scaffold material modifications for load-bearing applications in bone tissue engineering, International journal of oral and maxillofacial surgery 35(10) (2006) 928-934.
[96] N. Mohan, P. Senthil, S. Vinodh, N. Jayanth, A review on composite materials and process parameters optimisation for the fused deposition modelling process, Virtual and Physical Prototyping 12(1) (2017) 47-59.
[97] T.D. Ngo, A. Kashani, G. Imbalzano, K.T. Nguyen, D. Hui, Additive manufacturing (3D printing): A review of materials, methods, applications and challenges, Composites Part B: Engineering 143 (2018) 172-196.
[98] T. Wohlers, Wohlers Report 2017 3D Printing and Additive Manufacturing State of the Industry Annual Worldwide Progress Report. Wohlers Associates, Inc., Fort Collins, Colorado, USA, 2017.
[99] R.I. Campbell, H. Jee, Y.S. Kim, Adding product value through additive manufacturing, © The Design Society, 2013.
[100] M. Javaid, A. Haleem, Additive manufacturing applications in orthopaedics: a review, Journal of clinical orthopaedics and trauma 9(3) (2018) 202-206.
[101] L. Kumar, Q. Tanveer, V. Kumar, M. Javaid, A. Haleem, Developing low cost 3 D printer, Int J Appl Sci Eng Res 5(6) (2016) 433-447.
[102] J.W. Choi, N. Kim, Clinical application of three-dimensional printing technology in craniofacial plastic surgery, Archives of plastic surgery 42(3) (2015) 267.
[103] R.K. Chen, Y.-a. Jin, J. Wensman, A. Shih, Additive manufacturing of custom orthoses and prostheses—a review, Additive Manufacturing 12 (2016) 77-89.

[104] L.H. Hsu, G. Huang, C. Lu, D. Hong, S. Liu, The development of a rapid prototyping prosthetic socket coated with a resin layer for transtibial amputees, Prosthetics and orthotics international 34(1) (2010) 37-45.
[105] N. Herbert, D. Simpson, W.D. Spence, W. Ion, A preliminary investigation into the development of 3-D printing of prosthetic sockets, Journal of rehabilitation research and development 42(2) (2005) 141.
[106] A.S. Salles, D.E. Gyi, Delivering personalised insoles to the high street using additive manufacturing, International Journal of Computer Integrated Manufacturing 26(5) (2013) 386-400.
[107] J. Pallari, K. Dalgarno, J. Munguia, L. Muraru, L. Peeraer, S. Telfer, J. Woodburn, Design and additive fabrication of foot and ankle-foot orthoses, Proceedings of the 21st Annual International Solid Freeform Fabrication Symposium–An Additive Manufacturing Conference, 2010, pp. 9-11.

Chapter 2
Back brace for scoliosis

1. INTRODUCTION

The term *scoliosis* derives from the Greek word σκολιος that means curvature. In Orthopaedics, it indicates a lateral curvature of the spine, which, normally, when viewed from the front or back, doesn't show any lateral deviation [1, 2]. Scoliosis is a sideways curvature of the spine that occurs most often during the growth spurt just before puberty [1, 3]. Even if scoliosis can be caused by conditions such as cerebral palsy and muscular dystrophy, the cause of most scoliosis is unknown and about 3% of adolescents have scoliosis.

The many causes of scoliosis include neuromuscular problems, and inherited diseases or conditions caused by the environment. An estimated 65% of scoliosis cases are idiopathic, about 15% are congenital, and 10% are secondary to neuromuscular disease [4]. The prevalence of scoliosis in early childhood is about 1–2% [5], among adolescents it reaches about 5% [6] and it has been shown to spread out in elder subjects [7].

Most cases of scoliosis are mild, but some spine deformities continue to get more severe as children grow. Severe scoliosis can be disabling. An especially severe spinal curve can reduce the amount of space within the chest, making it difficult for the lungs to function properly [8].

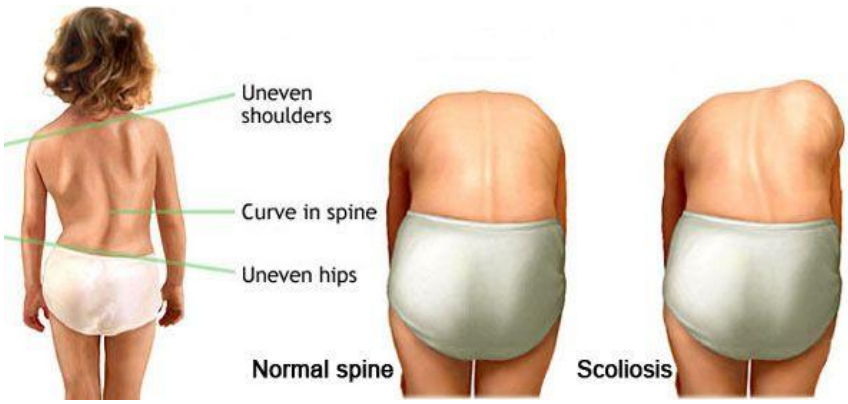

Figure 19 Example of idiopathic scoliosis

Idiopathic scoliosis represents a majority of cases, but its causes are largely unknown. Recent studies indicate potential heritability of the disorder. About 38% of variance in scoliosis risk is due to genetic factors while 62% is due to the

environment. The circumstances of discovery of scoliosis are multiple. Screening must be done during visits to the paediatrician, the general practitioner, during a visit from school medicine or on the occasion of a fitness test.
Scoliosis can also be discovered by the child or his family because of body morphological changes (mostly observed in summer during bathing activities).
Screening for scoliosis is based on the search for morphological abnormalities of the trunk, testifying to the torsion spinal. Scoliosis can generate asymmetries (height shoulders, positioning shoulder blades, waist fold), and especially the presence of a gibbosity, witness of the rotation vertebral torsion and trunk torsion (*Figure 19*). The existence of a gibbosity allows the diagnostic distinction between scoliosis and the scoliosis attitude [9].
Back braces for the correction of curvature of the spine (scoliosis) have been known for more than a hundred years [10]. Children who have mild scoliosis are monitored closely, usually with X-rays, to see if the curve is getting worse. In many cases, no treatment is necessary [8, 11]. Some children will need to wear a brace to stop the curve from worsening. Others may need surgery to keep the scoliosis from worsening and to straighten severe cases of scoliosis [12]. Orthotic treatment in adolescent idiopathic scoliosis is used to manage or even reduce spinal curvatures while waiting for skeletal maturation. By applying specific pressure points on the torso, the brace treatment attempts to modify mechanically the scoliotic spine shape and control progression of the spinal curvature [13]. The efficacy of bracing for the treatment for idiopathic scoliosis is controversial, with some authors reporting control of curve progression with bracing [14-16] and others reporting that bracing fails to alter the natural history [2, 17]. Currently, the main problems related to the use of traditional aids for postural support and correction of musculoskeletal deformities consist in the high stiffness and weight and the reduced transpiration of these systems, often causing irritation of the parts of the body in contact, lack of comfort and low acceptance by patients. The objective of the this chapter is to give an overview of the current state of the art about the realization of back brace for scoliosis with an introduction of the innovative approach that will be proposed in this thesis that combine innovative materials and 3D printing techniques.

2. SCOLIOSIS

Scoliosis is defined as a lateral curve of the spine whit fixed rotation and permanent deformation of the vertebrae. More precisely, scoliosis is a deformity of the spine

in all three space's planes: frontal plane (lateral curvature), horizontal plane (rotation of the vertebrae) and sagittal plane (deformity in lordosis or kyphosis) [1, 3]. On the contrary, the true scoliotic curves are structural, characterized by distorted vertebrae with the body shifted toward the convex side of the thorax; moreover, the segment of spine with scoliotic curve shows a lack of normal flexibility [18, 19]. So the vertebral column can be defined as an elastic supporting structure, consisting of a series of semi-rigid bodies, the vertebrae, supported and constrained by visco-elastic elements; the ligaments and disks represent the intrinsic constraints, while the muscles, the rib cage and the abdominal cavity represent the extrinsic ones [20]. The transverse variations of the spine are called scoliosis (*Figure 20*) and can be functional or structural.

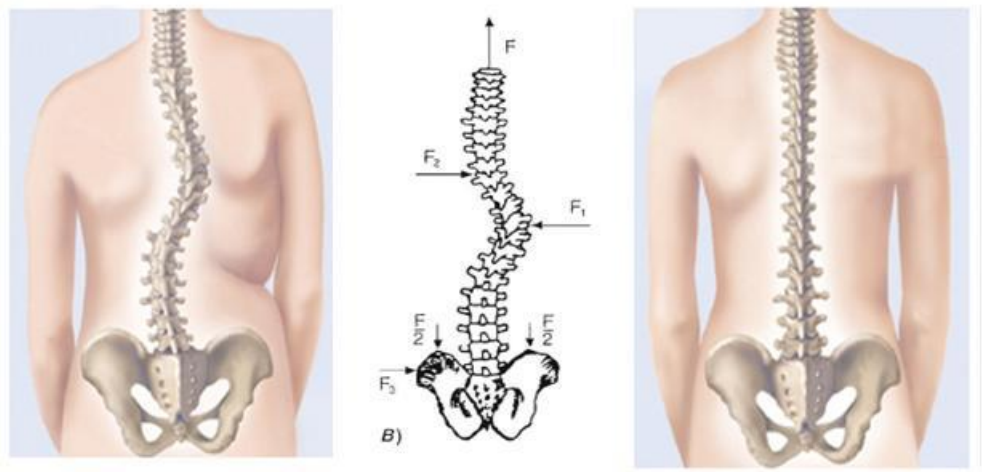

Figure 20 Representation of the forces to be applied for the correction of the scoliotic back

According to etiology, the scoliosis can be distinguished into two principal forms: congenital scoliosis and acquired scoliosis [21]. The congenital scoliosis reflects anomalous development in utero and are due to congenital abnormalities, such as failure of formation (wedge, hemivertebrae), failure of segmentation (unilateral bar, fusion), myelomeningocele, meningocele, spinal dysraphism [1, 22]. The acquired form must be divided into two groups: a) secondary scoliosis (or of known etiology), due to neuromuscular (poliomyelitis), myopathic, mesenchymal, metabolic, nutritional and endocrine disorders, traumatic causes (such as fracture or dislocation, deformities following thoracoplasty, neurofibromatosis, osteochondrodystrophies), Sheuermann's disease, Marfan's disease, Ehlers-Danlos disease, infection, tumour (cord tumours), syringomyelia and rheumatoid diseases); b) idiopathic scoliosis (of unknown etiology). The lateral deviations of the spine

are divided into functional scoliosis and structural scoliosis [23, 24]. The former, to be preferably defined as “scoliotic attitudes” to differentiate them from structural scoliosis, develop only in the antero-posterior plane and disappear in a built-in position; moreover, they do not involve morphological alterations of the vertebrae and do not possess evolutionary characteristics [25]. Functional scoliosis, therefore, does not represent a segmentary pathology, but rather a global phenomenon that is expressed in the central nervous system and, more precisely, in the centers of posture and balance. For this reason, it is good to call these deviations “primitive scoliotic attitudes”. In other circumstances, they are characterized by phenomena of compensation for longitudinal heterometries of the lower limbs or by pathologies of various types but not necessarily related to the spine. Scoliotic attitudes are, in general, self-resolving and the treatment, if the indication exists, is addressed not so much to the spine as to the triggering causes [26].
The structural scoliosis, to which reference must be made when adopting the term “scoliosis”, have, instead, a three-dimensional development, do not disappear in the discharge phase, involve morphological alterations of the vertebrae, of the disks, of the capsuloligamentous structures and of the rib cage. These alterations give the deviation the typical characteristics of rigidity and evolution [20]. Idiopathic scoliosis, in the absence of a treatment specific, can worsen until the achievement of bone maturity.

2.1 Idiopathic scoliosis

The idiopathic scoliosis is the most common of all forms of scoliosis and accounts for 80-90 per cent of cases. In this form of scoliosis, the deformity consists of lateral deviation of the spine with rotation of the vertebrae [1, 25]. Frequently, a single major curve is observed, accompanied by one or two compensatory curves that compensate for the spinal vertical alignment. It occurs during the growing years.
The idiopathic scoliosis is classified according to location, age at on set and magnitude. According to location, the curves are described in relation to the position of the end vertebrae and the apical vertebra *Figure 21*.

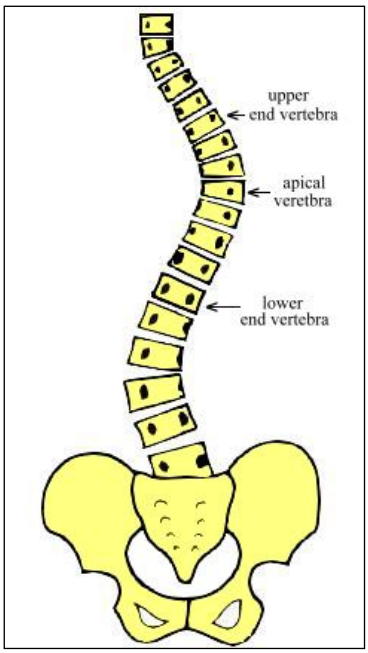

Figure 21 End vertebrae and apical vertebra are shown. See in the page for legend

The idiopathic scoliosis have been classified by Ponseti and Friedman into five classes [26, 27]. *Cervicothoracic*: the apical vertebra is T3, the upper end vertebra C7 or T1 and the lower end vertebra T4 or T5. *Thoracic*: the apical vertebra is T8 or T9, the upper end vertebra at T6 or T7 and the lower end vertebra at T11 or T12. *Thoracolumbar*: the apex is T11 or T12, the upper end vertebra at T6 or T7 and the lower end vertebra at L1 or L2. *Lumbar*: the apex is L1 or L2, the upper end vertebra at L11 or L12 or T1 and the lower end vertebra at L4 or L5. *Combined thoracic and lumbar*: the thoracic curve has its apex at T6 or T7, the lumbar curve has its apex at L2 [27]. The degree of vertebral rotation is estimated by the position of the shadows of the pedicles and is classified into four grades [28]. Zero rotation: the pedicle shadows are equidistant from the sides of the vertebral bodies. Grade I rotation: the pedicle shadow on the convexity has moved from the edge of the vertebral body. Grade II rotation: rotation intermediate between Grade I and Grade III. Grade III: the pedicle shadow is close to the centre of the vertebral body; Grade IV: the pedicle shadow is past the centre of the vertebral body.

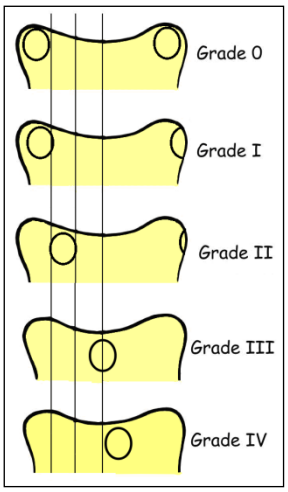

Figure 22 Schema of the 5 degrees of vertebral rotation

Once the curve and the end vertebrae have been identified, the magnitude and extent of each curve is determined by Cobb-Lippman technique of measurement [29]. The angle of the scoliotic curve is formed between two lines: a line is drawn at the upper end of the cranial end vertebra along the end-plate (or by marking the upper or lower edges of the pedicle shadows). A second line is drawn at the lower end of the caudal vertebra at the inferior end-plate of the body (or the lower end of the pedicle shadows). The angle is formed between two lines drawn at right angle to the two-end vertebral lines (*Figure 22*).

The idiopathic scoliosis is a structural, lateral, rotated curvature of the spine that arises in otherwise healthy children at or around puberty (*Figure 23*) [25]. The diagnosis is one of exclusion and is made only when other causes of scoliosis, such as vertebral malformation, neuromuscular disorder, and syndromic disorders, have been ruled out. The aetiopathogensis of this disorder remains unknown, with misinformation about its natural history [27]. Non-surgical treatments are aimed to reduce the number of operations by preventing curve progression. Although bracing and physiotherapy are common treatments in much of the world, their effectiveness has never been rigorously assessed. Technological advances have much improved the ability of surgeons to safely correct the deformity while maintaining sagittal and coronal balance. However, we do not have long-term results of these changing surgical treatments [30].

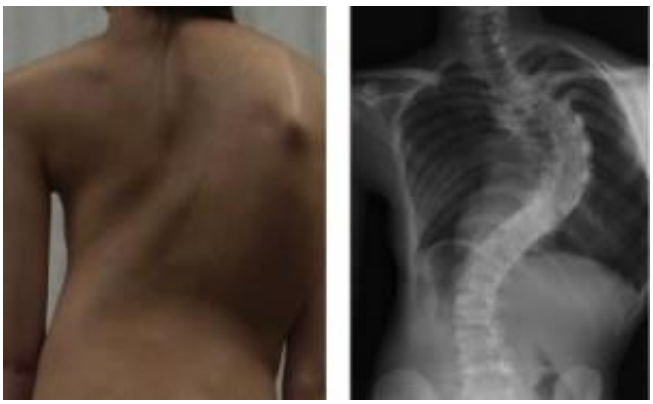

Figure 23 Idiopathic scoliosis

Non-operative treatment includes the use of different type of brace, in relation to the age and the location of the curve. Brace treatment of scoliosis remains the only widely accepted and documented affective non-operative treatment of progressive idiopathic scoliosis [2, 31-34]. The size of the curve tends to increase over the entire lifetime, but the degree of progression over a lifetime and the time-at-risk varies with many factors. Clinicians and patients need to be aware of the risk of curve progression as they make treatment decisions. Factors predicting curve progression include maturity (age at diagnosis, menarchal status, and the amount of skeletal growth remaining), curve size, and position of the curve apex [30].

Besides the degree of lateral curvature, other factors such as high degrees of thoracic lordosis and vertebral rotation and decreased respiratory muscle strength affect pulmonary function. Unlike early onset (age 0–8 years) idiopathic scoliosis, in which substantial loss of vital capacity and forced expiratory volume in first could cause pulmonary hypertension, right heart failure, and death, these problems rarely arise in AIS. Large curves (greater than 50°) with a thoracic apex have been associated with reduced vital capacity and more frequently with shortness of breath and severe cardiopulmonary disease.

The age at onset is the age at which the deformity is first noted, which is not necessary the same as the time the curvature appears. Anyway, according to the age at onset, the idiopathic scoliosis is classified into 5 groups: 1) scoliosis of the new-born (from 1 month old to 12 months); 2) infantile (from 1 years old to 3 years); 3) juvenile from 4 years old to onset of puberty (according to Stagnara approach, we divide this stage into three subgroups: juvenile I: from 4 to 7 years old; juvenile II: from 8 to 10 years old; juvenile III: from 11 years old to onset of puberty [35]); 4) adolescent (from puberty to 18 years old); 5) adult (after 18 years old).

It is known that scoliosis appearing later in adolescence usually has a better prognosis; in fact, the curvature ceases to progress about 1 year before complete ossification. A rapid increase in the curve on serial radiographs has a poor prognostic significance. Fortunately, only 5 to 10 per cent of idiopathic curves become severe enough to require surgical treatment [36]. In general, the earlier the onset, the worse the prognosis, because the idiopathic scoliosis develops during the growing years; so a scoliotic curve that appears during infantile age can increase much more than one appearing during adolescent age. Nevertheless, a large number of new-born scoliosis disappears spontaneously without treatment; these are the typical self-resolving idiopathic curves. This spontaneous resolution of the curve is noted less often in juvenile and adolescent curves.
When the scoliosis started after ten years of age, the increase was gradual in most of the patients [37]. The prognosis could often be evaluated after two or three successive examinations, taken at intervals of three months. If there is the increase of the curve, the prognosis was usually poor. On the other hand, if there was only a minor progression of the curve during this period of observation, the prognosis was much better. When the scoliosis started in children under ten years of age, it often did not increase much for a few years and then increase suddenly. This scoliosis of early onset usually carried a poor prognosis, in spite of its slow increase during the first years, for this reason it is important to act soon [38].

2.2 Osteogenesis Imperfecta

Osteogenesis imperfect (OI) is characterised by fragility of skeletal bones [39]. The cause is unknown. Cases may be grouped as pre-natal and post-natal, but there is no clear-cut distinction between the two groups except in the date of the first fracture that depends upon the severity of the disorder. Pre-natal cases are on the average decidedly more severe; many die at birth or survive only a few days or weeks. The exact proportion of surviving to fatal cases is unknown. A child may sometimes survive several months despite birth fractures of many ribs [40].
“Osteogenesis imperfecta tarda” is the term often applied to the occurrence delay of the first fracture. The scoliosis caused by this disease will be studied for the thesis project [41]. The prevalence of scoliosis in association with OI is high [42]. Progression rates of scoliosis in children with OI are variable, depending on the Sillence type of osteogenesis imperfecta [43].
Curves develop early (age five to six) and generally progress rapidly (*Figure 24*). Early bracing, although somewhat effective, may well compress the soft osteoporotic rib cage without controlling the spinal curvature.

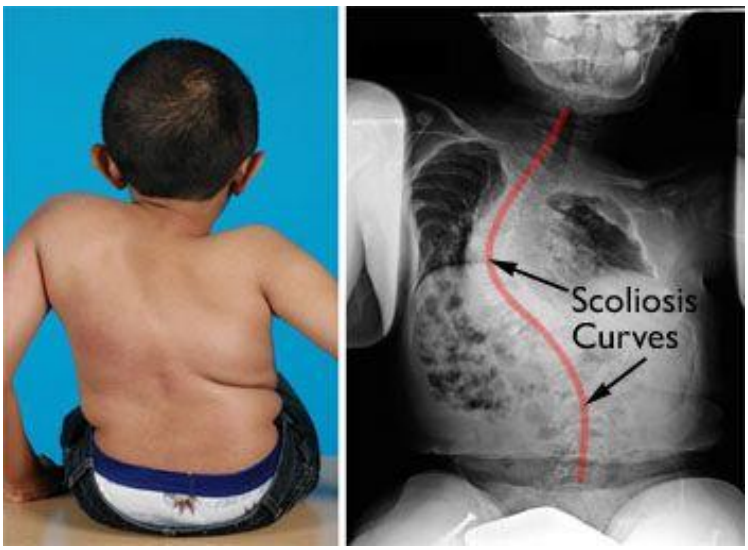

Figure 24 Osteogenesis imperfecta

The pulmonary compromise created by the scoliosis is compounded by the chest cage deformity secondary to bracing. In the patient with severe disease (thin bones and numerous fractures), posterior correction and fusion, with or without Harrington instrumentation is the preferred approach. This should be done early, as the osteoporotic bone does not tolerate the hook forces well; the correction is correspondingly limited. The use of methylmethacrylate bone cement around the hook provides redistribution of forces and more stable fixation. In the patient with mild disease (thick bones and few fractures), treatment should be similar to that of patients with idiopathic scoliosis. The chest cage should be carefully observed to avoid deformity from placement of the lateral or posterior pad.

2.3 Treatments for scoliosis

The main index for establishing if a person has scoliosis is the deformation on the frontal plane, whose severity is defined by the Cobb angle, i.e. the maximum angle between the vertebrae, as depicted in *Figure 25*.

Choosing the most suitable treatment for scoliosis relies heavily on accurate and reproducible Cobb angle measurement from successive radiographs. The objective is to reduce variability of Cobb angle measurement by reducing user intervention and bias. Custom software to increase automation of the Cobb angle measurement from posteroanterior radiographs was developed using active shape models [44].

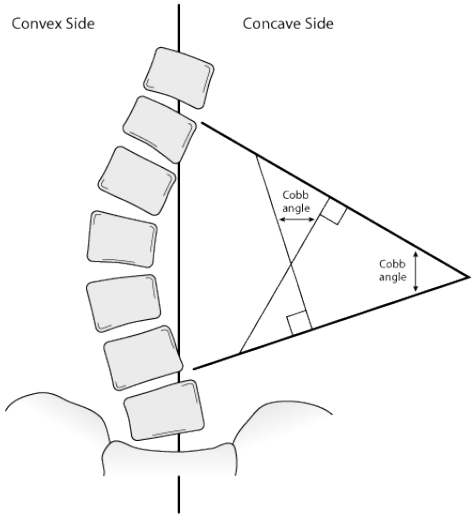

Figure 25 Cobb's angle

We can thus distinguish between mild scoliosis, when the Cobb angle is below 25°, moderate scoliosis if it is between 25° and 45°–50°, and severe scoliosis if above [7, 45]. The recommended treatments for moderate-sized scoliosis, especially for pre-adolescent children, involve close visits to control the degree of scoliosis and the practice of corrective gymnastics [25, 46, 47]. In the case of medium/high grade scoliosis, it is necessary instead to provide a brace such as the corrective back brace that is made to measure on the patient. Only for very high grade scoliosis is a surgical operation called spinal fusion [48].

Figure 26 Treatments for the cure of scoliosis: (from left to right) corrective gymnastics, back brace, surgical operation.

The typical treatment for mild and moderate scoliosis is based on physical exercise, both for stretching and for strengthening the muscles, and on the use of an external orthosis, called back brace (*Figure 26*).

There exist different versions and models of this orthotic device, from the very rigid and old Milwaukee brace, to the newest and extremely soft SpineCor as will be described in the next paragraphs. The correction is produced by passive

response to the forces applied by the brace; or brace-wearing engenders active contractions of trunk muscles, and those muscle forces correct the scoliosis (Figure 20) [49].

The purpose of orthoses is to act mechanically on an injured spine, either by modifying its dynamic nature with external constraints or by favoring a better distribution of loads in order to avoid a concentration of tensions. Since a stress cannot, for anatomical reasons, be exerted directly on the vertebral column, the orthosis must act, through interposed tissues and organs, through appropriately selected constraints and pressure points, such as to condition the type and extent of the desired forces, at the site of the injury [50].

The expectation of treatment with bracing is to prevent progression of the curve until the patient reaches skeletal maturity, at which time the risk of curve progression (and hence the risk of surgery) greatly diminishes. This type of device, in most cases, consists of very rigid structures in thermoplastic polymer, which to be truly effective must be worn continuously for many hours a day. The use of these braces can be prescribed at any age, from the newborn to the elderly and concerns a very wide range of pathologies. The aim is generally to impose a correct body position, recovering the normal functions of the interested parties. In some cases, when properly worn, these systems can guarantee the right blood circulation and help the patient's normal breathing [51].

Distinctive features of these aids are represented by efficiency, simplicity of use and the possibility of combining the rehabilitation of the musculoskeletal system with the cardio-respiratory system care methods. Unfortunately, the high stiffness, weight and reduced breathability of these systems often cause sweating of the parts of the body in contact, lack of comfort and low acceptance by the patients. In addition to causing physical discomfort, these systems also end up also having a negative psychological effect on younger patients.

If we consider the potential of these wearable devices in achieving the goals of excellent care, better quality of life and the possibility of full social inclusion, we immediately recognize the need to have systems with less space, better fit, simplicity and psychological acceptability and lower cost. From this point of view, the correct design and personalized realization (customization) could offer a strong and practical contribution to the resolution of the aforementioned critical issues and limit the physical discomfort of patients subjected to these treatments [47].

The back braces in charge of treating scoliosis are all made of thermoplastic polymer, made to measure starting from the plaster cast (classic technique) or via

CAD-CAM (computerized technique) and are based on the principle of three points: a push on the main curve and two counterthrusts [52].
The evolution of plastic materials has made the construction of corrective back orthoses easier and has improved tolerability [31]. All this, together with a refinement of diagnostic skills and prognostic evaluations, has made the treatment of scoliosis by means of orthopedic busts even more effective. The latter essentially aim to hinder the aggravation of the curve and reduce unstructured deformations, with obvious aesthetic success, through the following action mechanisms:

- Traction on the column axis;
- Derotation obtained by stressing the column axis from the convexity to the concavity;
- Lateral deflection thrust that requires two counter thrusts at the upper and lower ends of the larger curve.

3. BACK BRACE FOR SCOLIOSIS

Bracing treatment intends to apply restorative strengths on the spine to discharge stack on the inward (internal) some portion of the bend and increment stack on the raised (external) some portion of the bend [2, 13, 15, 32, 53]. The idea is that a bone encountering pressure will become less and a bone encountering diversion (less or no pressure) may develop more. Bracing tries to back off the scoliosis bend's bone development as an afterthought that should be prevented, and accelerate development as an afterthought that necessities to accelerate. While bracing will not regularly invert or remedy the scoliosis, it can moderate or decrease any movement of the bend until the child/adolescent achieves skeletal development. After this point, the bones fairly set so the bend is probably not going to advance (if it is less than 40 degrees).
The correct components of bracing are still under scrutiny. However, research shows that the brace should be rigid (hard) so that it can apply strong and consistent pressure on the scoliosis bend to have an impact.

3.1 Types of Scoliosis Braces

There are a number of non-bending back braces available today to treat scoliosis. These braces can shift in how weight is connected to the spine and ribs to keep a scoliosis bend from advancing. Some non-bending braces require full-time wear, regularly in the proximity of 16 and 23 hours a day, though others are just worn around 8-10 hours for each night while resting [13, 16, 53].

3.1.1 Boston Brace

The most commonly used brace for scoliosis today is the Boston brace (*Figure 27*). Large number of people knows the Boston brace as a kind of thoracic-lumbar-sacral orthosis (TLSO). Different kinds of Boston brace models are available, for instance, a CTLSO (TLSO with a neck augmentation) for a high thoracic bend, but they are not as common.

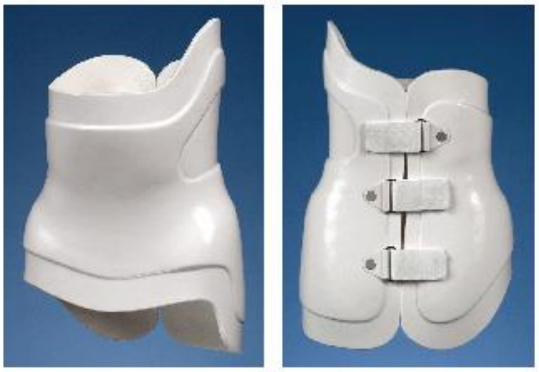

Figure 27 Boston brace

The Boston brace works by applying restorative weight on the angled (outside) side of the curve and removing contrasting zones of assistance on the inward (interior) side of the bend so the spine can advance toward that path [53].

3.1.2 Wilmington Brace

Wilmington brace is another commonly available brace for Thoracic-Lumbar-Sacral Orthosis (TLSO). However, the Wilmington brace is quite different from Boston brace (*Figure 28*). It is custom-fitted based on a replica taken from the patient back curvature [14, 34]. After having the replica, the counteractive forces are designed to the specific requirements of the patient's spinal curvature. This support goes onto the body like a tight coat and is known as a full contact TLSO brace due to its lack of gaps or open spots [34].

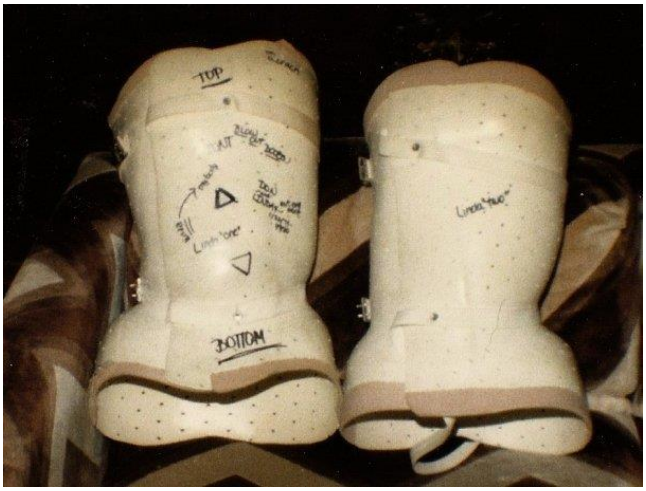

Figure 28 Wilmington brace

3.1.3 Milwaukee Brace

The Milwaukee brace was the first Cervico-Thoraco-Lumbo-Sacral Orthosis (CTLSO), meaning that the brace extended from the cervical spine (neck), thoracic spine (mid back), lumbar spine (lower back) to the sacrum (bone in the middle of the pelvis). The Milwaukee design was originally used to keep patients from moving after scoliosis surgery (*Figure 29*) [54]. The Milwaukee brace was later adapted and at one time was the most commonly prescribed (but not the most effective) scoliosis brace. Today we rarely see the Milwaukee brace design because it is wrong application can cause significant damage to the jaw and neck of patients [33].

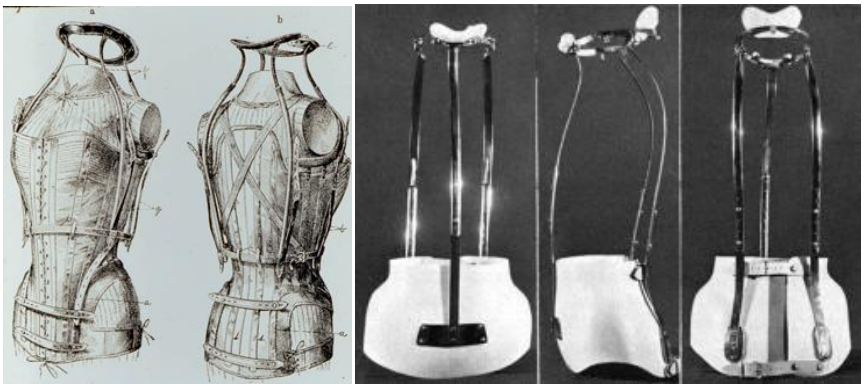

Figure 29 Milwaukee brace

3.1.4 Providence and Charleston Brace

The Providence and Charleston scoliosis braces are “part-time” braces designed to be worn only at night (*Figure 30*). This type of brace has a significant bend and cannot be worn for any length of time while standing [55]. The design is limited to use while the patient is in bed sleeping. The original concept relied on the growth of the child taking place mainly at night. By wearing the brace at night, it was believed the child would grow into a straighter spine. Unfortunately, research has shown that this type of bracing is only effective on very small curves. It is specially made from the replica of the patient's middle. After the replica is made, the remedial forces are included to the brace based on the measurements taken from the spine x-ray [56].

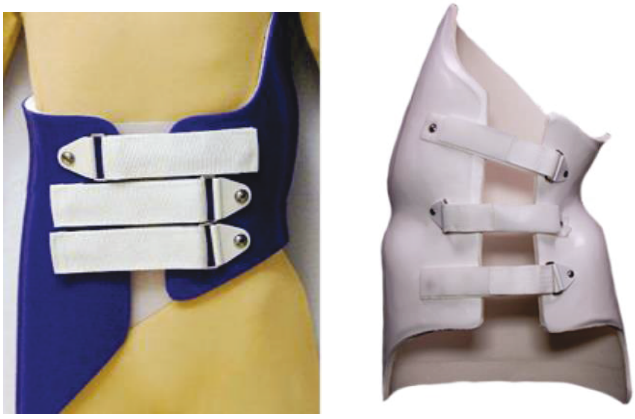

Figure 30 Providence and Charleston Brace

3.2 Back brace manufacturing techniques traditional vs proposed approach

It is possible to classify the chest brace production processes into traditional, modern and proposed processes as depicted in *Figure 31* [57].

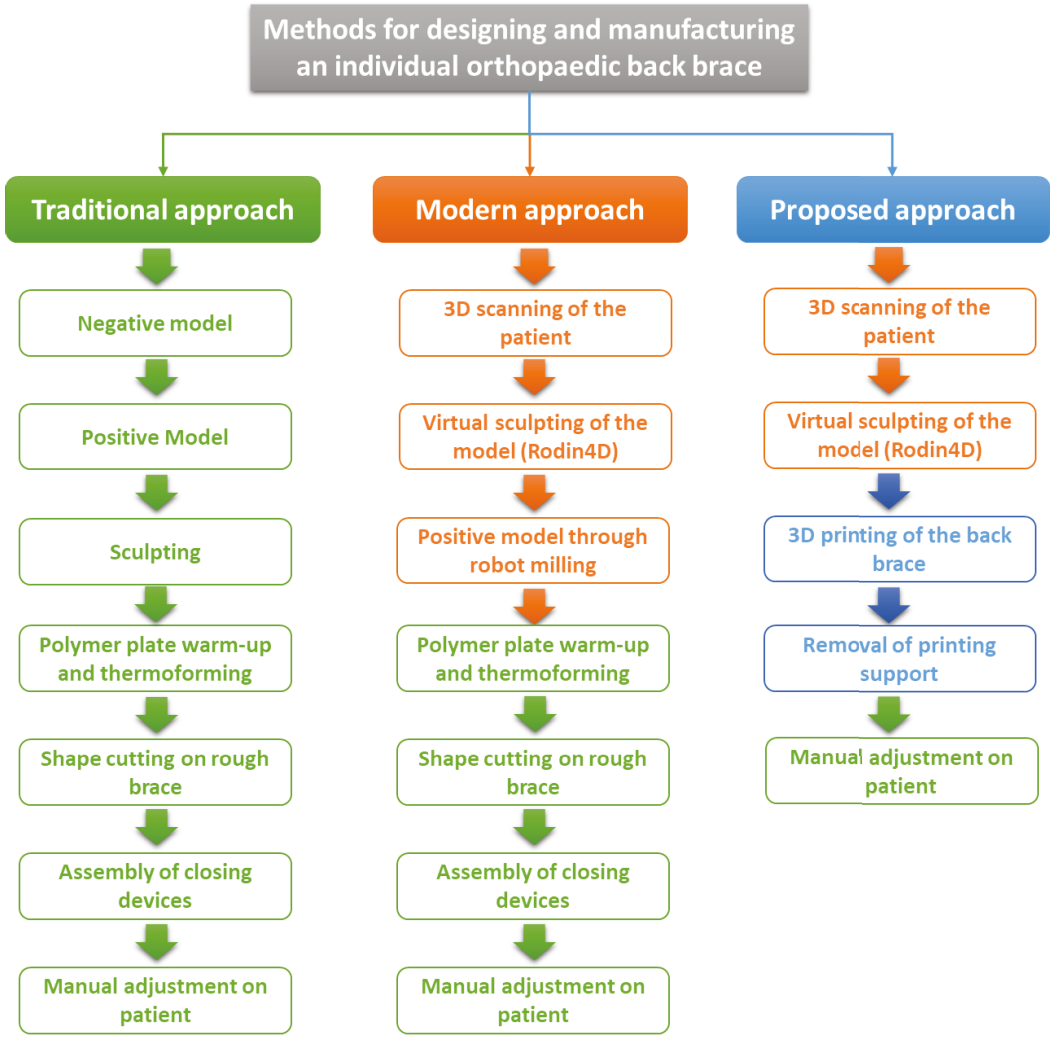

Figure 31 Proposed summary scheme of the distinct production processes presented in the present paper.

3.2.1 Traditional approach

The traditional sequence of operations starts with the creation of a negative cast with plaster of Paris bandages (*Figure 32a*). This is then filled with liquid plaster, left to dry and solidify, and finally the orthotist scuplted the mold by making the necessary corrections in agreement with the orthopedic (*Figure 32b*). Finally a thermoplastic layer sheet of polyethylene (PE), polystyrene (PS) or polypropylene (PP) is then applied onto the mold to produce the back brace that will be finished with laces, padding and protections (*Figure 32c*). Eventually the orthosis can be worn by the patient to test it and apply small corrections to obtain a customized

product. The entire production takes several days due to the drying time of the plaster [32, 57].

Figure 32 Major steps of the traditional brace design process: (a) creation of a negative cast with plaster of Paris bandages, (b) realization and refining of the positive mold and (c) realization of the back brace through a thermoformed polymer sheet.

3.2.2 Modern approach

Recently, the introduction of some new technologies has changed this approach, especially in the early stages of the orthosis creation process (*Figure 33*). With the expression "modern process", we consider the introduction of new technologies in the first steps of the procedure that have already been adopted today in orthopedic centers. More precisely the use of 3D scanners and associated software allow the creation of personalized virtual models of the body surface, avoiding the need for a negative cast with a clear saving of time and material (*Figure 33a*). The main systems are provided by Rodin4D, Biosculptor and Vorum. Once the computer models have been modified and finalized, they can be produced using numerical control machines. An equipment, with a drilling system, works a cylinder of polyurethane rotating at low speed (*Figure 33b*). The production is commonly achieved using an anthropomorphic robot with a drilling end effector coupled with

a rotating plate. The operator places a cylinder of polyurethane on the plate that is then worked by the robot while twisting at low speed. The created positive model is finally used to be wrapped with the plastic layer during the thermoforming step (*Figure 33c*). This procedure avoids the creation of a physical negative model, thus reducing the overall time to a full working day in best cases, by removing the part required for the plaster to solidify. Nevertheless, the present virtual sculpting step is not complete and requires a further manual sculpting phase of the milled positive mold and, at the same time, it adopts a material that is not recyclable nor reusable [7, 57].

Figure 33 Major steps of the modern approach: (a) 3D scanner of the patient, (b)the 3D CAM machine realizes the polyurethane positive model, (c) the thermoformed polymer sheet is thermoformed on the mold to obtain the final back brace

3.2.3 Proposed approach

After the innovations achieved in the first steps of the modern production process, the production is now evolving further, trying to improve the second part as well. The idea relies on the substitution of the thermoforming of the plastic plate on the 3D physical positive model with the introduction of the 3D printing [58]. Moreover, it has been tested in the field of orthotics and prosthetics (O&P) for cases of wrist orthosis, pelvis splint and lower limb prosthesis socket, where the

shape modelling was limited or simplified. In order to pass to such a manufacturing process, the orthotist should adopt a fully virtual sculpting phase, abandoning the creation of the physical positive model required by the thermoforming. The proposed method, reported in (*Figure 34*), regards the combined use of 3D scanner and AM techniques for the final realization of the back brace. The model that comes out of the 3D scanner is subsequently tessellated (surface mesh STL/OBJ) by using a specialized software, such as Autodesk Meshmixer (*Figure 34a*) [57]. After the creation of the CAD files the orthosis can be modelled by the previously described software: Rodin4D, Biosculptor or Canfit [59, 60]. The file is subsequently sliced by dedicated software and send to the 3D printing machine (*Figure 34b*). Due to the big volume of the back brace the most convenient printer is the one based on the Fused Deposition Modelling (FDM) technology, already described in the previous chapter. Among the other advantages of the FDM, we can mention the wide choice of materials available on the market and the low initial investment required for both machine and materials.

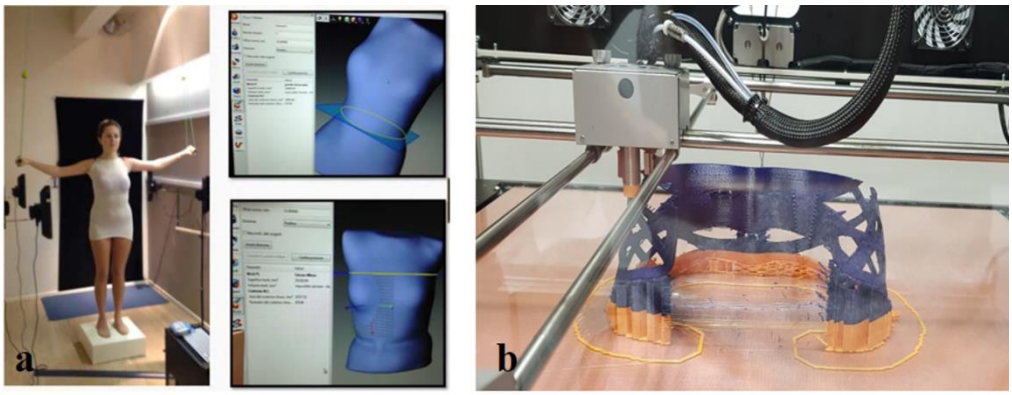

Figure 34 Major steps of the modern approach: (a)3D scanner of the patient and modelling of the CAD file, (b)3D printing of the back brace by FDM technique

After the model was printed, a series of standard operations was performed by the orthotist to verify the post-processability of the product. These operations regarded the support removal, the smoothing of the border and the drilling of holes for applying the straps used for closing the orthosis on the patient's body. The accuracy of a back brace is a fundamental prerogative for a therapy [61].

Old approach	Current Approach	Proposed approach
Traction system	**Cad-cam system**	
• Invasive for the patient • Slow process • Need for more operators • Disposal of plaster • Creation of a plaster negative and a plastic positive (double processing)	• Low cost of infrared sensors • Acquisition speed • Reduced discomfort for the patient • Greater system accuracy • No positive in plaster • No disposal of the plaster cast	
Brace realization	**3D printing**	
• Need for creation of a positive • Need for disposal of the positive • Increased bulk of the final product • Higher costs	• Reduced processing time (direct transition from scanning to printing) • Low construction costs • Greater wearability • Possibility of extreme customization of the product • Greater lightness of the final product • No waste material	

Table 1 Comparison between traditional approach and 3D printing techniques for back brace making

With the elimination of some steps of the traditional procedure, the reduction of acquisition and production times considerably reduces the margin of error. To further increase the accuracy of the back brace, there is also the greater control of the system and the possibility of subsequently modeling it with the aid of a heat gun.

Also not to be underestimated is the economic aspect: since both the acquisition, the design and the consequent printing of a back brace are made in the 3D world, there are no waste materials (unlike the traditional procedure which also foresees the disposal of gypsum blocks) and the costs are considerably reduced [62]. Finally, the aesthetic aspect is also noteworthy because the different textures that can be made, in addition to the aesthetic component, can also be used to improve the biomechanical principles of the back brace.

Furthermore, in *Table 1* a comparison between traditional, current and proposed technique is reported highlighting how they are evolving and what are the advantages brought by the new production approaches that involve digitalization with respect to the old method of making the plaster cast with artisan processing.

4. ENVIRONMENTAL IMPACT OF 3D PRINTING

The balance of lifecycle impacts of 3D printing has been investigated in some initial studies in the area, with the conclusion that electricity in the in-use phase is the dominant environmental impact. However, there are many uncertainties and variations in such analyses. Whether 3D printing has lower or increased environmental impact to alternative manufacture methods depends which manufacture technique the 3D printer is replacing and the impacts being taken into account in the assessment [63]

Industry 4.0 can provide support through continuous energy and resource management. By providing detailed information on each point of the production process, resource and energy use can be optimized over the entire value network (this means optimal resource and energy productivity, optimal resource and energy efficiency). In addition, systems can be optimized continuously during production process in terms of resources and energy consumption or emission output. This can make a substantial contribution to the sustainable development of the company. It is also possible to consider resource and energy efficiency already in the planning stage of the company by the optimization of rooms, spaces, pathways or lines, by the design of centralized and decentralized supply and disposal systems or by creating closed material and energy cycles [64]. Moreover, the impact of utilization levels on energy consumption with 3D printing will depend upon the specific printing technology. Some printers require extensive idle energy in the form of atmosphere generation, warm up and cool down between jobs, whilst others are able to print nearly without interruption FDM does not benefit significantly from full capacity utilization and can be used to generate output part-by-part without incurring a significant energy efficiency loss.

Figure 35 Waste in the currently production of back brace

In the production of back braces, currently, energy consumption must be added to the production of waste derived from the creation of the positive on which thermoplastic polymer sheets are thermoformed (*Figure 35*). By producing the back brace using 3DP techniques, the reduction of waste is huge and the material used for the brace can be re-spun and reused in FDM technologies (*Figure 36*).

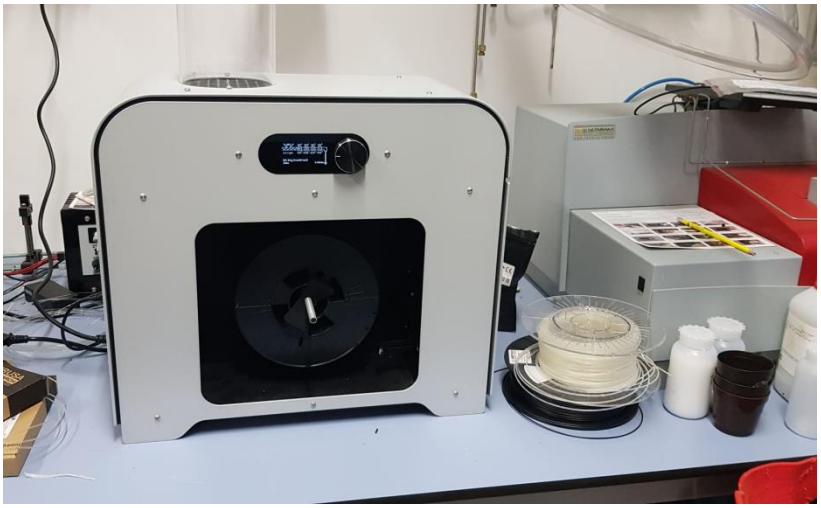

Figure 36 Polymer filament extruder

There is uncertainty about the potential to recycle waste material and printed parts due to potential changes in the material properties post-printing and pigments that if used may interfere with plastic separation processes. Although there are products in development that are intended to enable a closed loop recycling process by shredding and/or extrusion of waste prints into new filament [65, 66].

Extrusion devices can save over 90% of the costs of purchasing filament, and can enable production of filament on demand, in whatever length or colour is required for a specific job [67, 68]. However, the use of additional devices needs to be balanced with their added embodied energy and in use energy impacts.
Environmental impacts can be minimised by optimising part orientation and number of parts printed simultaneously, by minimising waste in support materials, by ensuring high usage of the minimal number of printers, and by optimising material selection and processing for strength, surface finish, embodied energy and melting point. In particular, in recent comparative studies, FDM processes showed a greater potential for reduced environmental impact in small print volume scenarios compared to other technologies [69]

References

[1] T. Esposito, B. Varriale, G. DiMartino, M. Chierchia, A.G. Carnevale, D. Ronca, SCOLIOSIS: CAUSES, GENETICS.
[2] C.J. Goldberg, D.P. Moore, E.E. Fogarty, F.E. Dowling, Adolescent Idiopathic Scoliosis: The Effect of Brace Treatment on the Incidence of Surgery, Spine 26(1) (2001) 42-47.
[3] C.J. Goldberg, D.P. Moore, E.E. Fogarty, F.E. Dowling, Scoliosis: a review, Pediatric surgery international 24(2) (2008) 129-144.
[4] T.S. Illés, F. Lavaste, J.F. Dubousset, The third dimension of scoliosis: The forgotten axial plane, Orthopaedics & Traumatology: Surgery & Research (2019).
[5] P. Trobisch, O. Suess, F. Schwab, Idiopathic scoliosis, Dtsch Arztebl Int 107(49) (2010) 875-884.
[6] K.M. Rafael, S. Hüsseyin, K. Rüdiger, Epidemiology of adolescent idiopathic scoliosis, Journal of Children's Orthopaedics 7(1) (2013) 3-9.
[7] D.F. Redaelli, F.A. Storm, E. Biffi, G. Reni, G. Colombo, A Virtual Design Process to Produce Scoliosis Braces by Additive Manufacturing, Springer International Publishing, Cham, 2020, pp. 860-870.
[8] S. Yang, L.M. Andras, G.J. Redding, D.L. Skaggs, Early-onset scoliosis: a review of history, current treatment, and future directions, Pediatrics 137(1) (2016) e20150709.
[9] L. Mainard-Simard, L. Lan, D. Fort, The advantages of 3D imagery in diagnosing and supervising children's and teenagers' scoliosis, Archives de pediatrie: organe officiel de la Societe francaise de pediatrie 24(10) (2017) 1029-1035.
[10] A.J. Danielsson, A.L. Nachemson, Back pain and function 22 years after brace treatment for adolescent idiopathic scoliosis: a case-control study—part I, Spine 28(18) (2003) 2078-2085.
[11] N.W. Gummerson, P.A. Millner, (ii) Scoliosis in children and teenagers, Orthopaedics and Trauma 25(6) (2011) 403-412.
[12] H. Shakil, Z.A. Iqbal, A.H. Al-Ghadir, Scoliosis: review of types of curves, etiological theories and conservative treatment, Journal of back and musculoskeletal rehabilitation 27(2) (2014) 111-115.
[13] D. Périé, C.-E. Aubin, Y. Petit, M. Beauséjour, J. Dansereau, H. Labelle, Boston Brace Correction in Idiopathic Scoliosis: A Biomechanical Study, Spine 28(15) (2003) 1672-1677.
[14] N.J. ALLINGTON, J.R. BOWEN, Adolescent Idiopathic Scoliosis: Treatment with the Wilmington Brace. A Comparison of Full-Time and Part-Time Use*, JBJS 78(7) (1996) 1056-62.
[15] C. Coillard, M.A. Leroux, K.F. Zabjek, C. Rivard, SpineCor – a non-rigid brace for the treatment of idiopathic scoliosis: post-treatment results, European Spine Journal 12(2) (2003) 141-148.
[16] H. Labelle, J. Dansereau, C. Bellefleur, B. Poitras, Three-dimensional Effect of the Boston Brace on the Thoracic Spine and Rib Cage, Spine 21(1) (1996) 59-64.
[17] C.J. Goldberg, F.E. Dowling, J.E. Hall, J.B. Emans, A statistical comparison between natural history of idiopathic scoliosis and brace treatment in skeletally immature adolescent girls, Spine 18(7) (1993) 902-908.
[18] J. Legaye, Three-dimensional assessment of the scoliosis, Recent Advances in Scoliosis (2012) 119.

[19] E. Berthonnaud, J. Dimnet, Analysis of structural features of deformed spines in frontal and sagittal projections, Computerized Medical Imaging and Graphics 31(1) (2007) 9-16.
[20] F.P.L. Quagliarella, Biomeccanica Ortopedica e Traumatologica.
[21] J. Cobb, Outline for the study of scoliosis, Instr Course Lect AAOS 5 (1948) 261-275.
[22] M.J. McMaster, K. Ohtsuka, The natural history of congenital scoliosis. A study of two hundred and fifty-one patients, JBJS 64(8) (1982) 1128-1147.
[23] J.E. Shelton, R. Julian, E. Walburgh, E. Schneider, Functional scoliosis as a long-term complication of surgical ligation for patent ductus arteriosus in premature infants, Journal of pediatric surgery 21(10) (1986) 855-857.
[24] R. Smith, R. Dickson, Experimental structural scoliosis, The Journal of bone and joint surgery. British volume 69(4) (1987) 576-581.
[25] S.L. Weinstein, L.A. Dolan, J.C. Cheng, A. Danielsson, J.A. Morcuende, Adolescent idiopathic scoliosis, The Lancet 371(9623) (2008) 1527-1537.
[26] S. Weinstein, I. Ponseti, Curve progression in idiopathic scoliosis, The Journal of bone and joint surgery. American volume 65(4) (1983) 447-455.
[27] I.V. Ponseti, B. Friedman, Prognosis in idiopathic scoliosis, J Bone Joint Surg Am 32(2) (1950) 381-395.
[28] C. Nash, J.H. Moe, A study of vertebral rotation, J Bone Joint Surg Am 51(2) (1969) 223-229.
[29] T. Vrtovec, F. Pernuš, B. Likar, A review of methods for quantitative evaluation of spinal curvature, European spine journal 18(5) (2009) 593-607.
[30] M. Inoue, S. Minami, Y. Nakata, Y. Otsuka, M. Takaso, H. Kitahara, M. Tokunaga, K. Isobe, H. Moriya, Preoperative MRI analysis of patients with idiopathic scoliosis: a prospective study, Spine 30(1) (2005) 108-114.
[31] I. Weisz, R. Jefferson, A. Carr, A. Turner-Smith, A. McInerney, G. Houghton, Back shape in brace treatment of idiopathic scoliosis, Clinical orthopaedics and related research (240) (1989) 157-163.
[32] C. Andrew, L. Edmond, H. Doug, Review of current technologies and methods supplementing brace treatment in adolescent idiopathic scoliosis, Journal of Children's Orthopaedics 7(4) (2013) 309-316.
[33] W.A. Carr, J. Moe, R. Winter, J.E. Lonstein, Treatment of idiopathic scoliosis in the Milwaukee brace, The Journal of bone and joint surgery. American volume 62(4) (1980) 599-612.
[34] G.S. Bassett, W. Bunnell, G. MacEwen, Treatment of idiopathic scoliosis with the Wilmington brace. Results in patients with a twenty to thirty-nine-degree curve, The Journal of bone and joint surgery. American volume 68(4) (1986) 602-605.
[35] I.A. Stokes, L.C. Bigalow, M.S. Moreland, Three-dimensional spinal curvature in idiopathic scoliosis, Journal of Orthopaedic Research 5(1) (1987) 102-113.
[36] J. James, Kyphoscoliosis, The Journal of bone and joint surgery. British volume 37(3) (1955) 414-426.
[37] C. Picault, J. Demauroy, B. Mouilleseaux, G. Diana, Natural history of idiopathic scoliosis in girls and boys, Spine 11(8) (1986) 777-778.

[38] L.-E. Peterson, A.L. Nachemson, Prediction of progression of the curve in girls who have adolescent idiopathic scoliosis of moderate severity. Logistic regression analysis based on data from The Brace Study of the Scoliosis Research Society, The Journal of bone and joint surgery. American volume 77(6) (1995) 823-827.
[39] H.T. Fairbank, OSTEOGENESIS IMPERFECTA: Osteogenesis Imperfecta Cystica, The Journal of bone and joint surgery. British volume 30(1) (1948) 164-186.
[40] R.H. Engelbert, C.S. Uiterwaal, A. van der Hulst, B. Witjes, P.J. Helders, H.E. Pruijs, Scoliosis in children with osteogenesis imperfecta: influence of severity of disease and age of reaching motor milestones, European Spine Journal 12(2) (2003) 130-134.
[41] K. Yong-Hing, G.D. MAcEWEN, Scoliosis associated with osteogenesis imperfecta, The Journal of bone and joint surgery. British volume 64(1) (1982) 36-43.
[42] D. Hanscom, R. Winter, L. Lutter, J.E. Lonstein, B. Bloom, D. Bradford, Osteogenesis imperfecta. Radiographic classification, natural history, and treatment of spinal deformities, The Journal of bone and joint surgery. American volume 74(4) (1992) 598-616.
[43] A.K. Anissipour, K.W. Hammerberg, A. Caudill, T. Kostiuk, S. Tarima, H.S. Zhao, J.J. Krzak, P.A. Smith, Behavior of scoliosis during growth in children with osteogenesis imperfecta, JBJS 96(3) (2014) 237-243.
[44] S. Allen, E. Parent, M. Khorasani, D.L. Hill, E. Lou, J.V. Raso, Validity and reliability of active shape models for the estimation of Cobb angle in patients with adolescent idiopathic scoliosis, Journal of digital imaging 21(2) (2008) 208-218.
[45] M. Wong, A. Mak, K. Luk, J. Evans, B. Brown, Effectiveness and biomechanics of spinal orthoses in the treatment of adolescent idiopathic scoliosis (AIS), Prosthetics and orthotics international 24(2) (2000) 148-162.
[46] R.P. Keiser, H.L. Shufflebarger, The Milwaukee brace in idiopathic scoliosis: evaluation of 123 completed cases, Clinical orthopaedics and related research (118) (1976) 19-24.
[47] R.T. Morrissy, School screening for scoliosis, Spine 24(24) (1999) 2584.
[48] L.A. Dolan, S.L. Weinstein, Surgical rates after observation and bracing for adolescent idiopathic scoliosis: an evidence-based review, Spine 32(19) (2007) S91-S100.
[49] G.T. Wynarsky, A.B. Schultz, Optimization of skeletal configuration: studies of scoliosis correction biomechanics, Journal of biomechanics 24(8) (1991) 721-732.
[50] T.P. Andriacchi, A.B. Schultz, T. Belytschko, R. Dewald, Milwaukee brace correction of idiopathic scoliosis. A biomechanical analysis and a restrospective study, The Journal of bone and joint surgery. American volume 58(6) (1976) 806-815.
[51] J.A. Sullivan, R. Davidson, T.S. Renshaw, J.B. Emans, C. Johnston, M. Sussman, Further evaluation of the Scolitron treatment of idiopathic adolescent scoliosis, Spine 11(9) (1986) 903-906.
[52] F. Desbiens-Blais, J. Clin, S. Parent, H. Labelle, C.-E. Aubin, New brace design combining CAD/CAM and biomechanical simulation for the treatment of adolescent idiopathic scoliosis, Clinical biomechanics 27(10) (2012) 999-1005.
[53] Y. Olafsson, H. Saraste, V. Söderlund, M. Hoffsten, Boston brace in the treatment of idiopathic scoliosis, Journal of pediatric orthopedics 15(4) (1995) 524-527.

[54] W.P. Blount, A.C. Schmidt, E.D. KEEVER, E.T. Leonard, The Milwaukee brace in the operative treatment of scoliosis, JBJS 40(3) (1958) 511-525.
[55] D.D. Bohl, C.J. Telles, N.S. Golinvaux, B.A. Basques, P.A. DeLuca, J.N. Grauer, Effectiveness of Providence nighttime bracing in patients with adolescent idiopathic scoliosis, Orthopedics 37(12) (2014) e1085-e1090.
[56] R. Gepstein, Y. Leitner, E. Zohar, I. Angel, S. Shabat, I. Pekarsky, T. Friesem, Y. Folman, A. Katz, B. Fredman, Effectiveness of the Charleston Bending Brace in the Treatment of Single-Curve Idiopathic Scoliosis, Journal of Pediatric Orthopaedics 22(1) (2002) 84-87.
[57] D.F. Redaelli, E. Biffi, G. Colombo, P. Fraschini, G. Reni, Current and Future Manufacturing of Chest Orthoses, Considering the Case of Osteogenesis Imperfecta, ASME 2018 International Design Engineering Technical Conferences and Computers and Information in Engineering Conference, 2018.
[58] H.-R. Weiss, N. Tournavitis, X. Nan, M. Borysov, L. Paul, Workflow of CAD / CAM Scoliosis Brace Adjustment in Preparation Using 3D Printing, Open Med Inform J 11 (2017) 44-51.
[59] N. Cobetto, C.E. Aubin, J. Clin, S. Le May, F. Desbiens-Blais, H. Labelle, S. Parent, Braces Optimized With Computer-Assisted Design and Simulations Are Lighter, More Comfortable, and More Efficient Than Plaster-Cast Braces for the Treatment of Adolescent Idiopathic Scoliosis, Spine Deform 2(4) (2014) 276-284.
[60] P.G. Knoops, C.A. Beaumont, A. Borghi, N. Rodriguez-Florez, R.W. Breakey, W. Rodgers, F. Angullia, N.U. Jeelani, S. Schievano, D.J. Dunaway, Comparison of three-dimensional scanner systems for craniomaxillofacial imaging, J Plast Reconstr Aesthet Surg 70(4) (2017) 441-449.
[61] S. Rudicel, T.S. Renshaw, The effect of the Milwaukee brace on spinal decompensation in idiopathic scoliosis, Spine (Phila Pa 1976) 8(4) (1983) 385-7.
[62] Q. Sun, Effect of processing conditions on the bonding quality of FDM polymer filaments, Rapid Prototyping Journal 14(2) (2008) 72-80.
[63] A. Pasricha, R. Greeninger, Exploration of 3D printing to create zero-waste sustainable fashion notions and jewelry, Fashion and Textiles 5(1) (2018) 30.
[64] M. Gabriel, E. Pessl, Industry 4.0 and sustainability impacts: Critical discussion of sustainability aspects with a special focus on future of work and ecological consequences, Annals of the Faculty of Engineering Hunedoara 14(2) (2016) 131.
[65] C. McAlister, J. Wood, The potential of 3D printing to reduce the environmental impacts of production, Proceeding of the ECEEE (2014) 213-221.
[66] P. Dudek, K. Zagórski, Cost, resources, and energy efficiency of additive manufacturing, E3S Web of Conferences, EDP Sciences, 2017, p. 01040.
[67] M. Lušić, A. Barabanov, D. Morina, F. Feuerstein, R. Hornfeck, Towards zero waste in additive manufacturing: a case study investigating one pressurised rapid tooling mould to ensure resource efficiency, Procedia CIRP 37 (2015) 54-58.
[68] T. Campbell, C. Williams, O. Ivanova, B. Garrett, Could 3D printing change the world, Technologies, Potential, and Implications of Additive Manufacturing, Atlantic Council, Washington, DC 3 (2011).

[69] J. Faludi, N. Cline-Thomas, S. Agrawala, 3D printing and its environmental implications, The Next Production Revolution. Implications for Governments and Businesses (2017).

Chapter 3
An innovative process to produce back brace scoliosis by 3D printing

1. INTRODUCTION

Scoliosis is a three-dimensional deformity of the spine and a musculoskeletal disorder. In structural scoliosis, there is usually a certain amount of spinal torsion and a disturbance of the sagittal profile coupled to the lateral deformation [1]. Therefore, scoliosis must be more accurately regarded as a three-dimensional (3D) deformity of the spine and trunk, which may progress quickly during periods of rapid growth [2]. The typical treatment for the treatment of scoliosis is composed of physical exercise, both for stretching and for strengthening the muscles, and of the use of an external device, called scoliosis brace [3]. Orthopaedic bracing is the conservative treatment generally prescribed to control curve progression in adolescent idiopathic scoliosis (AIS) showing curves between 20° and 40° of Cobb angle [4-6]. There exist different versions and models of this orthotic device, from the very rigid and old Milwaukee brace, to the newest and extremely soft SpineCor [7-9]. If the first type is now less common because of the limited comfort and low quality of life of the patients, the last seems to have a limited effectiveness and is appropriate only to light scoliosis, under 20° of the Cobb angle [10]. However, the treatment outcomes rely on multiple factors such as timing with adolescent growth spurt, spine flexibility, and patient compliance to treatment [11-13]. So, depending on the type and severity of scoliosis and on the number and locations of the contact regions, the effects of orthopaedic braces can be limited to stabilization or also spine curvature correction [14, 15]. There exist a wide variety of orthopaedic braces depending on the type and severity of scoliosis and on the available contact region [16, 17]. The aim of the device is to support the chest and, in most of the cases, to realign the spine by applying a correction based on the tree point bending system. The type of load depends on the extent of deformation, on the location along the spine and on the characteristics of the patient. The orthopaedist can decide for the proper brace and asks the orthotist to apply the patient specific correction to the models [5, 10, 16]. In order to realign the spine, the orthosis is shaped in a way that produces forces in precise regions, unloading other region [18, 19]. Three main phases define the traditional back brace fabrication: positive mold creation, sculpting and manufacturing. The full

process is usually long, from a full day to a week depending on the technology, and still expensive. At present, back braces can be produced using the following two methods: i) design and manufacture of plaster of Paris, ii) design and manufacture using 3D digitization and CNC milling. The traditional manufacturing process that is currently adopted for the custom made orthosis is based on the thermoforming of a plastic plate around the patient's positive mold [18]. This model can be obtained in different ways according to the available technology and to the experience of the orthotists. The traditional method is to reconstruct the negative shell mold of the patient using plaster of Paris bandages. This is then filled with liquid plaster, left to dry and solidify and finally sculpted manually by an expert orthotist. The entire production takes several days due to the drying time of the plaster. The "modern" method, instead, regards the use of a 3D scanner to acquire the shape of the patient's body and pass it to the computer [10, 18]. A specialized software is adopted for a first phase that consists on virtually sculpting and preparing the CAM file to control the computer numerical control (CNC) machine. This machine, typically a lathe or robot arm, produces the positive model milling a cylinder of polyurethane foam [5, 10].

Nowadays, the use of scanning technologies combined with computer aided design (CAD) and 3D printing (3DP) have shown great advantages over conventional techniques for the fabrication of customised medical aids, devices, implants and accessories [20, 21]. Because of technological advances, 3DP has recently gained recognition in medicine due to its potential benefits [5, 20, 22]. The greatest advantage that 3D printers provide is the freedom to produce custom-made medical products and equipment [22, 23]. The use of 3DP to customize prosthetics and implants can provide great value for both patients and physicians due to its ability to produce items more quickly and cheaply than traditional manufacturing methods [20-23]. Traditional manufacturing methods remain less expensive for large-scale production; however, the cost of 3DP is becoming more and more competitive for small-customized productions [24]. Moreover, 3DP can be inexpensive, less time consuming and more controllable than traditional manufacturing techniques for custom-made orthopaedic devices: costs for moulds and waste produced in machining by chip removal are saved; milling, forging and finishing phases are not necessary; less manual handwork is needed, reducing the risks of human errors [23, 24]. Among 3DP techniques, FDM is the most common and inexpensive method and is available for a wide range of materials such as thermoplastic polymers, elastomers and investment casting wax as reported in the previous chapter [25-27].

In this chapter, an innovative rapid manufacturing approach for the fabrication and characterization of customized orthopaedic back braces for scoliosis treatment will be presented.
Moreover, due to limited information regarding the physico-chemical properties of commercial filament, an accurate characterization of two commercial polymers (PLA and PETG) have been conducted in terms of mechanical, thermal and morphological properties to optimize the final printing process of the back brace.
In conclusion, it is possible to summarize the purposes of this chapter in the following three points:

1) To investigate and evaluate suitable materials for the fabrication of back braces by means of FDM 3DP;
2) To describe the reverse engineering and the production process of an orthopaedic back brace by 3DP;
3) To realize a cost model for the realization of the back brace and compare it with the traditional manufacturing technique.

2. MATERIALS AND METHODS

2.1 Preliminary material screening

Common materials currently used in the thermoformed and off-the-shelf braces include PE, PP, Podialene. Their mechanical properties, *i.e.* Elastic Modulus, Yield Stress and Elongation, were compared to those of the available commercial filaments, using the CES Edupack software database. When selecting potential filaments, we opted when possible for materials that are already broadly used for biomedical applications.

	ABS	PLA	PETG	Nylon	ASA	PC	PP	PVA
Ultimate strength (MPa)	40	65	53	40-85	55	72	32	78
Durability	✓✓✓	✓	✓✓✓	✓✓✓	✓✓✓	✓✓✓	✓✓✓	✓✓
Coefficient of Thermal Expansion (μm/m·°C)	90	68	60	95	98	69	150	85
Price (per kg) (€)	9-36	9-36	18-54	22-60	35-40	40-75	60-120	40-110
Printability	✓✓	✓✓✓	✓✓✓	✓✓	✓✓	✓✓	✓	✓
Extruder Temperature (°C)	220-250	190-220	230-250	220-270	235-255	260-310	220-250	185-200
Bed temperature (°C)	95-110	45-60	75-90	70-90	90-110	80-120	85-100	45-60
Impact resistant	✓✓✓	✓	✓✓	✓✓	✓✓✓	✓✓✓	✓	✓
Water resistant	✓	✓	✓✓✓	✓	✓	✓	✓✓✓	✓
Chemically resistant	✓	✓	✓✓✓	✓	✓	✓	✓	✓
Flexibility	✓	✓	✓✓	✓✓	✓	✓	✓✓✓	✓✓
Fatigue resistant	✓	✓	✓✓✓	✓✓✓	✓	✓✓✓	✓✓✓	✓✓✓
Medical grade	N.A.	A	A	N.A.	N.A.	A	A	A

Table 2 Basic mechanical properties of typical materials available for FDM 3D printers

Among the materials listed in *Table 2*, PLA and PETG were the best scoring materials, but PETG was preferred due to its better mechanical properties.

After a first screening of the potential filaments, hemicylindrical samples were chosen as simple models of brace sections, to have a mechanical characterization of materials in conditions that are as close as possible to the final application. The main advantages of using such geometry are: i) the possibility to test the real printing settings for the final back brace, as opposed to printing flat specimens; ii) the hemicylinders are more stable than flat samples when printing vertically; and iii) it allows the evaluation of deposition accuracy and correct adhesion in higher layers with such curved path.

The hemicylinders of 150 mm diameter, 50 mm in height and 2 mm of thickness (*Figure 37*) were created with the CAD software Autodesk Inventor and exported as stl file with the preset high level of accuracy, thus obtaining 1190 triangles. The dimensions were decided after measuring the section of a real brace on the reverse engineered 3D model. A short straight part of 30 mm was extruded on an end of the hemicylinder as it is representative of the regions on the back of the brace, where the curvature decreases and tends to zero. The file was imported in Ultimaker Cura 3.6 that performed the slicing and applied the printing settings creating the .gcode file. In order to improve the adhesion with the printing bed, a small brim composed of 5 lines at the first layer was added.

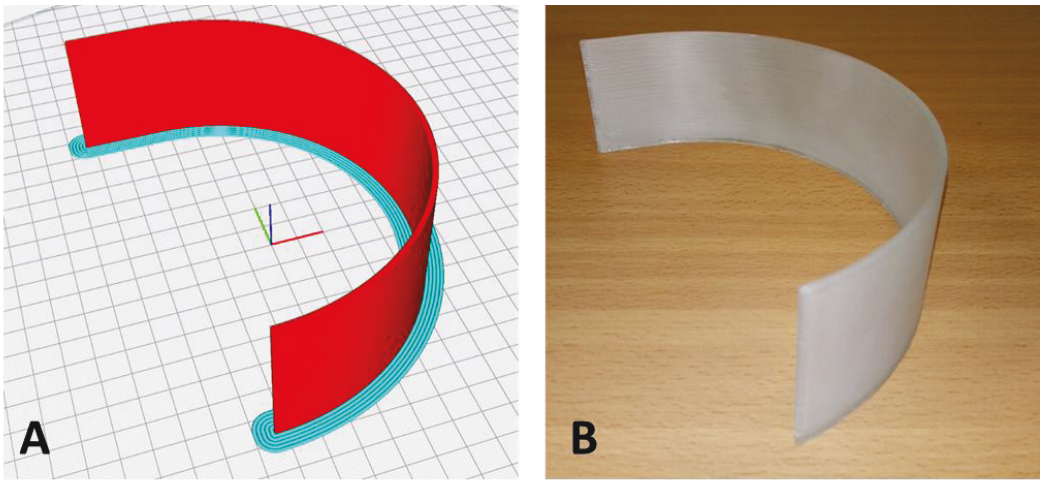

Figure 37 Gcode and printed hemycilinder representative of a back brace section

The hemicylinder has been used as standard object to compare the different materials and the printing settings in substitution to the traditionally proposed flat printed specimens or to the ideal possibility to 3D print a whole orthosis for each material and printing setting parameter. The hemicylindrical samples were manufactured using an i3D® Pivotmaker 3D printer. Preliminary tests were performed to identify the most appropriate printing settings for each selected material, including: extruder temperature (T_E), printing bed temperature (T_B) and printing speed (V_P) as reported in *Table 3*.

Material	Brand	Description	T_E (°C)	T_B (°C)	V_P (mm/s)
PETG	Filoalfa	PETG	235	90	50
	Sunlu		240		
PLA	Filoalfa	Alfaplus	205	50	50
	TreedFilaments	EcoGenius	208	60	40
	Filoalfa	Bianco	200	50	50
	TreedFilaments	Shogun	200	60	50
	Filoalfa	Rosso	200	50	50
	Filoalfa	Trasparente	200	50	50
PLA-Graphene	Filoalfa	Grafylon	200	50	50
TPU	Filoalfa	BioFlex	200	50	50

Table 3 Printing parameters of the selected polymer (PLA and PETG)

Two polymers were selected for the realization of the 3D printed back brace: a polylactic acid (PLA) and a polyethylene terephthalate-glycol (PETG) that will be described in the next chapters. For each polymer, different commercial filaments were considered (*Figure 38*) and a first mechanical screening have been conducted by tensile test as described in the following chapter. The reasons for choosing these materials are as follows:

- Health-conscious materials that do not cause medical complications in contact with the skin;
- Both materials belong to the cheapest polymers that can be purchased on a regular basis, so they are not difficult to produce;
- During manufacture itself, by the chosen technology, there is no complication and no special conditions need to be created during the additive manufacture of medical devices by the chosen technology [13];
- PLA material has features that are particularly suited to the application. This material is a biocompatible polymer that, in some forms, is used for the manufacture of various medical devices, whether for external or internal use (i.e. placement in a human body). Another important feature is its forming ability, under certain conditions. This material is so soft when it is heated over the T_g that it is possible to shape/form it.

- PETG material is a health-conscious material that showed good mechanical properties (strength, elasticity) among the polymers used in FDM technology.
- The detail description of material properties of PETG and PLA materials has been researching and described in the following paragraphs.

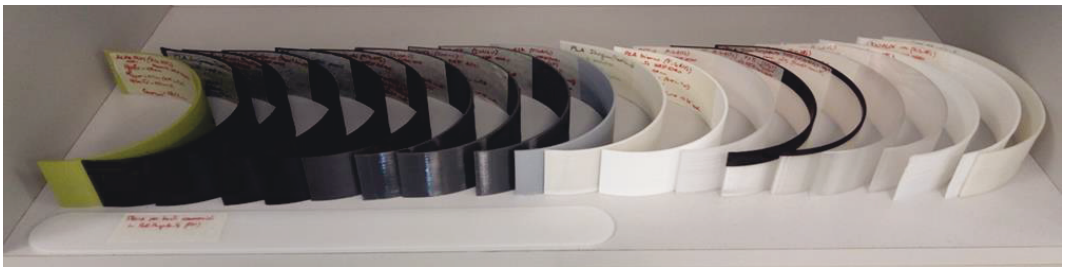

Figure 38 3D printed hemycilinder with different types of commercial filament for the first evaluation screening.

The properties of the 3D printed samples have been compared with a commercial Polypropylene (PP) back brace realized with the traditional manufacturing method. In addition, a commercial thermoplastic polyurethane filament (TPU) have been also characterized for the realization of the internal part of the back brace to improve the comfort of the orthosis once it will be used by the patient.

2.2 Polylactic acid (PLA)

Polylactic acid (PLA) is a thermoplastic polyester commonly used in FDM technique. It is made from renewable sources like cornstarch, tapioca roots or sugarcane [28-30]. An important aspect is that PLA degrades naturally when exposed to environmental conditions. PLA is currently applied in various industrial functions ranging from packaging of food materials and in some cases medical implants that include temporary tissue screws, sutures and tacks (*Figure 39*). Over a few weeks PLA will dissolve in the body [29].

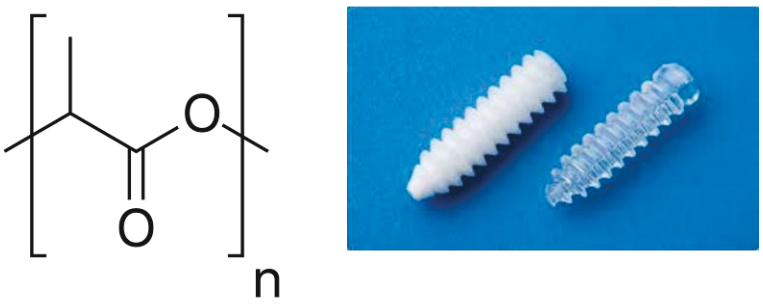

Figure 39 Structural formula of PLA and an example of PLA medical devices

PLA can be classified in various grades which include scientific, food safe, medical and type used in PLA printing. The melting point for PLA is around 180ºC and usually it is combined with other plastics to make it stronger when used in 3D printing [31]. PLA is not thermally contractive and is normally efficient when used to print huge pieces. One shortcoming of PLA is its brittleness if compared to other tough plastics. The other imperative thought when printing parts with PLA fiber is understanding what temperatures the part will be subjected to. PLA plastic begins to soften like rubber at temperatures of 80°C and will disfigure if utilized in conditions that stay over those temperatures for any drawn-out time.

2.3 Polyethylene terephthalate glycol (PETG)

Glycol - modified polyethylene terephthalate (PETG) is a thermoplastic polymer, with an excellent high – impact and chemical resistance, simultaneously with flexural strength. PETG is obtained from polyethylene terephthalate (PET) by copolymerization [32]. Cyclohexane dimethanol (CHDM) is added to the PET backbone in place of ethylene glycol making the resulting resin clearer and less brittle than the original PET as depicted in *Figure 40*.

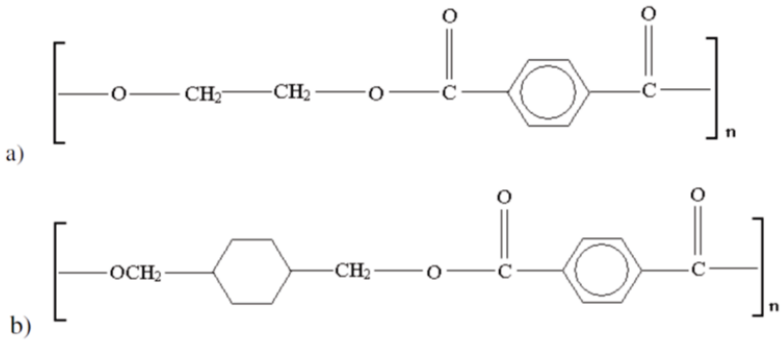

Figure 40 Chemical difference between the chemical structure of PET (a) and PETG (b).

The resulting copolymer has a lower melting temperature and is a useful material for thermoforming applications that require complex shapes. Specifically, PETG is a random copolymer consisting of 31 mol% PCT and 69 mol% PET. PET and PETG both exhibit quite similar deformation behaviour, have a similar glass transition temperature, and are visually nearly indistinguishable. Yet there is one substantial difference: PET readily undergoes strain-induced crystallization, whereas crystallization is nearly impossible to achieve in PETG at processing temperatures [33]. PETG is used in many fields, including medicals, electronics, automobiles etc. As a 3D printing filament, PETG has proven its worth as a

durable material that is easy to use. It normally combines some significant features of ABS filament which include mechanical properties and rigidity with those of PLA materials [34]. 3D printed PETG parts exhibit good layer adhesion and can be used to produce many end use parts, prototypes, jigs, and fixtures.

2.4 Characterization of 3D printed samples

The specimens for physico-chemical characterization were obtained from the 3D printed hemicylinders. Materials were characterized in terms of mechanical and thermal properties. Moreover, a surface analysis by scanning electron microscopy (SEM) was conducted to understand the effect of printing parameters on the surface finishing of the 3D printed parts. Two different fibres orientation have been chosen for the mechanical test: parallel to fibres orientation to test the material elastic modulus and perpendicular to the fibres orientation to test the fibre-fibre interface. In addition, two different layer thickness were assessed for the 3D printed specimens: 0.4 and 0.6 mm.

2.4.1 Tensile test

A tensile test is an essential qualification test for all engineered materials. Under the tensile test the important strength parameters can be determined including yeld stress (σ_y), yield strain (ε_y), elongation at break (ε_r), and Young's modulus (E'). This tensile test is done by applying a load longitudinally (lengthways) on standard tensile specimen with known dimensions of the material. The tensile test is applied at a specific strain rate until the failure of the specimen. The applied load and expansion are recorded during the test to calculate the properties of Ultimate Tensile Strength, Yield Strength, Percentage Elongation and Percentage Reduction in Area. Tensile properties were evaluated at room temperature by an Instron machine using a load cell of 1kN and a crosshead speed of 1 mm/min. Dumbbell shape samples were cut from the 3D printed hemicylinder according to the ASTM D1708 standard [35]. The study was carried out through analysis of five samples for each type of scaffold. The test was performed at room temperature considering two fibre orientations: parallel to the elongation direction (L) and transversal to the elongation direction (T) (*Figure 41*). The tensile modulus was calculated between 0.05% and 0.20% strain by a linear regression calculation. Then mean value and standard deviation was reported in next chapter.

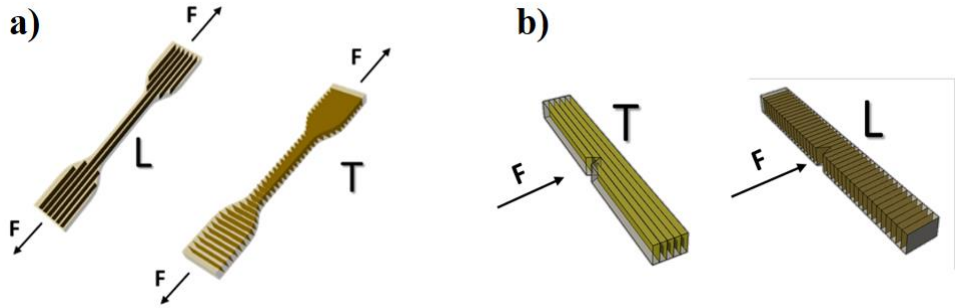

Figure 41 Fibres orientation with respect to force direction for a) tensile and b) impact test

2.4.2 Charpy impact test

Charpy impact tests were performed to correlate the energy absorption of the different materials with fibers orientation and layer thickness. The Charpy device is a dynamic three-point flexural test of a notched specimen. Samples (13.0 mm wide (w) 2.5 mm thick (t) and 60 mm long) with a notch depth-to-width ratio of 0.3 were fractured at room temperature by using an impact energy of 3.6 J and an impact speed of 1 m/s. At least five samples for each material were performed by using an Instron CEAST 6545 apparatus equipped with a Charpy pendulum hammer (mass: 3.65 Kg) positioned at a starting angle of 30°. The experimental setup consists on the specimen, the anvils where the specimen is freely supported, a pendulum with a defined mass attached to a rotating arm pinned at the machine frame. The pendulum is raised to a known height and allowed to fall. It falls following a circular trajectory and hits the specimen at the middle span length transferring kinetic energy to it and rising to a measured height. The difference in the initial and final heights is directly proportional to the amount of energy lost due to fracturing the specimen. The total energy of fracture (E_T) is determined by Eq.1 [36].

$$E_T = m \cdot g(h_0 - h_f) \quad (1)$$

The test results are expressed in terms of amount of energy absorbed by the material during fracture and was reported in *Table 3*.

As for the tensile test, impact test were evaluated considering two different fibres orientation: parallel (L) and transversal (T) to the impact force as depicted in *Figure 41b*. The absorbed energy per unit cross-sectional area (kJ/m^2) or impact strength E_c is defined as (following the standard ASTM D6110) [37].

$$E_c = \frac{E_T}{w \cdot t} \quad (2)$$

Where w and t are the width and the thickness of the specimen, respectively.

2.4.3 Differential scanning calorimetry

Differential scanning calorimetry (DSC) was conducted using a TA Instruments Q1000. The specimens (7-12 mg) were heated from 0°C to 250°C at 10°C/min, cooled from 200°C to 0°C at 10°C/min and then re-heated up to 250°C at 10°C/min. Glass transition temperature and melting temperatures were calculated from the first heating scan and results are reported in *Table 5*. DSC analysis have been conducted on PLA and PETG sample pre- and post-processing in order to understand the effect of 3D printing on materials thermal properties.

2.4.4 Surface morphological analysis

Scanning electron microscopy (SEM) was performed to obtain qualitative information related to the surface morphology of the 3D printed parts as a function of printing parameters. Analysing the quality of the interlayer adhesion. The specimens were gold sputtered and observed with a FEI QUANTA 200 FEG scanning electron microscope.

2.5 Brace manufacturing by FDM

2.5.1 Virtual design of the back brace

As written before, for the initial steps a commercial 3D scanner has been used for the scanning of the patient. The model that comes out of the 3D scanner (*Figure 42a*) is tessellated (surface mesh STL/OBJ) using a dedicated orthopaedic software for modelling and sculpting the virtual 3D model of the skin (*Figure 42b*). The main systems are provided by Rodin4D, Biosculptor and Vorum composed of laser scanners or cheaper sensors and dedicated proprietary software [38, 39].

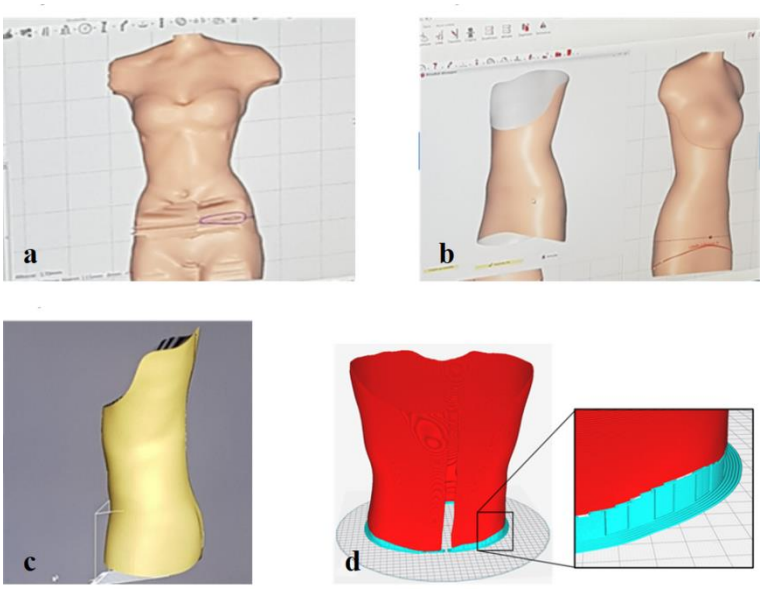

Figure 42 Processing step for the realization of 3D printed back brace: a) 3D scan of patient body, b) 3D surface modelling based on patient needs, c) realization of stl file, (d) Printing setup of the brace in Ultimaker CURA, where the model is depicted in red and the supports in blue.

This software enable the direct deformation of the tessellated surface with commands similar to the manual sculpting operations that the orthotist would perform on the physical positive model.

The second step regards the application of the thickness to the 3D model (*Figure 42c*). This step is necessary for passing the model to the software that realize the slicing required for creating the commands of the 3D printer. However, this step does not always perform well in all the software and so, after the sculpting phase was completed in the Rodin4D software, we preferred to pass the brace model as an open surface version in Rhinoceros in order to cut the edge and apply the thickness in a more stable way. After the thickness has been applied, the 3D files was exported in the STL format into software Autodesk Meshmixer in which was possible to further reduce the number of triangles of the mesh and to work exactly to the required number and size of the given triangles. These processes were performed using the crossover functions, as in the previous case, and then by the triangle number reduction function. In the last step, it was possible to create a STL back brace model, which is automatically generated according to the number of triangles in the mesh. The stl file was subsequently imported in the FDM machine software for the slicing process and the creation of the support structures. As has already been mentioned, the back brace manufacturing will be made by FDM

machine due to the big volume of the printed object and the high speed of printing if compared with other 3D printing techniques.

2.5.2 Back brace manufacturing process

The setting of the printer and the orientation of the orthosis in the printer are critical for the result. Among all the parameters available in the slicing software, for example Simplify3D software (*Figure 43*), the most important ones regard the printing speed, the choice of the layer height and the temperatures of the nozzle and of the printing bed. On a side, it is important to understand the limits about the fusion and the suggested bed temperature associated to the chosen material in order to exceed the melting point and provide good adhesion of the first layer. On the other side, the combination with the nozzle size, the layer height and the printing speed will determine whether the filament is able both to flow through the nozzle and to stick to the previous layer.

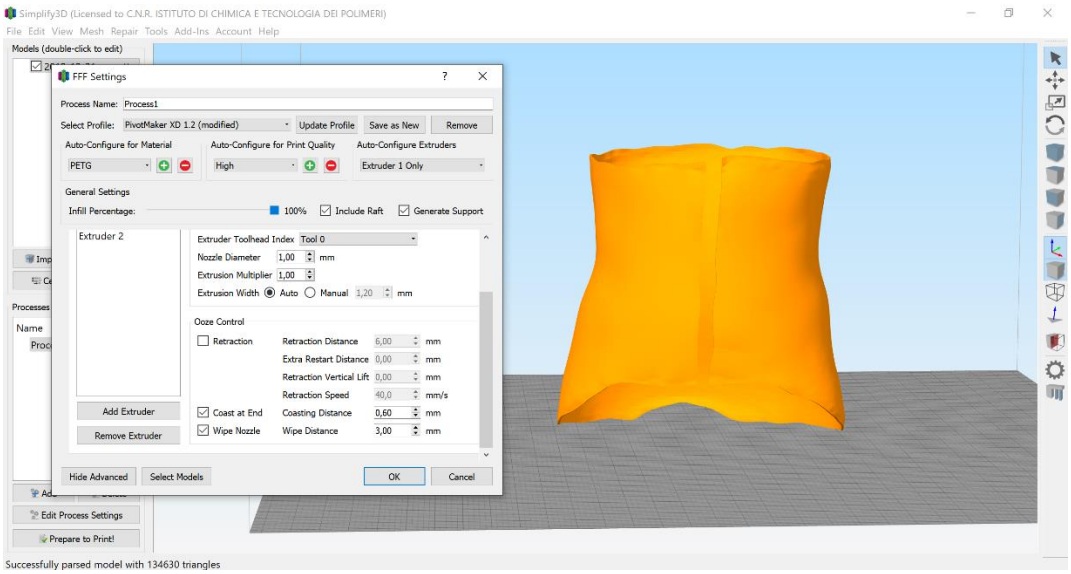

Figure 43 setting of the slicing and printing parameters for the final realization step of the back brace.

General indications are usually provided by the filament producer and can be found in literature or in specialized websites with tips from experts and other users. However, the proposed characterization of this chapter has been conducted in order to optimize the 3D printing process.

3. RESULTS AND DISCUSSIONS

3.1 Preliminary materials screening

A first choice among the available materials can be performed comparing the mechanical properties of the 3D printed selected materials with the polymers used for the traditional braces. For a first screening, a tensile test have been conducted on the filament reported in *Table 3*. Results of the mechanical characterization are reported in *Figure 44*.

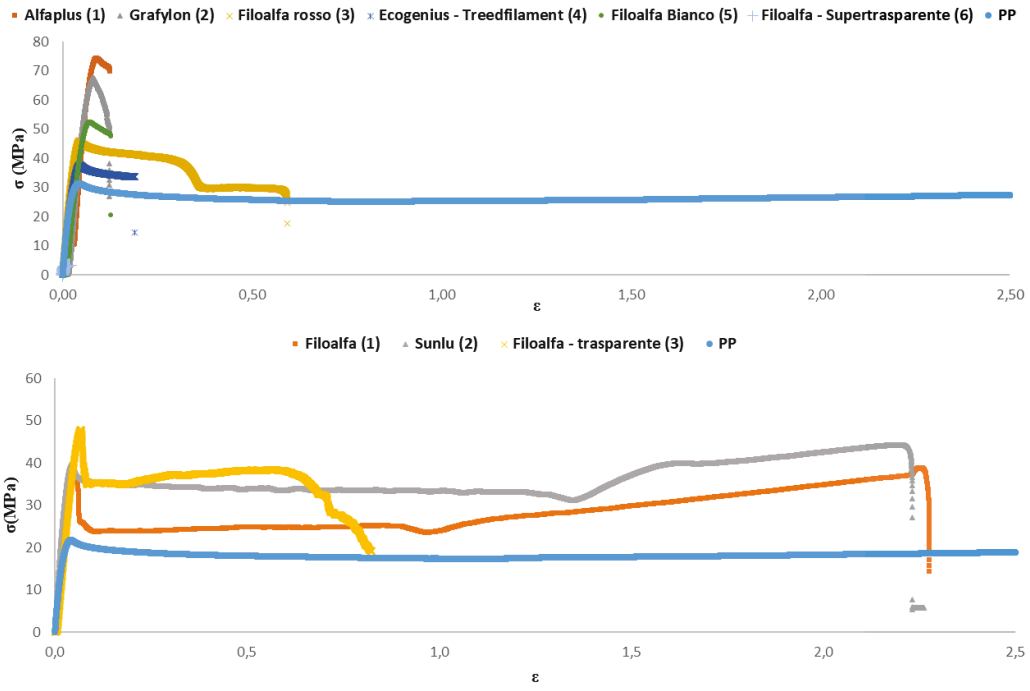

Figure 44 stress-strain diagram for the selected commercial filament compared with the properties of a traditional PP back brace.

As it is possible to see from the first screening results, PLA showed a typical brittle behaviour if compared to PETG properties. In term of elastic modulus both PLA than PETG resulted more rigid than PP. However, big differences have been found in the elongation at break (ε_b). In fact, ε_b of PLA is one order of magnitude inferior to that of PETG samples. PLA showed the typical brittle behaviour with no plastic deformation. The only interesting PLA is the PLA (Filoalfa) that has good elongation at break and elastic modulus similar to the PP samples. Due to the first screening results, three commercial filaments will be fully characterized

in the next chapter from mechanical, thermal and morphological point of view: PLA (Filolalfa), PETG (Sunlu) and PETG (Filoalfa).

3.2 Mechanical morphological and thermal characterization of selected polymers

An extensive mechanical characterization was conducted onto the selected filament to study the effects of layer thickness and fibres orientation on elastic modulus (E'), ultimate strength (σ_b) and elongation at break (ε_b) of printed specimens. Results of the characterization showed that FDM parts presented different mechanical response depending on how the layers were placed regarding the direction of the load. The modulus of elasticity (E'), the ultimate tensile strength (σ_{max}) and elongation at break (ε_{max}) of different configurations were reported in *Figure 45*. Furthermore, sample from commercial back brace mad of polypropylene (PP) and polyethylene (PP) were tested to compare the 3D printed materials with the thermoformed ones. PP and PE showed an elastic modulus of 1114.75±72.20 MPa and 420.94±80.03 MPa respectively and an elongation at break of 302.7±59.7 and 1377.5±198.6 respectively. As expected, the 3D printed samples showed anisotropic mechanical behaviour depending on fibres/force angle while layer thickness do not have great influence on mechanical performance. Looking at the result it is clear that PETG showed better mechanical properties in terms of both elastic modules and elongation at break. In tensile test, when the fibres were aligned with the applied force (*Figure 41a-L*) the samples showed the higher mechanical properties in terms of E' and ε_{max} both for PLA and PETG. On the contrary, when the force applied forms a 90° angle with the fibres (*Figure 41a-T*) the sample shower similar elastic modulus but elongation at break substantially lower. This is because when the force were applied parallel to the fibres direction (L) the sample strength is mainly dependant on the bulk material properties while when the forced is applied transversal to the fibres direction the sample strength is mainly dependent on the inter-fibres bonding. In this case, layer adhesion significantly affects the tensile strength since the inter-fibres fusion bonds between adjacent layers withstood most of the applied load. Comparison of 0.4 and 0.6 mm layer thicknesses showed that the layer thickness does not influence the mechanical properties of the samples.

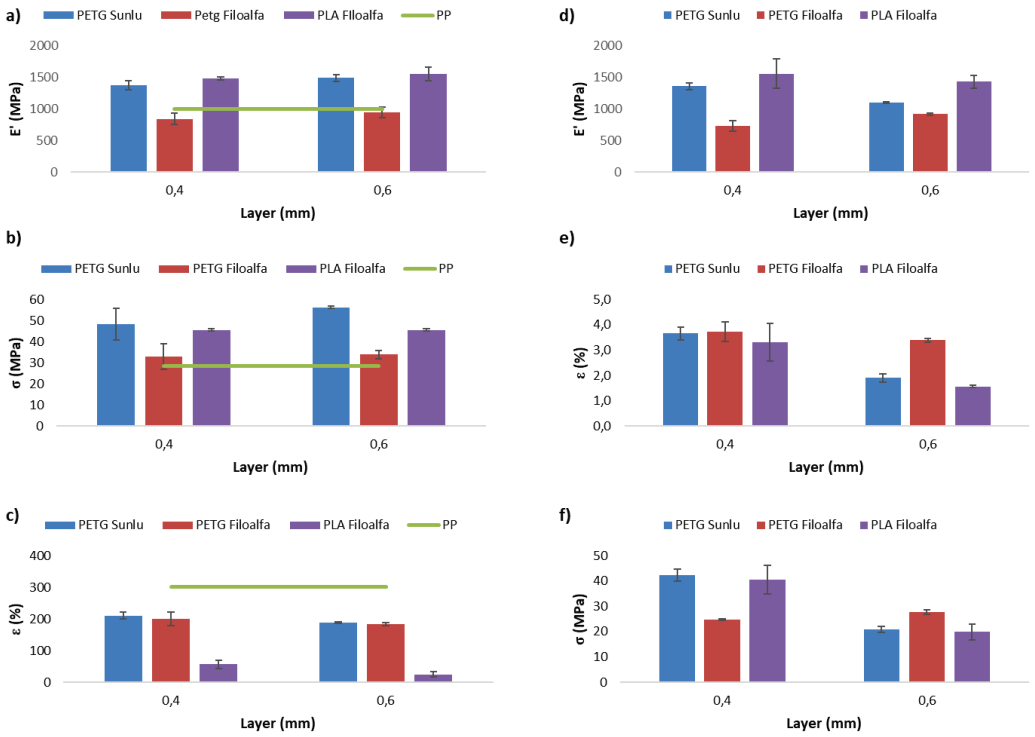

Figure 45 Effect of layer thickness and fibres orientation on mechanical properties of PLA and PETG samples

Looking at *Figure 45* it is evident that PETG (Sunlu) and PLA (Filoalfa) expressed the best mechanical properties in terms not only of elastic modulus but also of elongation at break with an elastic modulus of 1377.30±73.63 and 1480.93±23.85 MPa respectively. However, the two polymers exhibit different behaviour in term of elongation at break that are 211.00±11.00 % for PETG and 56.34±13.89 % for PLA. PETG Filoalfa, also if showed good elongation at break presented an elastic modulus too low if compared with PP and elongation at break inferior to the PETG Sunlu.

Impact tests are very useful for understanding the basic fracture mechanics of a material, as they measure the amount of energy that is absorbed by a material during high-strain-rate conditions before failure. The essential function of an impact test is to get a measure of the toughness or "fracture resistance" of a material by measuring the amount of energy required to break a sample completely [40]. Essentially, the measured energy is the total energy required to initiate a crack in the sample and grow it for a length equal to the length of the sample (for fracture resistance) or initiate and grow a fracture equal in surface area to the sample's cross-sectional area. Each sample set consisted of five

specimens for a given group of process parameters. The average impact strength (E_c) were taken as the results and they were reported in *Table 4*. Looking at the results it is possible to notice that build orientation significantly influenced the impact resistance of the samples highlighting a remarkable anisotropy. The effect of layer thickness on the impact strength was strongly dependent from fibers orientation. In the case of L samples, impact loading was parallel to the adjacent layers and so the applied load was mostly absorbed by the inter-layer boding.

Material	**Brand**	**Orientation**	**h_l** (mm)	**E_c** (kJ/m^2)
PETG	Sunlu	L	0.4	3.16 ± 0.77
			0.6	2.88 ± 0.44
		T	0.4	122.27 ± 1.60
			0.6	112.04 ± 4.33
	Filoalfa	L	0.4	1.17 ± 0.23
			0.6	0.85 ± 0.29
		T	0.4	10.72 ± 2.30
			0.6	7.73 ± 0.46
PLA	Filoalfa	L	0.4	2.28 ± 0.29
			0.6	2.29 ± 0.20
		T	0.4	3.45 ± 0.42
			0.6	3.23 ± 0.31

Table 4 Impact properties of the considered commercial filaments as a function of fibres orientation.

Therefore, for L samples the test measure the quality of interface bonding between adjacent layers and the layer thickness slightly affected the E_c both for PETG than for PLA. Looking at the results it is possible to notice that increasing the layer thickness the E_c tended to decrease. This effect can be explained by considering that with increased layer thickness, fewer layers were needed for a given total thickness, and so the number of interlayer bonds was reduced and E_c decreased. Similarly, for the T samples, impact strength decreased as the layer thickness increased. In this case, impact loading was perpendicular to the individual layers and so the resistance is mainly dependent on the mechanical properties of the fibres. In fact, they withstood most of the applied load for a given thickness increasing layer thickness decrease the number of layers. Moreover, looking at the result it is possible to see that the E_c values of PETG in T direction resulted two

order of magnitude higher respect the values of PLA going from 122.27 kJ/m^2 of PETG 0.4 mm to the 2.28 kJ/m^2 of PLA 0.4 mm. Therefore, it is possible to assess that PLA samples showed a typical brittle behaviour both in T and L directions. The result form mechanical characterization proved that PLA is not suitable for the realization of back brace due its typical brittle behaviour than result too different from the commercial PP actually in use in the orthopaedic field. On the opposite, PETG samples revealed better mechanical properties in terms of elongation at break and energy absorbed during impact and so it is more suitable for the realization of the back brace.

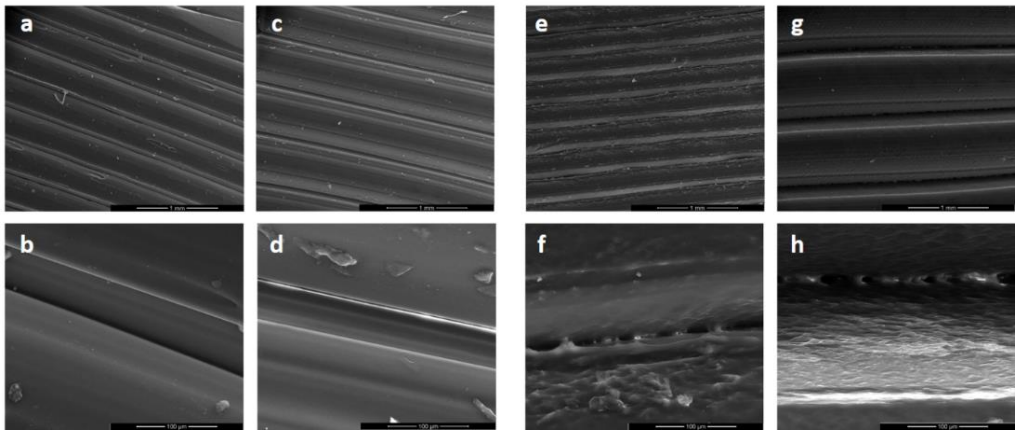

Figure 46 Scanning electron microscopy image of 3D printed PLA and PETG samples showing microscale roughness and layer interfaces quality for different layer thickness (a, c, e, g magnification 100 X , scale bar 1mm; b, d, f, h magnification 1000X , scale bar 100µm).

SEM images in *Figure 46* show the morphology of the PLA and PETG test samples with increasing magnification. At 100X magnification (*Figure 46a, c*) it is clear that the PETG samples showed a good surface finishing both for 0.4 and 0.6 mm layer thickness. Moreover looking at the images at higher resolution (*Figure 46b, d*) the samples revealed optimal cohesion between layers with a continuous interface without defects. PLA samples (*Figure 46e, g*), instead, showed worse surface finishing characterized by macroscopic defects. Furthermore, looking at the images with higher magnification (*Figure 46f, h*) it is possible to see a discontinuous interface between layers. The morphological analysis supported the results of mechanical analysis highlighting a better surface finishing for PETG samples with a smooth surface and a continuous interface between layers.

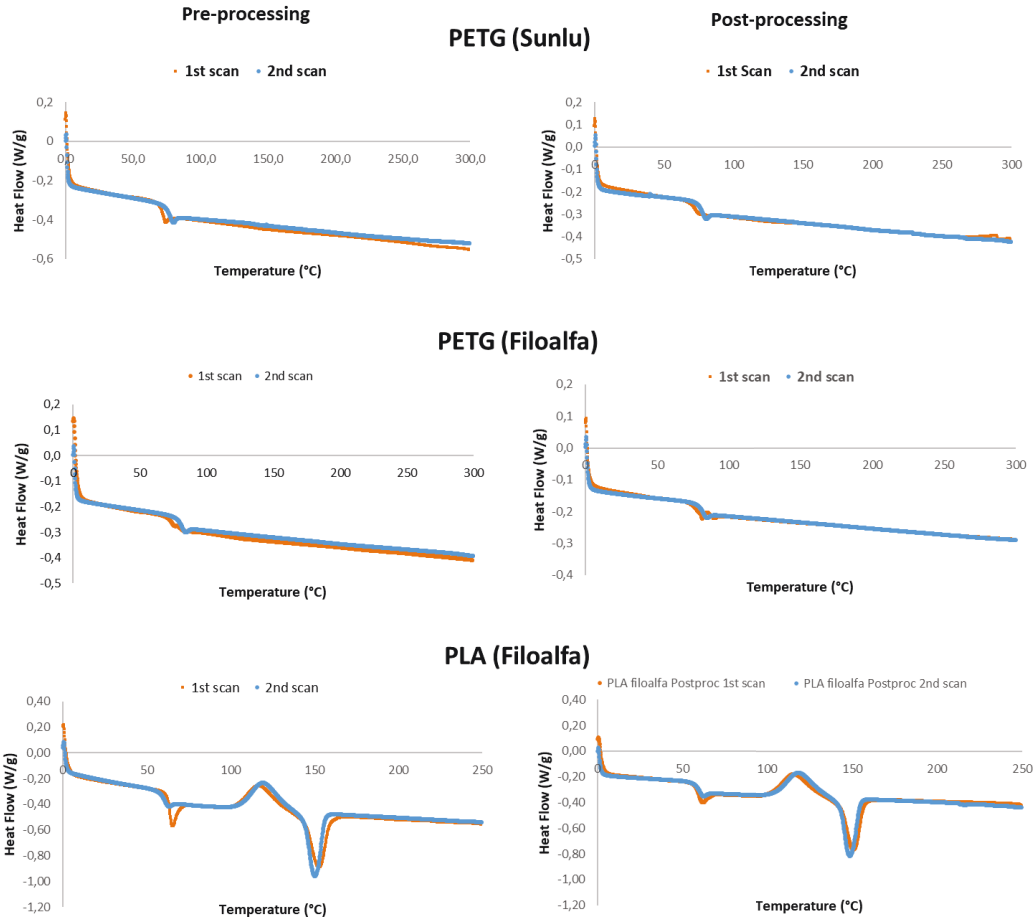

Figure 47 DSC analysis for PETG and PLA samples per and post-processing

Figure 47 shows a DSC graph of heat flux (W/g) versus temperature (T) for the PLA and PETG spool (pre-processing) and 3D printed materials (post-processing). Results have been reported in *Table 5*. The spectra of PLA showed three features typical of semi-crystalline thermoplastics, from left to right: heat flux at the glass transition temperature (T_g), an exothermic peak associated with cold crystallization, and a melting endothermic peak. The T_g of the spool material at the first scan is 62.39 °C and it is slightly higher than the T_g in the second scan. Melting temperature (T_m) showed the same behaviour with low differences between the first and the second scan. The T_g of the printed PLA shifts to a slightly lower temperature (58.49 °C), as well as T_m that decrease from 152.72 to 150.57 °C. This effect has been seen by other authors in the case of PLA which has been attributed to the formation of multiple crystalline states which can form during printing process [41]. Indeed, both the spool material and printed sample showed clear evidence of cold crystallization, a process associated with the

exothermal self-nucleation of the crystalline phases above the glass transition temperature. The cold crystallization peak is present in both samples, though it is noted to shift from a peak centred at 117.2 °C to a broad peak centred at about 120.1 °C following printing. The spectra of PETG revealed a completely different behaviour due to the amorphous nature of the polymers. In fact, PETG spectra revealed only a T_g transition around 70°C but not crystallization and melting peak have been recorded.

Sample		**T_g (°C)**		**T_m (°C)**		**ΔH_m (J/g)**	
		1st scan	2nd scan	1st scan	2nd scan	1st scan	2nd scan
PETG (Sunlu)	Pre	70.80	75.55	-	-	-	-
	Post	71.61	75.87	-	-	-	-
PETG (Filoalfa)	Pre	73.99	79.32	-	-	-	-
	Post	77.26	80.33	-	-	-	-
PLA (Filoalfa)	Pre	62.39	59.65	152.72	150.00	14.95	25.68
	Post	58.49	57.92	150.57	148.53	23.95	23.12

Table 5 Thermal characteristic of the considered polymers pre- and post-processing.

These results are in agreement with the literature that reported the PETG as a completely amorphous polymer. Also for PETG is possible to see low difference between the spool and the processed materials with a T_g that goes from 70.80 to 71.61 °C for the Sunlu and from 73.99 to 77.26 °C for the Filoalfa. The differences between the two materials could be ascribed to the presence of inorganic additives or contaminants. The overall results may indicate that the printing process result in changes in the nature and distribution of crystalline phases for PLA while slightly affected the behaviour of PETG polymers.

3.3 3D printing of the back brace

The orthosis was printed in the vertical and upside-down position in order to minimize the required supports (*Figure 48a*). Indeed, the top border of the orthosis (under the breast of the patient) was straighter than the lower border (around the hips) (*Figure 48b*). The chosen material was the PEG, due to the best mechanical and morphological properties described in the previous chapters. The nozzle temperature was set to 240 °C, which is in line with the range 230–250 °C recommended by the producer of the filament. The build plate temperature was set to 60 °C, in line with the suggested range 0-70 °C. We used a nozzle of 1.2 mm that could create the final thickness of 2.2 mm in two complete lines per layer.

Figure 48 Brace manufacturing. (a) Printing setup of the brace in the FDM machine, (b) 3D printed brace in the printer and (c) test on patient after final refinement by the orthotist

After the model was printed, a series of standard operations was performed by the orthotist to verify the post-processability of the product. These operations regarded the removal of the support, the smoothing of the border and the drilling of holes for applying the straps used for closing the orthosis on the patient's body (*Figure 48c*). The time for printing the brace was 4 h 33 min that can be compared to the standard "modern" process. The final weight of the back brace was 560 g that results very close to the actual weight of the thermoformed ones of 510g.

3.4 Cost model for the realization of the back brace by FDM technique

In this chapter of a cost model that is applicable for the proposed manufacturing processes of the back brace will be developed starting from the cost calculation model of Yim et al. [42, 43]. The parameters were then introduced regarding the type of printer used (in this study an FDM 3D printer I3D Pivotmaker), the materials used and the geometries of the back brace. The overall cost (C) was estimated by accumulation of four sub costs: machine purchase cost (P), machine operation cost (O), material cost (M), and labor cost (L) as shown in Eq.3.

$$C = P + O + M + L \tag{3}$$

P was computed by multiplying build time (T_b) and purchase cost (P_c) per hour as showed in Eq.4. It was assumed that the machine has 95% productivity during its useful life and so it is possible to calculate P as follow:

$$P = \frac{T_b \; x \; P_c}{0.95 \; x \; 24 \; x \; 365 \; x \; Y_{life}} \tag{4}$$

The operation cost (O) in Eq.3 was computed in Eq.5 by the product of operation rate (C_o) and build time (T_b). The operation rate is an empirically determined constant, correlated to factory overload, which is a complex function of maintenance, consumption of utilities, and cost of space.

$$O = T_b \; x \; C_o \tag{5}$$

The material cost (M) was computed in Eq. 6. The material cost was computed based on material cost (C_m) per unit weight. Furthermore, material cost was weighted by support structure factor (K_s) that take in account the additional material used to create support structure. The purpose of K_s is to capture the cost of additional material usage for building support structures. Without support structure, K_s is 1 and additional support structure increases K_s, which increases overall material cost M in Eq.3. Typically, K_s range from 1.1 to 1.5 and in our study we set it at 1.2. N, v, and ρ represent number of parts, part volume, and material density, respectively.

$$M = K_s \times N \times B \times C_m \times \rho \tag{6}$$

Finally, labor cost in Eq.3 was simply computed by the product of labor time (T_l) and labor rate (C_l) as shown in Eq 7.

$$L = \; T_l \times C_l \tag{7}$$

In particular, the build time model (T_b), can be deduced from Eq. 8 reported below. The construction time of the building was estimated from the sum of the processing time (T_s) and delay time (T_d) as shown in Eq. 8.

$$T_b = T_d + T_s \tag{8}$$

The delay time (T_d) in Eq.8 is computed by accumulation of delays before and after scanning each layer T_{pre} and T_{post}) and start up time $T_{strartup}$.

$$T_d = L_p \times \left(T_{pre} + T_{post}\right) + T_{startup} \tag{9}$$

For processes that require T_{pre} and T_{post}, appropriate values must be identified based on the machine's process parameters. In the case of the FDM used for the realization of the back brace, T_{pre} and T_{post} are zero.

The scanning time (T_s) in Eq.8 is a function of approximate geometric information as well as FDM process parameters. Therefore, computing T_s is more complex and consists of several intermediate computations to find the number of parts per batch, average cross section area, total scan length, and scanning time. The key idea of Eq. 10 is to calculate the number of bounding boxes (bounding boxes) that can be contained in an area of the two-dimensional platform.

In our case we set N = 1, since, considering the size of the back brace, it will be printed one at a time. Eq. 10 shows the method of computing number of parts for processes in which parts can be arrayed in two dimensions.

$$N = \frac{(PL_x + g_x - g_e)}{bb_x + g_x} + \frac{(PL_y + g_y - g_e)}{bb_y + g_y} \tag{10}$$

Where the descriptions of *PL*, *g* and *bb* are reported in *Figure 49*.

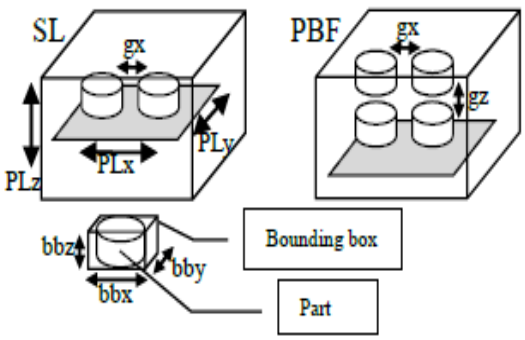

Figure 49: schematization of the printing surface and the bounding box

The term g_e represents the space between the piece to be printed and the edge of the platform. The average cross section area (A_{avg}) is computed by Eqs. 11 and 12.

$$\mathrm{A_{fn}} = \Upsilon \mathrm{e}^{\alpha(1-\gamma)} \tag{11}$$

$$A_{avg} = b_{bx} \times b_{by} \times A_{fn} \tag{12}$$

To approximate A_{avg}, a correction factor called area function (A_{fn}) was computed in Eq.12 where γ is a volumetric ratio (actual volume ÷ bounding box) and α is a constant with typical value of 1.5, so:
The total scan length (sl) is computed by Eq. 13.

$$sl = A_{avg}\left(\frac{n_{st}\ x\ L_p}{hr\ x\ d} + S_f\ \frac{L_s}{d}\right) \tag{13}$$

Where n_{st} is the number of single layer scans, h_r is the distance between two adjacent layer fibers, d the extruder diameter, S_f is the support factor and l_s the number of layers.
The key idea behind the calculation of the total scan length of Eq.13 is to calculate the length of a single line covering the average area of each level. The product of h_r and d determines the distance between two adjacent laser scans. Thus, any area divided by this product provides the scanning distance that covers the given surface assuming the area is a rectangle. The total length of the scan was calculated separately for the individual pieces and the supports separately and then they were put together. For the molded parts, the number of scans and the number of layers was multiplied by A_{avg} to obtain the total for the number of layers. For the supports, the support factor and the number of layers was multiplied by A_{avg} to consider the effect of the diffuse distribution of the supporting structures and then was put together for all the layers, respectively. The average scan speed (ss_{avg}) is computed in Eq.14 by the weighted (weight factor s_w) sum of scan speed (ss_s) and jump speed between two pieces (ss_j).

$$ss_{avg} = ss_s x\ s_w + ss_j\ x\ (1 - s_w) \tag{14}$$

Finally, the total scan time was computed by total scan length divided by average scan velocity as shown in Eq.15

$$T_s = \frac{N\ x\ sl}{3600\ x\ ss_{avg}} \tag{15}$$

The number of parts N was multiplied to accumulate scan length over all parts and factor 3600 is used to convert T_s to hours. In *Table 6* are reported the values of the cost model parameters used for the back brace application. However, the accurate estimation of those values will be highly dependent on the cost structure of the company that owns the machines.

PARAMETERS	USED VALUE
P (€)	13420
$\mathbf{Y_{life}}$ (years)	7
$\mathbf{C_o}$ (€/h)	4.75
$\mathbf{K_s}$	1.2
V (cm^3)	539.21
$\mathbf{C_m}$ (€/gr)	**PLA** = 0.033
	PETG = 0.029
ρ (gr/cm^3)	**PLA** = 1.24
	PETG = 1.25
$\mathbf{T_l}$ (h)	1
$\mathbf{C_l}$ (€/giorno)	25
$\mathbf{T_{startup}}$ (h)	0.25
$b_{bx} \times b_{by} \times b_{bz}$ (cm^3)	32.37 ×29.12×25.73
γ	0.02
α	1.5
$\mathbf{n_{st}}$	2
$\mathbf{h_r}$	1.4
d (cm)	0.1
$\mathbf{S_{upfac}}$	0.05
$\mathbf{L_s}$	33
$\mathbf{ss_s}$ (cm/s)	4
$\mathbf{s_w}$	0.7
$\mathbf{ss_j}$ (cm/s)	8

Table 6 Parameters used in the cost model

Table 7 report the quoted prices of the back brace based on our experimental setup. The costs are very similar for the two materials but certainly, compared to the costs of the current back braces (around 600-1000 €), they give an idea of the convenience that this new technology can bring to the production system of orthopaedic back braces.

Layer (mm)	PLA Back brace cost (€)	PETG back brace cost (€)
0.4	293.30	290.28
0.6	201.72	198.70

Table 7 Estimated cost for making the back brace with varying material and printing parameters

4. CONCLUSIONS

This chapter discusses the processes of design and manufacture of individual orthopaedic back brace by 3D digitization and FDM technique. The idea have been developed in collaboration with Clinica Medea (Bosisio Parini) in the context of EMPATIA project. With the combined approach of 3D medical imaging and FDM technique, it was possible to design and manufacture quickly and efficiently orthopaedic back brace, which have many advantages for the patients themselves as well as the doctors. They are:

- Low material consumption;
- Automated production;
- Easy, comfortable, airy and visually appealing solution for the patient;
- Cost savings;
- Higher accuracy of orthopaedic aids (by shaping the PLA material).

The current design process uses tools that can be improved by adding the information that we can obtain by the medical images. In particular, it is important to embed a part of reconstruction of the internal organs of the patients to be inserted in the patient model acquired by 3D scanning. Having such information would improve the resulting model of the scoliosis brace, considering the interaction of the device not only with the skin but also with the underlying skeleton. This could bring to the final version of the brace, avoiding the positive physical mold, necessary to 3D print it directly. Different materials have been proposed for the realization of the back brace: a Polylactic acid (PLA) and a polyethylene terephthalate glycol (PETG). The selected materials have been characterized from mechanical, thermal and morphological point of view in order to optimize the printing process. Results showed that FDM parts presented different mechanical response depending on how the layers were placed regarding the direction, of the load. Mechanical characterization and morphological analysis revealed that PETG parts showed better elongation at break and good interface between layers and so it is possible to conclude that is the best materials for the realization of back brace for medical applications. As we presented in the results, printing a complete back brace is feasible and the overall time for the production is comparable to the current one, but further research is required in terms of material choice and printing setup. For example, mechanical tests should prove the real characteristics of the printed product with the chosen parameters. We could better understand how changing temperature, speed, nozzle size and layer

height could influence in the properties of the real back brace and compare them to the other braces that are currently manufactured by thermoforming.

References

[1] H. Weiss, M. Moramarco, Scoliosis-treatment indications according to current evidence, OA Musculoskelet Med 1(1) (2013) 1.
[2] H.-R. Weiss, A. Kleban, Development of CAD/CAM based brace models for the treatment of patients with scoliosis-classification based approach versus finite element modelling, Asian spine journal 9(5) (2015) 661.
[3] J.A. Janicki, B. Alman, Scoliosis: Review of diagnosis and treatment, Paediatrics & child health 12(9) (2007) 771-776.
[4] A.L. Nachemson, L.-E. Peterson, Effectiveness of treatment with a brace in girls who have adolescent idiopathic scoliosis. A prospective, controlled study based on data from the Brace Study of the Scoliosis Research Society, JBJS 77(6) (1995) 815-822.
[5] N. Cobetto, C.-É. Aubin, S. Parent, S. Barchi, I. Turgeon, H. Labelle, 3D correction of AIS in braces designed using CAD/CAM and FEM: a randomized controlled trial, Scoliosis and spinal disorders 12(1) (2017) 24.
[6] J. Pruijs, M. Hageman, W. Keessen, R. Van Der Meer, J. Van Wieringen, Variation in Cobb angle measurements in scoliosis, Skeletal radiology 23(7) (1994) 517-520.
[7] C. Coillard, V. Vachon, A.B. Circo, M. Beauséjour, C.H. Rivard, Effectiveness of the SpineCor brace based on the new standardized criteria proposed by the scoliosis research society for adolescent idiopathic scoliosis, Journal of Pediatric Orthopaedics 27(4) (2007) 375-379.
[8] K.J. Noonan, S.L. Weinstein, W.C. Jacobson, L.A. Dolan, Use of the Milwaukee brace for progressive idiopathic scoliosis, JBJS 78(4) (1996) 557-67.
[9] A. Howard, J.G. Wright, D. Hedden, A comparative study of TLSO, Charleston, and Milwaukee braces for idiopathic scoliosis, Spine 23(22) (1998) 2404-2411.
[10] D.F. Redaelli, F.A. Storm, E. Biffi, G. Reni, G. Colombo, A Virtual Design Process to Produce Scoliosis Braces by Additive Manufacturing, International Conference on Design, Simulation, Manufacturing: The Innovation Exchange, Springer, 2019, pp. 860-870.
[11] A.G. Aulisa, M. Giordano, F. Falciglia, E. Marzetti, A. Poscia, V. Guzzanti, Correlation between compliance and brace treatment in juvenile and adolescent idiopathic scoliosis: SOSORT 2014 award winner, Scoliosis 9(1) (2014) 6.
[12] M.-L. Nault, S. Parent, P. Phan, M. Roy-Beaudry, H. Labelle, M. Rivard, A modified Risser grading system predicts the curve acceleration phase of female adolescent idiopathic scoliosis, JBJS 92(5) (2010) 1073-1081.
[13] M. Lusini, S. Donzelli, S. Minnella, F. Zaina, S. Negrini, Brace treatment is effective in idiopathic scoliosis over 45: an observational prospective cohort controlled study, The Spine Journal 14(9) (2014) 1951-1956.
[14] L.A. Dolan, S.L. Weinstein, Surgical rates after observation and bracing for adolescent idiopathic scoliosis: an evidence-based review, Spine 32(19) (2007) S91-S100.
[15] C.J. Goldberg, D.P. Moore, E.E. Fogarty, F.E. Dowling, Scoliosis: a review, Pediatric surgery international 24(2) (2008) 129-144.

[16] U. Von Deimling, U. Wagner, O. Schmitt, Long-term effect of brace treatment on spinal decompensation in idiopathic scoliosis. A comparison of Milwaukee brace--Cheneau corset, Zeitschrift fur Orthopadie und ihre Grenzgebiete 133(3) (1995) 270.
[17] J. Matussek, H. Mellerowicz, C. Klöckner, B. Sauerlandt, K. Nahr, G. Neff, 2-and 3-dimensional correction of scoliosis by corset treatment. Optimized conservative therapy of idiopathic scoliosis with the improved Cheneau corset, Der Orthopade 29(6) (2000) 490-499.
[18] D.F. Redaelli, E. Biffi, G. Colombo, P. Fraschini, G. Reni, Current and future manufacturing of chest orthoses, considering the case of osteogenesis imperfecta, ASME 2018 International Design Engineering Technical Conferences and Computers and Information in Engineering Conference, American Society of Mechanical Engineers Digital Collection, 2018.
[19] D. Law, M.-c. Cheung, J. Yip, K.-L. Yick, C. Wong, Scoliosis brace design: influence of visual aesthetics on user acceptance and compliance, Ergonomics 60(6) (2017) 876-886.
[20] I. Molnár, L. Morovič, Design and manufacture of orthopedic corset using 3D digitization and additive manufacturing, IOP Conference Series: Materials Science and Engineering, IOP Publishing, 2018, p. 012058.
[21] J. Saleh, K. Dalgarno, Cost and benefit analysis of fused deposition modelling (FDM) technique and selective laser sintering (SLS) for fabrication of customised foot orthoses, Innovative Developments in Design and Manufacturing, CRC Press2009, pp. 723-728.
[22] T.P. Mpofu, C. Mawere, M. Mukosera, The impact and application of 3D printing technology, (2014).
[23] J. Banks, Adding value in additive manufacturing: researchers in the United Kingdom and Europe look to 3D printing for customization, IEEE pulse 4(6) (2013) 22-26.
[24] L. Mertz, Dream it, design it, print it in 3-D: what can 3-D printing do for you?, IEEE pulse 4(6) (2013) 15-21.
[25] M. Fantini, F. De Crescenzio, L. Ciocca, Design and Rapid Manufacturing of anatomical prosthesis for facial rehabilitation, International Journal on Interactive Design and Manufacturing (IJIDeM) 7(1) (2013) 51-62.
[26] E.L. Nyberg, A.L. Farris, B.P. Hung, M. Dias, J.R. Garcia, A.H. Dorafshar, W.L. Grayson, 3D-printing technologies for craniofacial rehabilitation, reconstruction, and regeneration, Annals of biomedical engineering 45(1) (2017) 45-57.
[27] C. Lunsford, G. Grindle, B. Salatin, B.E. Dicianno, Innovations with 3-dimensional printing in physical medicine and rehabilitation: a review of the literature, PM&R 8(12) (2016) 1201-1212.
[28] M.A. Cuiffo, J. Snyder, A.M. Elliott, N. Romero, S. Kannan, G.P. Halada, Impact of the fused deposition (FDM) printing process on polylactic acid (PLA) chemistry and structure, Applied Sciences 7(6) (2017) 579.
[29] R. Kulkarni, K. Pani, C. Neuman, F. Leonard, Polylactic acid for surgical implants, WALTER REED ARMY MEDICAL CENTER WASHINGTON DC ARMY MEDICAL BIOMECHANICAL …, 1966.
[30] R.K. Kulkarni, E. Moore, A. Hegyeli, F. Leonard, Biodegradable poly (lactic acid) polymers, Journal of biomedical materials research 5(3) (1971) 169-181.

[31] T. Serra, J.A. Planell, M. Navarro, High-resolution PLA-based composite scaffolds via 3-D printing technology, Acta biomaterialia 9(3) (2013) 5521-5530.
[32] C. Marcauteanu, E.T. Stoica, C. Bortun, M.-L. Negrutiu, C. Sinescu, A. Tudor, Advantages of a Polyethylene Terephthalate Glycol-modified Coated with a Thermoplastic Polyurethane as an Occlusal Appliance Material, Rev. Chim.(Bucharest) 65 (2014) 734.
[33] R.B. Dupaix, M.C. Boyce, Finite strain behavior of poly (ethylene terephthalate)(PET) and poly (ethylene terephthalate)-glycol (PETG), Polymer 46(13) (2005) 4827-4838.
[34] E.C. Ching, R.K. Li, Y.W. Mai, Effects of gauge length and strain rate on fracture toughness of polyethylene terephthalate glycol (PETG) film using the essential work of fracture analysis, Polymer Engineering & Science 40(2) (2000) 310-319.
[35] A. Standard, D1708: Standard Test Method for Tensile Properties of Plastics by Use of Microtensile Specimens, ASTM International: West Conshohocken, PA, 2006.
[36] M. Caminero, J. Chacón, I. García-Moreno, G. Rodríguez, Impact damage resistance of 3D printed continuous fibre reinforced thermoplastic composites using fused deposition modelling, Composites Part B: Engineering 148 (2018) 93-103.
[37] A. International, Standard test method for determining the Charpy impact resistance of notched specimens of plastics. ASTM D6110-10, ASTM International West Conshohocken, Pennsylvania, 2010.
[38] N. Cobetto, C. Aubin, S. Parent, J. Clin, S. Barchi, I. Turgeon, H. Labelle, Effectiveness of braces designed using computer-aided design and manufacturing (CAD/CAM) and finite element simulation compared to CAD/CAM only for the conservative treatment of adolescent idiopathic scoliosis: a prospective randomized controlled trial, European Spine Journal 25(10) (2016) 3056-3064.
[39] A. Finnieston, BioSculptor CAD/CAM system: Technology for prosthetics & orthotics, CAD/CAM Systems in Pedorthics, Prosthetics & Orthotics (1988) 54-58.
[40] A.E. Patterson, T.R. Pereira, J.T. Allison, S.L. Messimer, IZOD impact properties of full-density FDM polymer materials with respect to raster angle and print orientation.
[41] A. Jalali, M.A. Huneault, S. Elkoun, Effect of thermal history on nucleation and crystallization of poly (lactic acid), Journal of materials science 51(16) (2016) 7768-7779.
[42] M. Schröder, B. Falk, R. Schmitt, Evaluation of cost structures of additive manufacturing processes using a new business model, Procedia CIRP 30 (2015) 311-316.
[43] S. Yim, D. Rosen, Build time and cost models for additive manufacturing process selection, ASME 2012 international design engineering technical conferences and computers and information in engineering conference, American Society of Mechanical Engineers Digital Collection, 2012, pp. 375-382.

Chapter 4
Clinical Trials

1. INTRODUCTION

The clinical trial was conducted in collaboration with the orthopaedic clinic "La Nostra Famiglia - Eugenio Medea" of Bosisio Parini (Lecco).
The main objective of the experimentation is the testing of the back braces produced through the combination of medical imaging and 3D printing overcoming the critical issues of traditional processes. The clinical investigation is a pilot study that will involve pediatric patients suffering from rachis alterations (idiopathic scoliosis and osteogenesis imperfecta) whose main objective will be the evaluation of the acceptance, safety and satisfaction of patients in the use of 3D printed back braces respect to the traditional ones with consolidated clinical effectiveness. The pilot study collected quantitative data during the experimentation (inertial sensor, infrared thermography) with the aim of quantifying in a preliminary manner any differences between the printed brace and the thermoformed brace.
This is a pilot study, carried out to acquire preliminary information on the device in order to adequately plan further development phases of the same, including design changes. These studies are characterized by a small sample of participating subjects and do not need to be dimensioned on a statistical basis. It is therefore considered that a number of 10 subjects can be adequate for the expected duration of the study.
Sensitive data collected by the participants will be treated according to the regulations in force and in respect of privacy. During all phases of the study, there is always a qualified and trained personnel present.

2. INCLUSION AND EXCLUSION CRITERIA

The general demographics, medical history, and physical examination of the patient were used to establish general admission criteria to the pilot test. The low-back pain history and evaluation of patient trunk strength and range of motion provided the outcome criteria for the study. Trunk strength and spine range of motion were evaluated using standard protocols.
Inclusion Criteria
Patients involved in clinical trials are affected by idiopathic scoliosis or osteogenesis imperfecta, according to the following criteria:

– For patients with idiopathic scoliosis:
    - Ages 6 to 17 years.
    - Lumbar or thoracolumbar scoliosis.
    - Gibbo higher than 5° on the scoliometer.
    - Angular values measured in degrees Cobb on the AP radiogram between 15° and 30°.

– For patients with osteogenesis imperfecta:
    - Ages 3 to 17 years.
    - Vertebral pain and / or vertebral deformities with a biconcave lens and/or deformity on the sagittal or frontal plane that can be partially reduced in a clinical test of traction, deflection and derotation.

Exclusion criteria

Patients with the following diseases are excluded from the clinical trial:

- Skin allergies.
- Behavioral and psychiatric disorders (e.g., emotional problems, anxiety, panic attacks).
- Dimensions of the trunk exceeding the printable dimensions.

3. PLANNED ACTIVITIES

The planned activities have been divided into the following phases:

1) Recruiting.
2) First visit: initial assessments and subject scanning.
3) Production of the brace.
4) Second visit: delivery of the printed back brace and intermediate evaluations.
5) Third visit: return of the printed brace and final evaluations.
6) Data analysis.

3.1 Recruiting

Patients with idiopathic scoliosis and osteogenesis imperfecta have been recruited, with inclusion and exclusion criteria indicated above. Only in the event that the patient shows interest and consents to participate in this research, the Informed

Consent Form for participation in the research will be signed. At the end of this initial visit, the patient is scheduled for the first visit.

3.2 First visit

The duration of the visit is estimated at about an hour. The activities planned during the first visit are the following:

- Clinical evaluation by the physician:
  - Posterior, frontal and lateral observation, in orthostatic position;
  - Measurement of the pelvis, test of reducibility in lateral flexion, possible rigidity in the sagittal plane and their location;
  - Measure on the AP and LL radiography of scoliotic curvatures and lateral curves in degrees Cobb.
  - Anthropometric measurements: weight and height in statics (height of the trunk from sitting for non-ambulatory subjects).
- Scanning of the area of interest: the scanning takes place by the Structure Sensor, a triangulation scanner with infrared structured light commonly used in orthopedics for the acquisition of anatomical segments. The data acquired represent with good fidelity the anatomy of the patient's bust but they are only preliminary information to help the doctor and the orthopedic technician for the production of the back brace, which will also intervene in the subsequent phases of the production process. This system is certified as a class 1 laser device. In the risk analysis, the precautions that will be adopted to further reduce the potential risks are indicated. All information is reported in a report that is then used by the orthopedic technician to proceed with the creation of the back brace.
- Evaluation by inertial sensor: the subject will be asked to wear the G-Sensor 2 sensor (BTS Spa), a wearable sensor classified as a class 1 medical device for gait analysis, while performing the following tests (with and without back brace thermoformed, if available):
  - Static acquisition with open / closed eyes (3 repetitions).
  - Timed Up and go (TUG) test (3 repetitions-*Figure 50*).

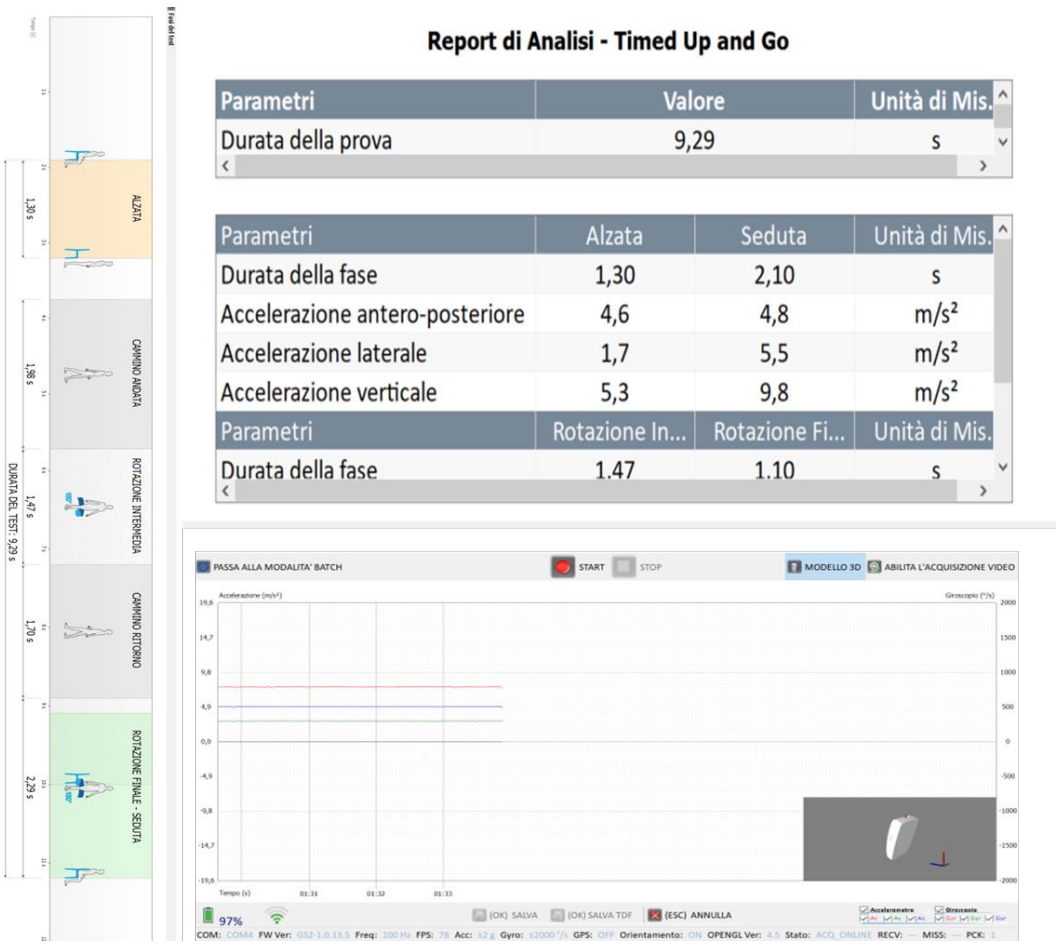

Figure 50: Evaluation by inertial sensor

– First questionnaire / patient interview, related to his experience of using the thermoformed back brace.

3.3 Realization of the back brace

The production process is based on computer modeling of the orthosis. The modeling activities will be carried out by an engineer who will work alongside the orthopedic technician, under the supervision of the doctor. Two possible cases that may occur during the clinical investigation will be presented below. In CASE A, an existing traditional back brace is reproduced by additive production (3D printing), in CASE B, the modeling of a new back brace starts from the anatomical scan of the patient. For CASE A the production step is reported below.

1.a Using 3D modeling software (Rhinoceros, Autodesk Meshmixer), the first operation concerns the cleaning of the scan file eliminating everything that

does not concern the surface of interest and smoothing the surfaces to reduce artifacts. The process then differs as follows.

2.a We proceed to the extraction of the surface of interest of the back brace. This procedure is carried out adequately with the use of Autodesk Meshmixer modeling software.

For CASE B the production step are the following

1.b Using the Rodin4D Neo modeling software the patient's model must be aligned according to the frontal, sagittal and horizontal axes. It is therefore based on the indications reported in the report by the doctor and on the experience of the orthopedic technician. It is therefore

2.b Identification of the area that must be corrected and the modifications to be made: straightening of the column, thrust zones and expansion zones, elongation to maintain a constant volume. These modifications represent the equivalent of the operations that the orthopedic technician performs manually with the traditional technique.

In both cases we reached a shaped surface representing the surface of the final back brace. After the scanning process, the surface must be converted in a solid object creating the desired thickness. The stl file is imported into print file generation software (Ultimaker Cura). Once the parameters have been set, the print file is acquired by the printer (WASP 4070 and I3D PIVOTMAKER) and produced using PETG as filament. The back brace is manually finished by the orthopedic technician to remove the supports, smooth the edges and apply the closing systems (riveted laces). Eventually it could become necessary, as for the traditional back brace, to add an additional soft layer of expanded polyethylene in areas critical for contact, like the area around the edge under axillary.

Finally, an orthopedic technician draws up the manufacturer's declaration of conformity to Directive 2007/47/EEC. For the evaluation of the production process, a sheet (manufacturing plan and back brace check) will be completed for each back brace as reported in *Figure 51*.

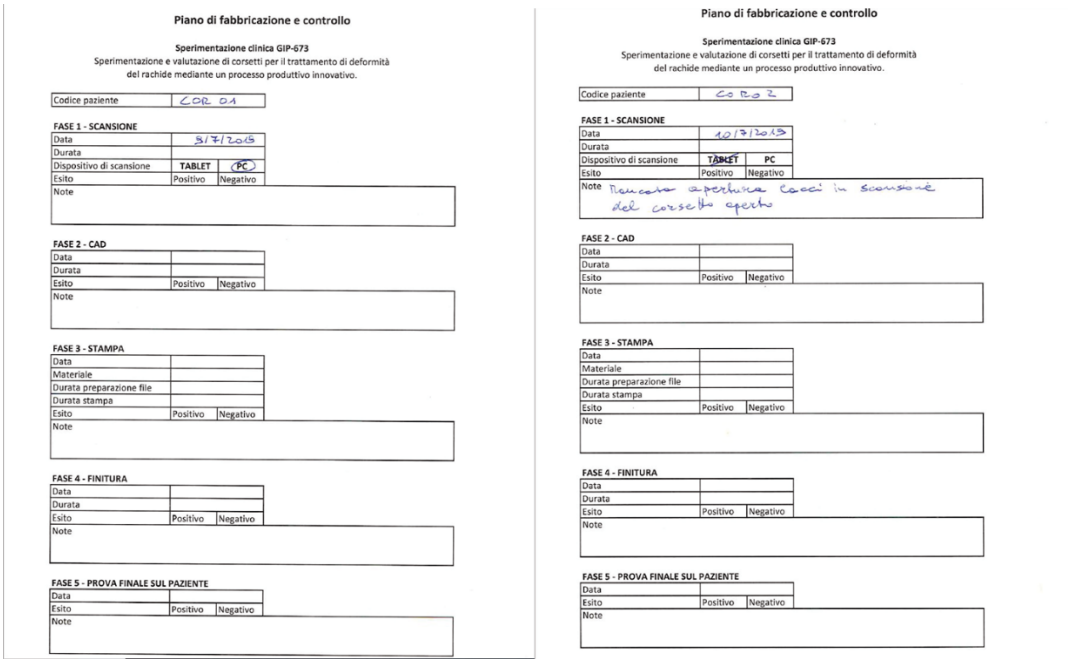

Piano di fabbricazione e controllo

Sperimentazione clinica GIP-673

Sperimentazione e valutazione di corsetti per il trattamento di deformità del rachide mediante un processo produttivo innovativo.

Codice paziente	COR 01

FASE 1 - SCANSIONE

Data	31/7/2015	
Durata		
Dispositivo di scansione	TABLET	(PC)
Esito	Positivo	Negativo
Note		

FASE 2 - CAD

Data		
Durata		
Esito	Positivo	Negativo
Note		

FASE 3 - STAMPA

Data		
Materiale		
Durata preparazione file		
Durata stampa		
Esito	Positivo	Negativo
Note		

FASE 4 - FINITURA

Data		
Durata		
Esito	Positivo	Negativo
Note		

FASE 5 - PROVA FINALE SUL PAZIENTE

Data		
Esito	Positivo	Negativo
Note		

Piano di fabbricazione e controllo

Sperimentazione clinica GIP-673

Sperimentazione e valutazione di corsetti per il trattamento di deformità del rachide mediante un processo produttivo innovativo.

Codice paziente	COR 02

FASE 1 - SCANSIONE

Data	10/7/2015	
Durata		
Dispositivo di scansione	TABLET	PC
Esito	Positivo	Negativo
Note	Necessita apertura cosci in scansione del corsetto aperto	

FASE 2 - CAD

Data		
Durata		
Esito	Positivo	Negativo
Note		

FASE 3 - STAMPA

Data		
Materiale		
Durata preparazione file		
Durata stampa		
Esito	Positivo	Negativo
Note		

FASE 4 - FINITURA

Data		
Durata		
Esito	Positivo	Negativo
Note		

FASE 5 - PROVA FINALE SUL PAZIENTE

Data		
Esito	Positivo	Negativo
Note		

Figure 51 Data sheet for manufacturing plan and back brace check

3.4 Second visit

The duration of the visit is estimated at about an hour. The planned activities are the following:

- Delivery of the back brace. If necessary, the back brace will be further refined by the orthopedic technician following the instructions of the doctor and the patient. The back brace will then be delivered, with the indication to wear it for at least 22h/day for 2 weeks. The patient will be given a diary (*Figure 55*) with the indication to report in writing the rough activities carried out during the day.
- Thermographic survey. The infrared sensor (One Pro, FLIR) converts the bodies thermal radiation into a visible image (thermogram) (*Figure 53*), has an accuracy of ±2°C and a visual resolution of 1440×1080 pixels. Infrared thermography is a non-invasive and harmless technology already used in clinical settings, even pediatric, for the study of diseases that are potentially associated with a change in surface temperature [1]. In the case of this, the information collected will be used exclusively to assess the wearability of the back brace.

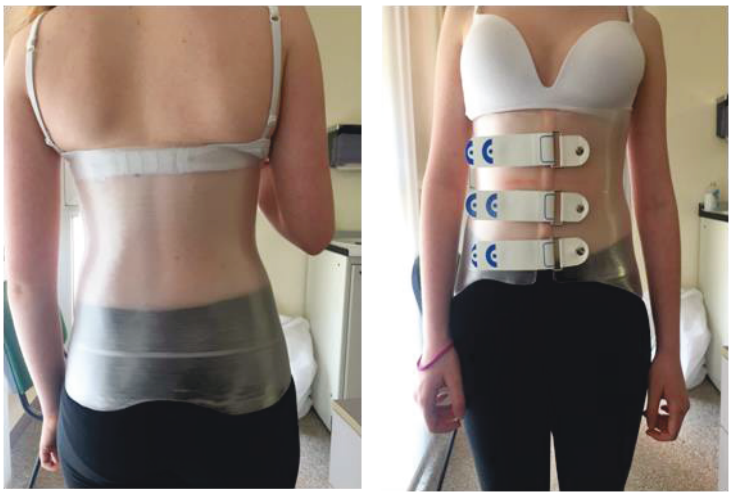

Figure 52 3D printed PEG back brace tested on a patient

3.5 Third visit

The duration of the visit is estimated at about an hour. At the end of the 2-week trial, the patient returns the back brace and the following evaluations are performed:

- Evaluation of the status of the back brace.
- Return of the diary.
- Measurements with wearable sensor, repeating the activities described during the first visit, but with and without the printed back brace.
- Second questionnaire/patient interview, related to his experience of using the printed back brace.

3.6 Data analysis and tolerability evaluation criteria

We have seen how, thanks to the inertial sensor, it is possible to evaluate the degree of mobility and ease in movements by wearing the back brace (*Figure 50*) but an analysis on the tolerability of the back brace can also be done with infrared sensors.

The data acquired by means of an infrared sensor will be processed with analysis software and will be used to highlight the anatomical fidelity of the printed back brace compared to the thermoformed back brace.

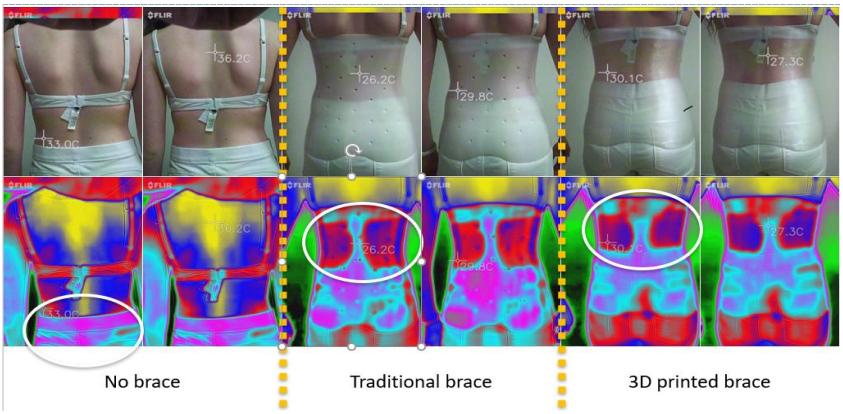

Figure 53 Evaluation by infrared sensor

The thermography produced by the infrared sensor (*Figure 53*) shows that the back brace showed better thermal dissipation compared to the thermoformed ones.

The acceptability of the back brace has been further tested with questionnaire for the evaluation of tolerability (*Figure 54*) and personal diary (*Figure 55*) referred to the activities performed during use.
The questionnaire also take in account the possible differences encountered by patients in wearing the new back brace compared to the old models, also in terms of self-image, indicating the degree of agreement by indicators from 1(not acceptable) to 7 (best).
The data collected through a questionnaire are used to evaluate the acceptance of the technology and the satisfaction in using the product back brace.

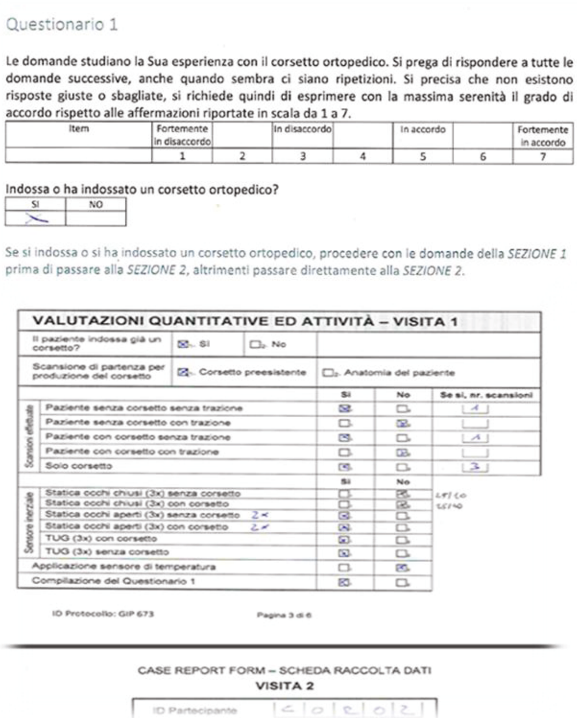

Questionario 1

Le domande studiano la Sua esperienza con il corsetto ortopedico. Si prega di rispondere a tutte le domande successive, anche quando sembra ci siano ripetizioni. Si precisa che non esistono risposte giuste o sbagliate, si richiede quindi di esprimere con la massima serenità il grado di accordo rispetto alle affermazioni riportate in scala da 1 a 7.

Item	Fortemente in disaccordo		In disaccordo		In accordo		Fortemente in accordo
	1	2	3	4	5	6	7

Indossa o ha indossato un corsetto ortopedico?

SI	NO
X	

Se si indossa o si ha indossato un corsetto ortopedico, procedere con le domande della *SEZIONE 1* prima di passare alla *SEZIONE 2*, altrimenti passare direttamente alla *SEZIONE 2*.

VALUTAZIONI QUANTITATIVE ED ATTIVITÀ – VISITA 1

Il paziente indossa già un corsetto?	☒ Sì	☐ No
Scansione di partenza per produzione del corsetto	☒ Corsetto preesistente	☐ Anatomia del paziente

		Sì	No	Se sì, nr. scansioni
Scansioni effettuate	Paziente senza corsetto senza trazione	☒	☐	1
	Paziente senza corsetto con trazione	☐	☒	
	Paziente con corsetto senza trazione	☒	☐	1
	Paziente con corsetto con trazione	☐	☒	
	Solo corsetto	☒	☐	3
		Sì	**No**	
Sensore inerziale	Statica occhi chiusi (3x) senza corsetto	☐	☒	
	Statica occhi chiusi (3x) con corsetto	☐	☒	
	Statica occhi aperti (3x) senza corsetto 2x	☒	☐	
	Statica occhi aperti (3x) con corsetto 2x	☒	☐	
	TUG (3x) con corsetto	☒	☐	
	TUG (3x) senza corsetto	☒	☐	
Applicazione sensore di temperatura		☐	☒	
Compilazione del Questionario 1		☒	☐	

ID Protocollo: GIP 673 Pagina 3 di 6

CASE REPORT FORM – SCHEDA RACCOLTA DATI

VISITA 2

ID Partecipante | C | O | R | O | 2 |

Figure 54 Questionnaire for the evaluation of tolerability

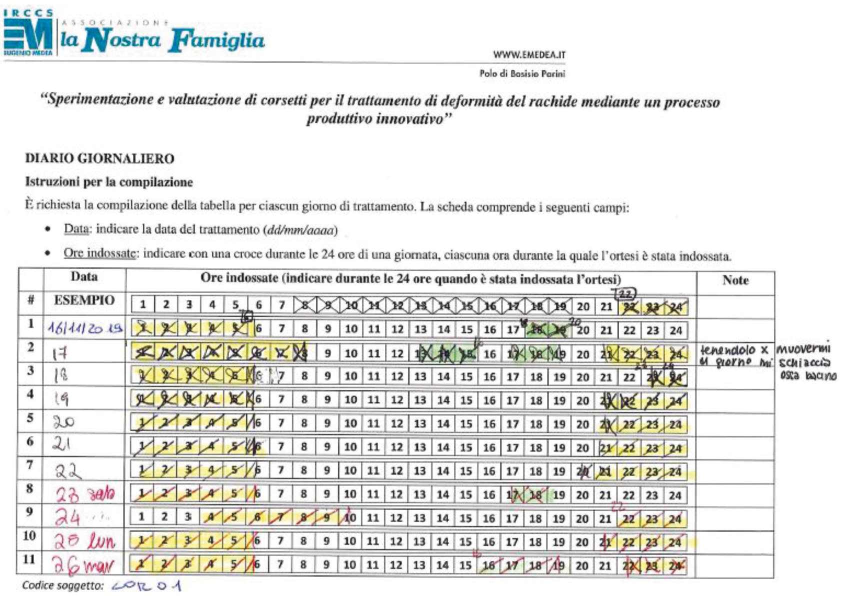

IRCCS EUGENIO MEDEA ASSOCIAZIONE la Nostra Famiglia

WWW.EMEDEA.IT

Polo di Bosisio Parini

"Sperimentazione e valutazione di corsetti per il trattamento di deformità del rachide mediante un processo produttivo innovativo"

DIARIO GIORNALIERO

Istruzioni per la compilazione

È richiesta la compilazione della tabella per ciascun giorno di trattamento. La scheda comprende i seguenti campi:

- Data: indicare la data del trattamento (*dd/mm/aaaa*)
- Ore indossate: indicare con una croce durante le 24 ore di una giornata, ciascuna ora durante la quale l'ortesi è stata indossata.

#	Data	Ore indossate (indicare durante le 24 ore quando è stata indossata l'ortesi)	Note
#	ESEMPIO	1 2 3 4 5 6 7 8 9 10 11 12 13 14 15 16 17 18 19 20 21 22 23 24	
1	16/11/2019	1 2 3 4 5 6 7 8 9 10 11 12 13 14 15 16 17 18 19 20 21 22 23 24	
2	17	1 2 3 4 5 6 7 8 9 10 11 12 13 14 15 16 17 18 19 20 21 22 23 24	tenendolo x il giorno mi muovermi schiaccia osta bacino
3	18	1 2 3 4 5 6 7 8 9 10 11 12 13 14 15 16 17 18 19 20 21 22 23 24	
4	19	1 2 3 4 5 6 7 8 9 10 11 12 13 14 15 16 17 18 19 20 21 22 23 24	
5	20	1 2 3 4 5 6 7 8 9 10 11 12 13 14 15 16 17 18 19 20 21 22 23 24	
6	21	1 2 3 4 5 6 7 8 9 10 11 12 13 14 15 16 17 18 19 20 21 22 23 24	
7	22	1 2 3 4 5 6 7 8 9 10 11 12 13 14 15 16 17 18 19 20 21 22 23 24	
8	23 sab	1 2 3 4 5 6 7 8 9 10 11 12 13 14 15 16 17 18 19 20 21 22 23 24	
9	24	1 2 3 4 5 6 7 8 9 10 11 12 13 14 15 16 17 18 19 20 21 22 23 24	
10	25 lun	1 2 3 4 5 6 7 8 9 10 11 12 13 14 15 16 17 18 19 20 21 22 23 24	
11	26 mar	1 2 3 4 5 6 7 8 9 10 11 12 13 14 15 16 17 18 19 20 21 22 23 24	

Codice soggetto: COR 01

Figure 55 Personal diary

Those analysis of the data acquired during all phases of the clinical investigation has made it possible to gather information on the acceptability, safety and satisfaction of patients in the use of printed back braces.
Furthermore, it was possible to obtain preliminary information on the advantages and limitations of the proposed innovative production process, which will allow the introduction of any corrective and improvement actions to the same.

4. LIMITATIONS

Since this clinical investigation is a pilot study aimed at acquiring preliminary feasibility information on the manufacture of a new custom-made device, it is not possible to estimate a number of expected dropouts. However, some of the possible causes of dropouts could be the following:

1) Problems during the production process not otherwise foreseeable that prevent the production of the back brace.
2) Difficulty in using the back brace for the minimum pre-established duration.
3) Inability to wear the back brace due to manufacturing problems

The risks associated with the use of custom-made devices object of the present clinical investigation are considered acceptable and comparable to the risks that a subject that uses orthoses and/or aids for the mobilization of body districts may face.

5. CONCLUSIONS

Adolescence, as a sensitive phase of a young person's development, requires a special degree of adaptation in the event of a chronic illness. For scoliosis patients this means, for instance, facing up to cosmetic impairments and subjectively significant physical defects. Scoliosis is a risk factor for impairment of the quality of life of children and adolescents and its impact is particularly marked if brace wearing is indicated. Particular attention needs to be paid to aspects of brace compliance. Cognitively the patient must come to terms with a commitment of time-consuming, confining, and sometimes uncomfortable treatment for a condition that does not always cause physical symptoms. Support for patients within the context of in-patient rehabilitative treatment has proved to be both necessary and helpful.

The development of an innovative production process based on a virtual processing can allow a high customization and a better wearability of the back braces thanks to a greater adherence to the anatomy of the patient. In fact, the 3D printed back brace has the potential to better respect the patient's anatomy, distributing the thrusts homogeneously with consequent better acceptance and the possibility of greater use times. Finally, 3D printing of back braces produces less waste material then craft processing. Among the tested materials, the PETG responds in an optimal manner to the needs of patients and physicians for the treatment of the pathologies included in the clinical trial.

The new production process thus conceived allows: reduce production costs, customize the back braces more and foresee a phase of recovery of the back braces once disused (the material can be re-spun and reused with the same technology). Moreover, the 3D printed back brace have been tested on patients and the first patients analyzed have found benefits in terms of wearability, comfort and psychological acceptability.

Acknowledgements

We would like to acknowledge Prof. P. Fraschini, Dr. F. Storm, Dr. D. Redaelli and all the staff of the "Associazione La Nostra Famiglia - IRCCS Eugenio Medea Bosisio Parini (LC) for the pre-clinical evaluation test of the back brace and the Project **EMPATIA** (Empowerment del PAzienTE in cAsa) for the financial support of the work.

References

[1] R.B. Knobel, B.D. Guenther, H.E. Rice, Thermoregulation and thermography in neonatal physiology and disease, Biological research for nursing 13(3) (2011) 274-282.